Integrated Physical-Fenton Remediation of Petroleum-Contaminated Soil Using Ethyl Lactate as a Green Solvent

by

Seyedeh Pegah Jalilian Ahmadkalaei

Department of Chemical and Environmental Engineering

THESIS SUBMITTED TO THE UNIVERSITY OF NOTTINGHAM FOR THE DEGREE OF DOCTOR OF PHILOSOPHY

AUGUST 2017

ABSTRACT

The huge amount of petroleum hydrocarbons contaminated sites is the heritage of a long history of fossil fuels usage. Reducing petroleum hydrocarbons levels in contaminated soils by Fenton reaction and with the aid of one or two agents such as solvents, surfactants, or vegetable oils has been studied in recent years, with successful reported results. Nonetheless, destruction of the aliphatic fraction of total petroleum hydrocarbon (TPH) by Fenton reaction has been studied to a lesser extent as compared to the aromatic fraction of TPH. Additionally, studies regarding the effect of humic acid (HA) on Fenton reaction reported contradictory results, and more research is necessary to clarify HA effects. Lastly, although achieving the highest efficiency is the main objective of soil remediation technologies, the environmental side effects of the applied processes should be considered as important as the efficiency. In light of these, the main aim of this project was to increase Fenton treatment efficiency by using an environmental friendly solvent, ethyl lactate (EL). The project objectives included determining optimum levels for the reagents of Fenton reaction and desorption process such as hydrogen peroxide (H_2O_2) and EL, identifying the kinetic of TPH desorption and destruction of petroleum hydrocarbons by Fenton reaction in addition to analysing the effects of EL on these processes. Through desorption tests, EL/water solution demonstrated great ability to increase the removal efficiency and desorption of sorbed TPH. Desorption by EL/water solution consisted of a very fast desorption stage followed by a slow stage. After 30 min of desorption, the removal efficiency of TPH increased from 63% to 81% for EL=25% and EL=100%, respectively. The initial desorption rate for 25% and 100% were

1.625 mg/min and 3.368 mg/min, respectively. The results of batch experiments indicated that EL%=10% was the optimum value for the EL-modified Fenton reaction. After 4 h, an increase in H_2O_2 concentration from 0.1 M to 2 M at L/S=2 and EL=25% increased the removal efficiency of TPH from 68.41% to 90.21%. HA addition up to 150 mg/l was also studied. For fraction 1, adding HA led to an increase in removal efficiency while for fraction 2, only HA=150mg/l had higher removal efficiency than the HA=0 case and for fraction 3, addition of HA in the studied range could not increase the removal efficiency. A good compatibility of zero-valent iron nanomaterial with H_2O_2 was proved. Laboratory column experiments were finally carried out to remove petroleum hydrocarbons from diesel-contaminated soil with EL to reproduce the conditions of in-situ treatment. The remaining diesel in soil decreased by increasing H_2O_2 molarity from 0.1 M to 0.5 M whereas a further increase to 2 M led to an increase in remaining diesel in soil. The stability of H_2O_2 in EL has been observed which signifies good potential for in-situ applications. Overall, the project has demonstrated the feasibility of EL-modified Fenton reaction for the remediation of petroleum-contaminated soil.

Keywords: Ethyl lactate; Fenton treatment; Soil remediation; Total petroleum hydrocarbons

LIST OF PUBLICATIONS

Jalilian Ahmadkalaei S.P., Gan S., Ng H.K., Abdul Talib S. (2016) Investigation of ethyl lactate as a green solvent for desorption of total petroleum hydrocarbons (TPH) from contaminated soil. Environ Sci Pollut Res 23:22008–2201

Jalilian A. S. P., Suyin Gan, Hoon Kiat Ng, Suhaimi Abdul Talib (2017) Evaluation of ethyl lactate as solvent in Fenton oxidation for the remediation of total petroleum hydrocarbon (TPH)-contaminated soil. Environ Sci Pollut Res, 24(21):17779-17789

Jalilian Ahmadkalaei S.P., Gan S., Ng H.K., Abdul Talib S. (2017) The role of natural organic matters in water and soil remediation. Proceedings of the 4th Postgraduate Colloquium for Environmental Research (POCER 2017), Melaka, Malaysia, 25-26 July 2017

ACKNOWLEDGEMENTS

I am deeply grateful to Prof. Gan Suyin, Prof. Ng Hoon Kiat and Prof. Suhaimi Abdul Talib for providing this funded PhD opportunity to carry out research within the field of soil treatment. They have supported me through the entire project. I am very thankful to my beloved parents and siblings, for their support and sharing and loving care and encouragement that give me the courage to face all problems. The Ministry of Higher Education (MOHE), Malaysia, is also gratefully acknowledged for its financial support towards this project under the Fundamental Research Grant Scheme (FRGS), FRGS/2/2013/TK05/UNIM/02/1.

LIST OF TABLES

LIST OF FIGURES

LIST OF ABBREVIATIONS

AAS	Atomic absorption spectrometry
AOT	Advanced oxidation technique
BTEX	Benzene, toluene, ethylbenzene, and xylene
BTX	Benzene, toluene and mixed xylene
DCM	Dichloromethane
DNAPL	Dense non-aqueous phase liquid
EL	Ethyl lactate
EPA	Environmental Protection Agency
ET	Ethanol
FA	Fulvic acid
FAME	Fatty acid methyl esters
S-FAME	Synthesized fatty acid methyl esters
Fe^{2+}	Ferrous ion
Fe^{3+}	Ferric ion
FeO_2^+	Ferry ion [Fe(IV)]
$FeOH_3^+$	Perferryl ion
$FeSO_4 \cdot 7H_2O$	Ferrous sulphate heptahydrate
GC	Gas chromatographic
H_2O_2	Hydrogen peroxide
H_2SO_4	Sulphuric acid
HA	Humic acid
HCl	Hydrochloric acid

$HgCl_2$	Mercury chloride
HOC	Hydrophobic organic carbons
$[HN4]6Mo_7O_{24}•4H_2O$	Ammonium molybdate tetrahydrate
HS	Humic substances
$KMnO_4$	Potassium permanganate
Koc	Soil organic carbon-water partition coefficient
Kow	Octanol-water partition coefficient
L/S ratio	Solution to soil ratio
NAPL	Non-aqueous phase liquid
$(NaPO_3)_6$	Sodium hexametaphosphate
NOM	Natural organic matters
O_3	Ozone
•OH	Hydroxyl radical
PAH	Polycyclic aromatic hydrocarbons
PCE	Perchloroethylene
PCP	Pentachlorophenol
•R	Organic radical
R^2	Correlation coefficient of fitting
$S_2O_8^{2-}$	Persulfate
SOM	soil organic matter
TPH	Total hydrocarbon petroleum
U.S. EPA	United States environmental protection agency

LIST OF UNITS

%	Percentage
ºC	Degree Celsius
°C/min	Degree Celsius per minute
g	Gram
g/l	Gram per liter
g/ml	Gram per millilitre
h	Hour
l	Litre
m	Meter
mg/kg	Millie gram per kilogram
min	Minute
mmol	Millie mole
ml	Millilitre
ml/min	Millilitre per minute
M	Molar
ppm	Part per million
rpm	Rotation per minute
sec	Second
v/w	Volume per weight
wt%	Weight percentage
W/W%	Weight per weight percentage

TABLE OF CONTENTS

CHAPTER 1: INTRODUCTION

1.1 Research Background

The vast number of contaminated sites with petroleum hydrocarbons is the heritage of a long history of using fossil fuels. According to the European Environment Agency in 2006, crude oil (alkanes, alkenes and cycloalkanes) was one of the main pollutants in European contaminated sites forming 33.7% of total soil contaminants (Valentin et al., 2013). Around 450000 contaminated sites have been reported in America (Yap, 2012). Crude petroleum is a complex mixture constituted mainly of hydrocarbons, organic sulphur compounds, nitrogen, and oxygen. This mixture contains hundreds of thousands of hydrocarbons, ranging from light, volatile, short-chained organic compounds to heavy, long-chained, branched compounds. Compounds in crude oil can be divided into three general classes consisting of saturated hydrocarbons, aromatic hydrocarbons and polar organic compounds (Riser-Roberts 1998). Storage leakage, transport loss, land disposal of petroleum waste, accidental and intentional spills, refineries, aboveground tanks, terminals, marine oil spills, or pipelines are among the main sources that pollute soils with petroleum hydrocarbons (Heath et al., 1993; Zhang et al., 2010; Lim et al., 2016; Besha et al., 2017).

Oil-contaminated soil poses serious health and environmental risks through soil contamination itself, through water and groundwater pollution that can be toxic for aquatic life (Arias-Estevez et al., 2007; Garcia-Falcoan et al., 2004), and

through human consumption of contaminated food and water (Rey-Salgueiro et al., 2008). The presence of petroleum hydrocarbons in soil can change the physical, chemical and biological properties of soil (Rauckyte et al., 2009). Petroleum hydrocarbons will decrease the applicability of the soil for plantation by changing the soil properties from wet-soil to oil-soil (Lee et al., 2002). Thus, remediation of organic-contaminated soil is of concerns for both government and public (Cheng et al., 2015).

Remediation of petroleum-contaminated soil is a complicated process. Diesel and fuel oil are the most difficult fraction of petroleum hydrocarbons for remediation (Jamialahmadi et al., 2015). In conventional remediation methods for petroleum hydrocarbons polluted soil, the contaminants are transferred from one phase to the other, for example via utilizing a solvent without destruction or degradation. Recently soil washing/soil flushing (SW/SF) processes using extracting agents (surfactants, biosurfactants, cyclodextrins (CDs), cosolvents) are proven to be effective methods in removing contaminants (Trellu et al., 2015). More recent attempts have been carried out to not only remove the contaminants, but to also degrade them such as bioremediation, oxidation and thermal process. Among these, Fenton reaction which is classified as an advanced oxidation treatment has been proven to be a successful approach to soil remediation (Bogan et al., 2003, Romero et al., 2009, Yap, 2012,). Among unconventional remediation methods, we can mention the unconventional sorbents such as humic acid, electrokinetic remediation, non-thermal plasma treatment, vermiremediation and biocatalyst assisted remediation (Kuppusamy et al., 2016; Zhang et al., 2016). It is reported that SOM even showed higher

removal efficiency than a chelating agent in removing diesel fuel from contaminated soil (Lim et al., 2016).

1.2 Problem Statement

A wide range of processes for remediating contaminated soils have been applied including soil vapour extraction, thermal treatment, surfactant flushing, and chemical oxidation using Fenton reagent, permanganate and ozone as well as bioremediation including bioaugmentation, biostimulation, and bio-venting (Lim et al., 2016). Two general views could be recognized in the used methods for soil treatment. In the first, researchers dissolve the contaminants in a solvent and remove the solvent from the soil whereas in the second, they focus on destructing the contaminants by different methods such as oxidation. Combination of these two general views has also been considered.

Destruction of hydrocarbons by oxidation, and remediation of the high concentration soil contamination by Fenton reaction have long been proven to a very effective method with the high efficiencies (Watts et al., 1996; Watts et al., 2000; Neyens et al., 2003). In Watts et al. (2000)'s work, benzene, toluene, and mixed xylenes (BTX) were chosen as representative aromatic compounds, and *n*-nonane, *n*-decane, and *n*-dodecane (NDD) were selected as common aliphatic components of gasoline. NDD was destructed by 20% after 48 h, and BTX was destructed completely in 32 h.

Combination of Fenton reaction with solvent extraction is now recognized as a successful remediation strategy (Lundstedt et al., 2006, Jalilian et al., 2017). Fenton oxidants are more active in aqueous medium; this means that they can react with the dissolved form of contaminants more effectively than with the

adsorbed form. By applying a solvent, for instance ethanol (ET), the dissolution rate of contaminants will increase. By dissolving the contaminants, their destruction by Fenton reaction will be more efficient. The commonly used agents for dissolving petroleum hydrocarbons and increasing their desorption rate are organic solvents like n-hexane, low-molecular-weight alcohols (e.g., methanol, ethanol, tert-butanol, pentanol, acetone, and hexanol) (Khodadoust et al., 1999; Khodadoust et al., 2000; Silva et al., 2005; Li et al., 2012), and vegetable oils such as sunflower oil (Pannu et al., 2004; Gong et al., 2005).The higher efficiency of a green solvent, i.e. ethyl lactate (EL) for desorbing polycyclic aromatic hydrocarbons in comparison with ethanol has been reported by Yap et al. (2012/a). EL is a green solvent, which is 100% biodegradable, easily recyclable and non-corrosive. Its physicochemical properties make it an attractive alternative to conventional solvents. Properties such as high degree of solvency and miscibility in water, and low volatility enables it to be a suitable coupling solvent with other treatment processes such as Fenton reaction (Yap et al., 2012/a). The applicability of EL-Fenton treatment for degradation of four PAHs, i.e. phenanthrene, anthracene, fluoranthene and benzo[a]pyrene in soil was studied and was compared to ethanol-Fenton and conventional Fenton treatments. EL-Fenton treatment demonstrated a higher removal efficiency than the ethanol-Fenton reaction. A combination of pretreatment and treatment with EL-Fenton for 8-10 h reached to near 97% destruction which was an additional 40% removal by conventional Fenton reaction after 24 h (Yap et al., 2012/a). To date, the potential of EL with Fenton reaction for remediating diesel-contaminated soil has not been explored. Hence, this represents a good

opportunity to further investigate this novel remediation approach and develop an effective strategy for diesel-contaminated soils.

Significance of StudyWhilst there are substantial literature related to different remediation technologies of petroleum hydrocarbons-contaminated soil, lesser studies exist for the remediation of aliphatic fraction of petroleum hydrocarbons as compared to aromatic fraction. Comparatively too, very few studies on modified Fenton reaction with solvents for treatment of TPH-contaminated soil exist and to the best knowledge of the author, there is no study to date regarding the application of EL for Fenton remediation of TPH-contaminated soil. It needs to be mentioned here that the TPH named here is attributed to the aliphatic fraction of diesel hydrocarbons. Furthermore, the effects of humic acid (HA) on Fenton reaction have been demonstrated in many studies, but there are controversial arguments regarding the positive or negative effects of HA.

This thesis develops a modified Fenton reaction with EL for diesel-contaminated soil. As desorption of contaminants is one of the major limitations of the Fenton reaction, desorption study of TPH from contaminated soil by EL is studied. The integrated EL-Fenton reaction was carried out in both batch and column set-ups. The batch set-up was chosen to study the reaction in small-scale laboratory conditions. The column set-up was selected to represent field in-situ remediation. In some studied, HA increased the treatment efficiency while in other reported results HA was considered responsible of the decrease in treatment efficiency. Considering the contradictory findings on HA effects, this thesis also aims to determine how increasing HA dosage influence the removal efficiency of TPH and clarify its effects in the treatment. The results of this study

are crucial for developing an enhanced understanding of the effect of EL in modified Fenton reaction for diesel-contaminated soil and determining optimum values of EL and HA for Fenton soil remediation applications. The data obtained in this thesis would benefit further pilot-scale studies.

1.3 Research Objectives

The aim of the present study is to examine the potential of EL-based Fenton as an alternative treatment technique to conventional water-based Fenton treatment for total petroleum hydrocarbon (TPH)-contaminated soil. The objectives of this project are as follows:

1. Assessing the ability of EL/water system to desorb petroleum hydrocarbons from contaminated soil.
2. Modelling the desorption kinetics of petroleum hydrocarbons from contaminated soil using EL/water system.
3. Investigating the effectiveness of integrated EL/water-Fenton treatment for petroleum-contaminated soil via a batch parametric study and optimizing the process.
4. Modelling the EL/water-Fenton oxidation kinetics of petroleum hydrocarbons from contaminated soil.
5. Evaluating the effects of different operating variables on TPH removal efficiency in column set-up.

1.4 Research Approach and Scope

Figure 1-1 illustrates the scope of work carried out in this project. First, the soil material characteristics which affect the treatment efficiency such as soil texture, moisture content, soil pH, organic matter and total iron (Fe) available were determined. The TPH analytical technique was then established; diesel range of petroleum hydrocarbon, C9-C28, was passed through the gas chromatography (GC) column to separate the aliphatic fraction of petroleum hydrocarbons and was divided into three fractions, C9-C16, C16-C22, C22-C28, and TPH is the summation of three fractions. These variations enabled the study to gain further insight into the effects of hydrocarbons with different molecular weights on the treatment performance.

Next, choosing the best solvent for Soxhlet extraction of TPH was carried out in order to use the solvent with the highest desorption capacity. The initial concentration of 5000 mg/kg soil was selected for most experiments as it was the average contamination level value in the field. According to Contaminated Land Management and Control Guidelines No. 1: Malaysia Recommended Site Screening Levels for Contaminated Soil Land, the reported values in residential and industrial soils are 40000mg/kg and 400000mg/kg respectively. The applicability as well as kinetic of EL in desorption of TPH from contaminated soil was examined with different EL%.

Subsequently, the applicability of combination of Fenton treatment with EL was the focus of study. The effect of different variables on the removal efficiency of EL-Fenton reaction was studied. The extent of degradation was evaluated at different EL%, L/S ratio, and initial concentration of H_2O_2. As the studied soil

in this project had high organic matters, investigating the effects of humic acid (HA) was also included.

Finally, the performance of EL-based Fenton reaction in column set-up which is closer to field conditions was examined. A column with 5 cm diameter was chosen with 150 g soil in the column. The solution of EL with Fenton reaction reagents were injected into the column from top. The investigated variables affecting TPH removal efficiency in different sections included EL%, H_2O_2 concentration and L/S.

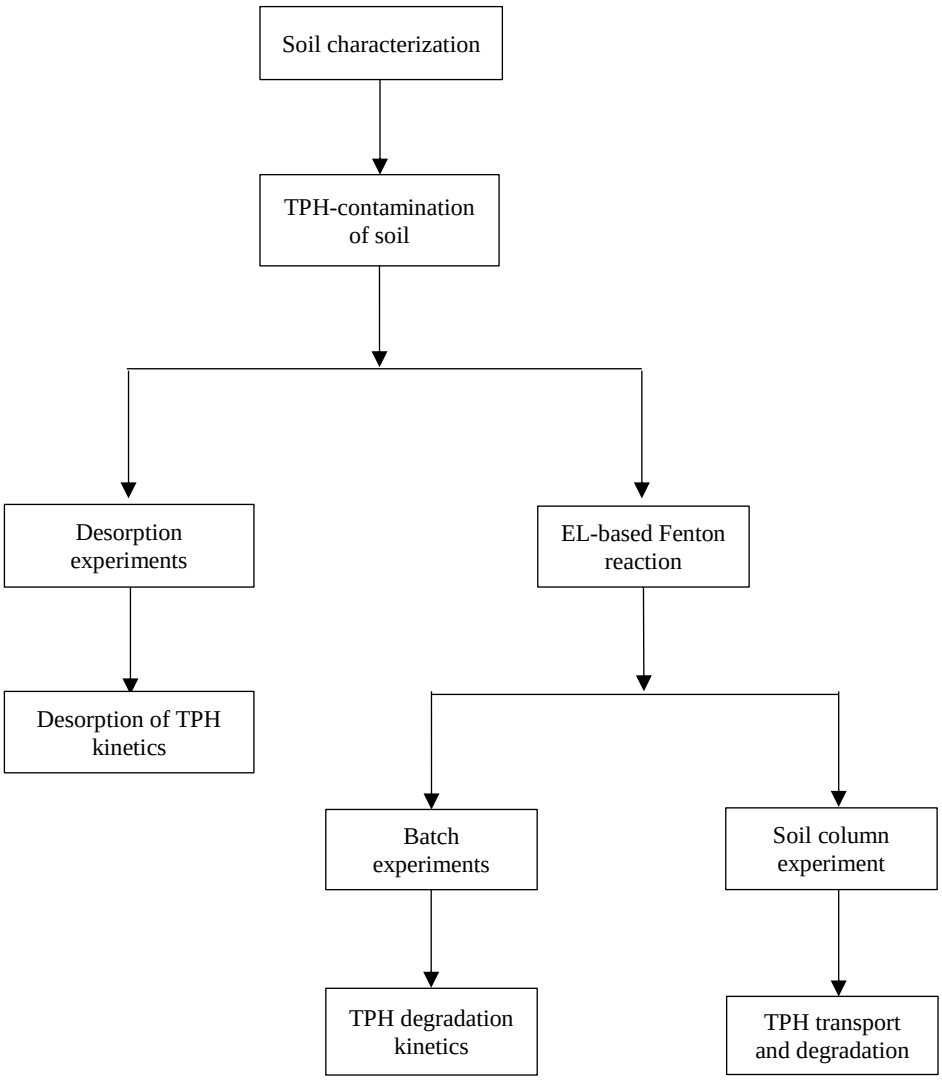

Figure 1-1: Scope of work

1.5 Thesis Structure

This thesis consists of seven chapters as follows:

Chapter 1 presents an introduction to the definition of TPH, the implications of TPH-contaminated soil, and the need for soil remediation. The problem statement and knowledge gap in this area is described along with the research objectives, approach and scope of work.

Chapter 2 is a comprehensive literature review that discusses the definition of TPH, the chemistry of Fenton reaction, modified Fenton reaction and its combination with other remediation processes, desorption processes of adsorbed contaminants with the effective variables in solvent extraction, and soil column set-up.

Chapter 3 summarises the analytical techniques involved in this research. They include soil spiking, soil characteristics determination, and TPH in soil and H_2O_2 residual concentration quantification. The methodology applied in other chapters for conducting the experiments were included in this chapter.

Chapter 4 reports the TPH desorption experiments using EL. Determining the best solvent for desorption experiment was the focus of the first part of this chapter. The applicability of EL in desorption of TPH-contaminated soil was examined was the subsequent focus in which the effects of different variables on removal efficiency was examined and desorption kinetic was determined.

Chapter 5 comprises the feasibility study of EL with Fenton reaction, including parametric and degradation kinetic studies on TPH removal from polluted soil. Using response surface methodology (RSM), the effects of involved variables in the Fenton reaction was studied and optimised.

Chapter 6 describes the application of soil column set-up to investigate the applicability of EL-Fenton reaction under field conditions. The effects of several variables including EL% on remaining amount of diesel in soil were elucidated.

Chapter 7 reviews the main results from this work. Conclusions are drawn and several recommendations for future work are suggested.

CHAPTER 2: LITERATURE REVIEW

2.1 Introduction

This chapter aims to review relevant literature related to remediation of petroleum hydrocarbons-contaminated soil. Firstly, petroleum hydrocarbons are defined as a broad range of hydrocarbons exist ranging from aliphatic to aromatic fractions. Next, solvent extraction is reviewed along with the sorption/desorption processes as this is a crucial part of the integrated Fenton remediation technology studied in this project. The main focus of this chapter lies in the application of Fenton treatment for soil remediation and coupling different methods with Fenton reaction. A final section discusses soil column set-up studies in simulating conditions close to actual field conditions.

2.2 Petroleum Hydrocarbons

Because of the wide variety of compounds in petroleum mixtures, their different partitioning behaviour, and the lack of physical and chemical data for each individual compound, the entire range of petroleum hydrocarbons is classified into different fractions. The fractions are chosen based on the similarity in their nature (aliphatic or aromatic) and their similarities in other physicochemical characteristics such as boiling point (TNRCC1006).

Separation of hydrocarbons in a gas chromatographic (GC) column is accomplished based on their boiling point range. By using this concept and applying the n-alkanes as the markers, the range of TPH is divided into different fractions. Each component, branched or aromatic, is identified based on their

carbon number and boiling point in comparison with the n-alkane with the same carbon number (TNRCC1006). The recognized carbon number is named as the approximate equivalent carbon number (EC) (TNRCC1006; Mackay et al., 1993). For example, as Mackay et al. (1993) explained, n-hexane with six carbon and boiling point of 69°C has EC=6. In determining the EC of benzene with the same number of carbon, i.e. 6, we need to know its boiling point, i.e. 80°C, which determines its retention time in a GC column. Based on this information, the EC of Benzene has been calculated as 6.5.

The n-alkane markers and the other TPH constituents are listed in Table 2-1. For example, the hydrocarbons between >nC7 to nC8 indicates that all hydrocarbons that elute after n-heptane and up to n-octane are included. Cyclization, or ring structures, can increase the boiling point, so all hydrocarbons with 8 carbons are not included in this range, including the aromatics ethylbenzene and the xylenes (TNRCC1006). Averaging the properties of all compounds in each fraction, and the empirical relationship represented by EC are among the proposed ways to use one value for each physicochemical properties of each fraction (Gustafson et al., 1997).

Table 2-1: n-Alkane marker compounds, carbon number, equivalent carbon number and boiling points. Note that Equivalent Carbon Number indicates approximate elution of the compounds (TNRCC1006)

Name and Approximate Order of Elution in a Boiling Point Column	*Actual Carbon Number*	*Boiling Point (°C)*	*Equivalent Carbon Number (EC)*
nC6	6	69	6
Benzene	6	80	6.50
nC7	7	98	7
Toluene	7	111	7.58
nC8	8	126	8
Ethylbenzene	8	136	8.50
m-Xylene	8	139	8.60
p-Xylene	8	138	8.61
o-Xylene	8	144	8.81
1,2,3 Trimethylbenzene	9	169	9.84
nC10	10	174	10
Naphthalene	10	218	11.69
nC12	12	216	12
Acenaphthylene	12	270	15.06
Acenaphthene	12	278	15.50
nC16	16	287	16
Flourene	13	295	16.55
Anthracene	14	340	19.43

Continued Table 2-1: n-Alkane marker compounds, carbon number, equivalent carbon number and boiling points. Note that Equivalent Carbon Number indicates approximate elution of the compounds (TNRCC1006)

Phenanthrene	14	339	19.36
Pyrene	16	360	20.80
nC21	21	357	21
Fluoranthene	16	375	21.85
Benzo(a)anthracene	18	435	26.37
Chrysene	18	448	27.41
Benzo(b)fluoranthene	20	481	30.14
Benzo(k)fluoranthene	20	481	30.14
Benzo(e)pyrene	20	493	31.17
Benzo(a)pyrene	20	495	31.34
Dibenze[a,h]anthracene	22	524	33.92
Benzo(g,h,i)perylene	21	525	34.01
nC35	35	499	35
Indeno[1,2,3-cd]pyrene	21	536	35.01

The whole range of TPH is usually divided into three ranges of gasoline, diesel and lube/motor oil/grease. Here, it is noteworthy to point out that these fractions do not have a clear-cut point. In other words, they have some overlap areas. The selected range for each of these three fractions differs in different standard methods. Generally, the commonly used divisions are C6-C12, C10-C28 and C20-C40 that are considered as the gasoline range, diesel range, and lube oil

range, respectively (caslab,2017). A diagram including these fractions is shown in Figure 2-1.

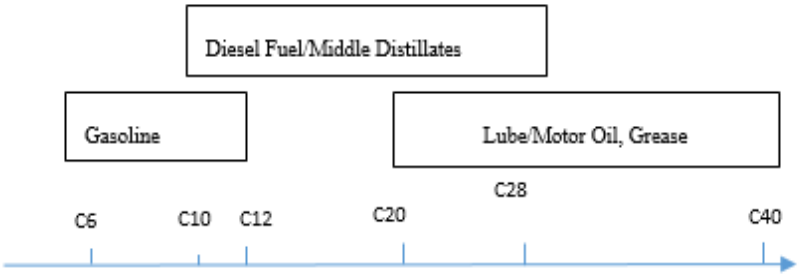

Figure 2-1: Carbon number ranges for TPH

In determining the concentration of one division, for example the diesel range, two different methods are mostly used. In the first method, the concentration of the whole detected area is considered by GC from the beginning marker until the last marker. The determined concentration in this method includes all the detected peaks, not only various diesel components such as normal-, iso-, cyclo-alkanes and aromatics, but also potential degradation products (Yeh et al., 2008). In the second method, the sum of some selected n-alkanes in the diesel range (for example C10, C12, C14, C16, C18, C20, C22 and C24), are calculated as an approximation of all petroleum hydrocarbon concentration (Yeh et al., 2008). The reported concentration in this way does not show the generated products through the reactions (Yeh et al., 2008).

Yeh et al. (2008) also detected the difference between the results of these two methods. After remediating the soil by ozone reaction, they reported that n-alkane did not show any considerable reduction, while the diesel range changed. Converting the diesel compounds to other hydrocarbon products led to the result that the amount of n-alkane remained constant, while diesel compounds were converted to other products.

Information related to the chemistry and the reaction of the contaminants with the soil particles, and hydrodynamic information related to their movement in the soil are necessary for predicting their movement. Among the different fractions of TPH, gasoline consists mostly of volatile components and hence, the downward movement would not happen for this petroleum fraction whereas in contrast, dissolving in groundwater is important for diesel range (Lee et al., 2002). The lack of sufficient information related to the diesel movement and the possible chemical reactions has resulted in diesel remediation being among the major environmental issues (Lee et al., 2002).

Different methods for the remediation of contaminated soil with petroleum hydrocarbons have been proposed. Among them, soil vapour extraction has been a widely used method for the treatment of gasoline-contaminated soil. This method requires a post-treatment for eliminating the extracted contaminants in the gaseous form (Lee et al., 2002). As non-volatile compounds are resistant to this method, it is not appropriate for diesel range hydrocarbons, or heavier fractions (Lee et al., 2002). Bioremediation is another used method, either as the main treatment process or a post-treatment one. Although diesel range hydrocarbons have shown good remediation efficiency with bio-reduction methods, but due to the high expenses involved in these methods, and in co-contaminant cases with heavy metals as they inhibit the degradation of hydrocarbons, this method is not recommended and it is especially not preferred for soils with high TPH concentration (Koshlaf et al., 2016; Yoo et al., 2016). Moreover, it has been reported that high concentration of non-aqueous phase liquid (NAPL) reduces the efficiency of the bioremediation process. NAPLs are immiscible in water and consist of refractory compounds, and they have high

tendency to adsorb to soil and this property affects the removal efficiency (Besha et al., 2017). Therefore, cost-effective methods with high efficiency are the focus of research for the treatment of contaminated soils with petroleum hydrocarbons. Oxidation of TPH by different oxidants like ozone and hydrogen peroxide is one of the most successful approaches that have been applied (Lee et al., 2002; Yu et al., 2007).

2.3 Solvent Extraction

Extraction of contaminants from the soil matrices using a solvent in its total meaning includes applying water, organic solvents, or vegetable oils and their derivatives. This total process is named as dissolution, desorption, soil washing, or in the special case of using water, it is termed as leaching (Guo et al., 2010). The different forces between contaminants and soil particles could be classified as chemical reactions, hydrophobic/hydrophilic properties (solubility), and surface forces (Bayley et al., 2005(a/b)). To successfully overcome the energy of contaminant/solid, at the point of the impact, a greater energy than the potential energy between the contaminants and solid surface must be applied (Bayley et al., 2005(a/b)). Some examples of different solvents in desorption (extraction) of petroleum hydrocarbons from contaminated soil are summarised in Table 2-2.

The hydrophobic contaminants' properties which affect their solubility are mainly the octanol-water partition coefficient (k_{ow}) and the water solubility. The higher these values are, the lesser the extraction efficiency (Sui et al., 2014). In this sense, compounds with $k_{ow} > 6$ are defined as the most hydrophobic with a high affinity toward the soil particles, and compounds with $k_{ow} < 6$ are

known as weakly sorbed compounds. Because of the presence of water in soil, water miscible solvents lead to a better extraction than the partially miscible or immiscible solvents (Subramanian et al., 2010).

Another determinative characteristic of solvents is their polarity. In extracting oil pollutants from soils, the solvent with the polarity closest to the oil pollutants could be more efficient in dissolving them (Li et al., 2012). In addition to dissolving the pollutants, solvents could enhance the extraction by reducing the interfacial tension between NAPL-water; as a result, the density and viscosity of the NAPL change and the NAPL solute can move as an aqueous solute and NAPL does not exist as a discrete phase any more (Lee et al., 2006).

Table 2-2: Selected solvent extraction studies of petroleum hydrocarbons-contaminated soil

Contaminants	Removal efficiency/ extracted pollutants	Solvent/Cosolvent	Solvent/Soil ratio	Reference
Polycyclic aromatic hydrocarbons (PAHs)	46% of total PAH	Fatty acid methyl esters (FAME)	1	(Gong et al. 2010)
12 PAHs	81–100%	Sunflower oil	1,2	(Gong et al. 2005/b)
12 PAH	field-moist soil batch extraction (67.2% and 81.5%) for the air-dried 90.2% and 97%	Sunflower oil	-	(Gong et al., 2005/a)
Xylene, naphthalene and hexadecane	95%	50% ethyl acetate, 40% of acetone and 10%	8	(Silva et al. 2005)
PCP	Extracting approximately 720 mg/kg PCP	water-ethanol mixtures as solvents	-	(Khodadoust et al. 1999)
PAHs	65 to 90% of the extractable PAHs	5% 1-pentanol, 10% water and 85% ethanol	1 g:4 ml soil:solvent extraction ratio	(Khodadoust et al. 2000)
Anthracene	Extraction efficiency was >90%	Peanut oil	-	(Pannu et al. 2004)
Pentachlorophenol (PCP)	montmorillonite (40–80%) and ignited sediment (~90%)	Lactic acid	-	(Subramanian et al. 2010)
TPH including 25 alkanes (C11–C35) and 16 US EPA priority polycyclic aromatic hydrocarbons	76–94 %	Petroleum ether	-	(Sui et al.,2014)

2.3.1 Effective variables in solvent extraction

Apart from the solubilization ability of the solvent, variables such as properties of soil (composition, water content, soil organic matter (SOM), pH, porosity,

etc.), NAPL properties (composition, wettability, etc.), and pore water properties (viscosity, density, etc.) affect the efficiency of the solvent extraction process (Lee et al., 2006; Sui et al., 2014). Operational variables like soil temperature are also important in determining the efficiency of soil remediation (Albergaria et al., 2012).

Li et al. (2012) examined the influence of various extraction variables (cosolvent (acetone) concentration, extraction time, L/S ratio, and extraction stages) on the removal of four oil fractions (saturates, naphthene aromatics, polar aromatics and nC7-asphaltenes) from soils. The highest reported removal of saturates, naphthene aromatics, polar aromatics and nC7-asphaltenes reached to 91%, 81%, 87% and 60% after 0.5 min, respectively, by applying a solution of 25% acetone.

Silva et al. (2005) studied the applicability of a mixture of solvents composed of ethyl acetate–acetone–water in removing contaminants in the diesel range with different functional groups: xylene, naphthalene and hexadecane. The studied variable on the effectiveness of the extraction was solid to liquid ratio S/L, with the values of 1: 1, 1: 2, 1: 3, 1: 4, 1: 8 (g/ml). By decreasing the ratio from 1: 1 to 1: 2, the removal efficiency of xylene, naphthalene, and hexadecane increased from 66.83% to 86.24%, 67.94% to 86.33%, and 68.78% to 87.33%, respectively. Therefore, in 10 min, 85% of removal efficiency was attained. Decreasing the ratio to 1:8 increased the extraction by just 8% on average.

Khodadoust et.al. (1999) used water-ethanol mixtures as the solvents for extraction of pentachlorophenol (PCP) from contaminated soils. The reasons for choosing ethanol were the high solubility of PCP in ET, its complete miscibility

with water, and its low cost. The mixture consisting of 50% ET showed the higher efficiency in comparison with 100% water or 100% ET.

The applicability of FAME, which are the major constituents of biodiesel, non-toxic and readily biodegradable, on the mobility and degradation of crude oil within artificial sand columns has been studied by Gong et.al (2005/b). The S-FAME (synthesized in the lab) demonstrated its ability in polycyclic aromatic hydrocarbons (PAH) removal from the soil as compared to other eluting agents, cyclodextrin, hydroxypropyl-b-cyclodextrin, and the synthetic surfactants, Triton X-100 and Tween 80. As an organic phase, FAME had the ability to bind PAH, which were dissolved into the FAME, resulting in a positive PAH removal process from contaminated soils.

Pannu et al. (2004) reported using vegetable oil in the remediation of PAH contaminated soil. They studied the application of peanut oil for extraction of PAH from soil. The efficiencies of the total PAHs extraction from weathered soil and the spiked soil were 83.7% and 91.4%, respectively.

Using more environmentally benign solvents has recently been the focus of researchers. The United States Environmental Protection Agency (U.S. EPA) has classified both lactic acid and its ethyl and butyl esters as Class4A inert compounds (Subramanian et al., 2010). Lactate esters have been found to be good cleaning agents for the removal of oils, greases, and paints (Subramanian et al., 2010). Lactic acid in soil has been found to enhance biodegradation of highly toxic compounds like toxaphene (Subramanian et al., 2010). Lactic acid used in mixed solvent systems of lactic acid–water was effective for the

extraction of PCP from montmorillonite and natural sediment (Subramanian et al., 2010).

EL (ethyl 2-hydroxypropionate) which is a clear and colourless liquid of low volatility and complete miscibility with water and most organic solvents is another studied green solvent (Lee et al., 2006). Extraction of toluene and perchloroethylene (PCE) as representative aromatic and chlorinated hydrocarbons were selected by Lee et al. (2006) to examine the applicability of EL for the solvent extraction process. Solubility of toluene and PCE was measured with increasing EL volume from 0 to 80% in laboratory batch and column studies. PCE and toluene solubility increased exponentially with increasing volume fraction of EL. EL was reported as the strongest cosolvent among methanol, ethanol, tertiary butyl alcohol and acetone. 50% of EL could result in a PCE solubility of up to 40000 mg/l, which was nearly a 200-fold increase over its solubility in water.

2.3.2 Ethyl lactate

Ethyl lactate is formed from ethanol and lactic acid. Ethyl lactate, with other names of Lactic acid ethyl ester; 2-Hydroxypropanoic acid ethyl ester, actylol, and acytol, is considered as a green solvent and is not named in Environmental Protection Agency's (EPA) Toxic Release Inventory (TRI) or listed in the Hazardous Air Pollutant (HAP) section (Jones et al., 2003, wikipedia). EL is 100% biodegradable and easy to recycle, without causing any health issues, so it is recently considered as a proper alternative for the conventional solvents, such as chlorinated hydrocarbons, especially because it can be obtained from renewable sources (Aparicio et al., 2008; Aparicio et al., 2009/a; Pighin et al., 2016). The solvency properties of EL is mentioned in Table 2-3.

Table 2-3: Solvating properties of ethyl lactate

Solvating properties	EL
Kauri Butanol(KB) Value	>1000
Solubility Parameters	
Hildebrand	21.3
Hansen	
Disperse	7.8
Polar	3.7
Hydrogen	6.1
Solubility	Miscible in Water and Hydrocarbons

EL formula is illustrated in Figure 2-2.

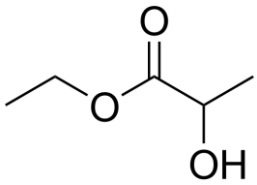

Figure 2-2: Illustration of EL formula

Guo et al., (2010) shows that EL can enhance the removal efficiency of copper from contaminated soil. It is also reported by Yap et al. (2012/a) that EL is able to increase the efficiency of Fenton reaction, because of its high cosolvency power. The hydroxyl and carbonyl groups make it possible to develop intermolecular hydrogen bonding, and EL is also able to disrupt the water-dominated network and it leads to decreasing the polarity of the fluid, these two reasons can explain why EL has high efficiency in remediation (Yap et al. 2012/a).

2.4 Sorption/Desorption

When two phases are in contact with each other and the concentration of one compound changes in those phases due to the accumulation or release from the interface, the process is named sorption (Dąbrowski, 2001). Sorption on the

surface is a general term that is applied for defining the adsorption and precipitation because of different forces. Through sorption, the solutes distribute between two phases or at interfaces that can affect the availability and the fate of contaminants (Huang et al., 2003). Many different types of physical, chemical and biological processes occur at the interface of two involved phases in a sorption process (Dąbrowski, 2001).

The whole sorption process can be divided into three general parts: external mass transfer, reaction on the interface, and internal mass transfer. External related resistances (external transport) means any resistance types that are out of the interfacial boundary between two phases. The external resistances involve transport from the mass bulk resistance and boundary layer (liquid film) near to the interface (Kannan et al., 2003; Mohan et al., 2004), the interface of the continuous liquid and a substrate, including the solid and non-continuous liquid. Phenomena such as poor mixing, high concentration, small particle size and high affinity of adsorbate for adsorbent (Mohan et al., 2004) lead to high external resistance. After reaching to the interface, the solutes through different ways pass this barrier to reach the internal parts of solid. Intraparticle diffusion, the next step, is that process is attributed to the substrate related diffusion in direction of net mass transfer after interface (Bogan et al., 2003; Birdwell et al., 2007; Qiu et al., 2009). For desorption, the same processes would happen in the reverse order. However, due to processes such as chemisorption and diffusion in internal pores, in most cases the rate of sorption and desorption is not equal.

2.4.1 SOM and its role in sorption/desorption

SOM could be classified into two major fractions, humic substances (HS) and non-humic substances (Sparks, 2003). Non-humic substances are not recalcitrant to biological attacks so they have a short lifetime in comparison with the other parts (Sparks, 2003). One of the main differences between these two groups is that non-humic substances have some specific characteristics to be defined, but humic substances cannot be recognized by distinct features (Sparks, 2003). The different fractions of NOM (natural organic matter), which is typically reported as total organic matter (TOM), are depicted in Figure 2-3 (Pagano et al., 2014).

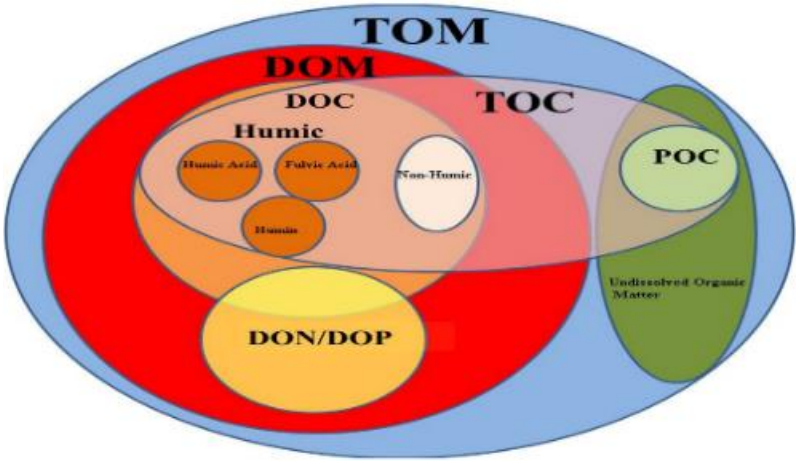

Figure 2-3. Total Organic Matter (TOM), Total Organic Carbon (TOC), Dissolved Organic Matter (DOM), Dissolved Organic Carbon (DOC), Particulate Organic Carbon (POC), Dissolved Organic Nitrogen (DON), and Dissolved Organic Phosphorus (DOP) are represented. (Pagano et al., 2014)

Humic substance (HS) is the main components of SOM. Three attributed fractions to this component, i.e. humic acid (HA), fulvic acid (FA), and humin, are differentiated based on their solubility behaviour in acidic and basic solutions. FA is soluble in both acidic and basic solutions while humin is insoluble in these solutions; meanwhile, HA after dissolution in basic acid is

insoluble in acidic solution (Song et al., 2002; Xiao et al., 2004; Huang et al., 2012). The percentages of main elements in HA and FA are listed in Table 2-4.

Table 2-4: Average elemental composition of SOM, HA, and FA in soil (Sparks, 2003)

	SOM (%)	*HA (%)*	*FA (%)*
Carbon	52-58	53.8-58.7	40.7-50.6
Hydrogen	3.3-4.8	3.2-6.2	3.8-7.0
Oxygen	34-39	32.8-38.3	39.7-49.8
Nitrogen	3.7-4.1	0.8-4.3	0.9-3.3
Sulfur	-	0.1-1.5	0.1-3.6
O/C	-	0.5	0.7

There are different ways to evaluate the effects of SOM on sorption/desorption and oxidation processes. In some studies, the role of SOM is analysed based on the actions that each fraction, such as HA, FA and humin, plays (Song et al., 2002; Xiao et al., 2004; Huang et al., 2008; Huang et al., 2012, Wang et al., 2016). In some others, SOM is studied based on its particulate and non-particulate features, as an influential variable on the transport and reactivity of hydrophobic organic carbons (HOC) (Sedlak et al., 1993; Diock et al., 2005).

Although some specific properties for each fraction have been reported, their characteristics may change over the time. For example, Gunasekara et al. (2003) reported that young SOM is made mostly from aliphatic carbons; old SOM has more aromatic fractions. Based on these observations, they have made the conclusion that both the aromatic and aliphatic fractions can participate in non-linear sorption that will be discussed later.

Among different parts of soils, clays, oxides and SOM are the constituents of the soil that are known as the main (de)sorption controlling parts. It is reported that organic matter and clay are the primary fractions that affect the (de)sorption of carbofuran (Heath et al., 1993). SOM is known as the part with the main role in adsorption with a high affinity to many non-polar compounds. Clay minerals after organic matters have the most adsorption ability thus they play a prominent role in adsorption/desorption in soils with low amount of organic matters 0.1-0.5% (Heath et al., 1993; Bermudez-couso et al., 2012).

Different findings that may seem contradictory relating to the effect of SOM on solubility and mobility have been reported. In some studies, SOM is considered as the adsorbent for the HOC, and hence, it decreases the desorption efficiency. In contrast, as they compete with HOC for the adsorption sites, they can increase the desorption efficiency. Their ability to form micelles like biosurfactants is also reported as a means of increasing the desorption efficiency (Sui et al., 2014).

SOM is among the most effective soil parts on adsorption/desorption processes. Other factors, such as mineral parts of the natural sorbents within the sediment matrix could have significant effects on sorption. However, He et al. (2006) have mentioned the higher effect of SOM in the adsorption of hydrophobic organic contaminants than the effect of mineral fractions, except in the absence of water. They related that the clay or SOM ability for the sorption depended on the type of organic contaminants. For instance, K-clay is a better adsorbent for carbaryl and dichlobenil while biphenyl could be better adsorbed to SOM than

clay particles. Atrazine, on the other hand, has the same affinity towards clay and SOM.

2.4.2 Sorption equilibrium isotherms

Adsorption isotherm models, which is an essential part of the adsorption science, relate the equilibrium concentration or pressure of a given component in the bulk phase and in the adsorbed phase at constant temperature (Quinones et al., 1998; Dąbrowski et al., 2001). The isotherm equation for an adsorbent-adsorbate system is a function of the adsorbate, adsorbent and solution properties (Parker, 1995). An isotherm equation is predictive in designing the process and defining the thermodynamic characteristic of the process (Alen et al., 2004). Table 2-5 summarises the isotherm models for single component adsorption.

The sorption processes are generally divided into two main groups of physical sorption and chemical sorption or chemisorption. Physical sorption is related to the weak Van der Waals' attraction forces at all time, and is reversible; in some cases, such as zeolites, electrostatic interactions are also included (Ruthven, 1984). The process which is totally called as partitioning is actually due to the physical forces. Chemisorption involves chemical forces bound between the adsorbent and adsorbate, which is irreversible, and can exist with electron transferring (Ruthven, 1984; Abdolali et al., 2014).

A simple assumption of linear partitioning between the solid and liquid phases is used widely, and it is reported as Eq.2-1.

$$K_d = \frac{q_e}{C_e} \qquad \text{Eq.(2-1)}$$

where K_d denotes the constant partition coefficient [$M^{-1}L^3$], C_e defines the aqueous-phase equilibrium solute concentrations [ML^{-3}], and q_e is the solid-phase equilibrium solute concentrations [MM^{-1}]. The assumption of this equation is that molecules are isolated from their neighbours, and adsorption takes place on a uniform surface (Ruthven, 1984). It is the limit of many non-linear isotherm models. However, it cannot explain all systems.

Other isotherms have been proposed to explain systems with deviation from linear assumption (Miller et al., 1986). Langmuir was the first one who proposed an equation for the "monomolecular adsorption on energetically homogeneous surfaces" and the constants in Langmuir isotherm model has physical meaning against constants in the Freundlich isotherm model (Dąbrowski, 2001). As is stated in Table 2-5, one of the assumptions of Langmuir isotherm is that the adsorbed molecules are not under the effects of their neighbours. This assumption cannot be true under all situations, and some other proposed isotherms had been used to correct this assumption (Quinones, 1996/b).

2.4.3 Sorption/desorption kinetics

Through adsorption kinetics, the changes in concentration within the adsorbed and dissolved phases are expressed versus time. The models that have been applied to describe the process of adsorption/desorption processes could be divided into two general categories: those that consider all involved processes as a whole process, and those that investigate the real underlying physical processes.

In the whole process group, the adsorption/desorption rate, which is usually expressed as $\frac{dq_t}{dt}$, is achieved through empirical equation, and is usually defined

as a function of the concentration of adsorption/desorption capacity. (Pseudo) first-order mass transfer kinetic, which consists of one, two and three compartment models, (pseudo) second-order mass transfer kinetic, and Elovich's equation (Qiu et al., 2009) are classified under this group. This group is also named as the adsorption reaction models or empirical sorption kinetics, which do not give definite mechanisms (Qiu et al., 2009; Wu et al. 2001) and are reported in Table 2-6. Once the adsorption equations are written based on the adsorption capacity instead of solution concentration, the equation would be called pseudo of that type of equation (Qiu et al., 2009).

The second group will focus on each step. The transfer of solute in a mobile-immobile systems involves different mechanisms that can be defined as different resistances that are mentioned earlier. The first one is the resistance from the bulk of mobile phase to the boundary layer around the sorbent; the movement of the solute in the bulk is based on the advective-dispersive transportation (Brusseau et al., 1990). After that, the diffusion in the boundary layer which is completed by the diffusion into the pores or surfaces which is otherwise known as "intra-aggregate diffusion", with the assumption that the sorption on the interface is instantaneous and the local equilibrium is assumed for the most systems (Brusseau et al., 1990).

The first process, bulk diffusion, is mostly considered as a rapid process that cannot be considered as a controlling factor. The major resistance is contributed to the remaining steps, film diffusion, sorption and intraparticle diffusion, which is the major goal of the second adsorption rate category. The processes that are mostly described by this group are diffusion related processes, the relatively

immobile liquid film diffusion (surface diffusion) and intraparticle diffusion that includes pore diffusion, (McKay et al., 1983), and solid phase diffusion (Haddadi et al.,2009). Depending on the process conditions, one of them can be the dominant process over the other. For example, in an agitation involved process, the film diffusion can be neglected while in a column study with low flow rate, it can have more significant effects (McKay et al., 1983).

Table 2-5: Sorption isotherms of single component systems, C_e:Aqueous-phase equilibrium solute concentrations [ML^{-3}], q_e: Solid-phase equilibrium solute concentrations, [MM^{-1}]

Name		Equation	Parameters and variables	Remarks/Explanations/Assumptions
Langmuir and Langmuir-modified isotherms	**Langmuir isotherm model (Ruthven, 1984)**	$q_e = \frac{K_L q_m C_e}{1 + K_L C_e}$ Linear forms: $\frac{C_e}{q_e} = \frac{1}{K_L q_m} + \frac{C_e}{q_m}$ $\frac{1}{q_e} = \frac{1}{q_m} + \frac{1}{K_L q_m}\frac{1}{C_e}$	q_m: Theoretical isotherm saturation capacity $[MM^{-1}]$ K_L: Langmuir adsorption constant related to the energy of adsorption $[M^{-1}L^3]$ T: Temperature [K] σ: Isotherm constants related to the degree of sorption ν, η: Exponents	• The simplest theoretical model for monolayer adsorption, the adsorbed layer on the adsorbent is one molecule thickness (Ruthven, 1984; Batzias et al., 2007; Foo et al., 2010) • All sites are energetically equivalent (Ruthven, 1984) • The molecules are not under the attraction of their neighbour molecules, it means no lateral interaction and steric hindrance, which lead to the constant enthalpy and sorption activation (Foo et al., 2010; Ruthven, 1984) • A general form of isotherm that start from the linear state for the C=0-0.3C_L , pass through the Freundlich isotherm (Weis 1966/a)
	Modified Langmuir – 1 isotherm model (Subramanyam et al., 2012)	$q_e = \frac{K_L T^{-n} C_e}{1 + K_L C_e}$		-
	Modified Langmuir – 2 isotherm model (Subramanyam et al., 2012)	$q_e = \frac{K_L C_e}{1+K_L C_e}\left(\frac{1+\sigma^2(1-K_L C_e}{2(1+K_L C_e)^2}\right)$		-
	Holl – Kirch , modified forms of Langmuir (Khan et al., 1997/b)	$q_e = \frac{q_m K_L C_e^{\nu}}{1 + a C_e^{\nu}}$		-
	Radke and Prausnitz modified forms of Langmuir (Khan et al., 1997/b)	$q_e = \frac{q_m K_L C_e}{1 + K_L C_e^{b}}$		-

Continued Table 2-5: Sorption isotherms of single component systems, C_e:Aqueous-phase equilibrium solute concentrations [ML^{-3}], q_e: Solid-phase equilibrium solute concentrations, [MM^{-1}]

	Marczewski and Jaroniec Isotherm (Generalized-Langmuir equation) (Parker et al., 1995)	$q_e = q_m \left(\frac{(K_L C_e)^\eta}{1 + (K_L C_e)^\eta} \right)^{\nu/\eta}$		• Reduces to the Langmuir isotherm for $\nu = \eta = 1$ • Reduces to Holl-Kirch isotherm for $\nu = \eta$ • Reduces to the Toth isotherm for $\nu = 1$
	Toth model	$q_e = \frac{q_{mT} C_e}{(b + C_e^D)^{1/D}}$	q_{mT}: Toth maximum adsorption capacity [MM^{-1}] *b*: Constant of the Toth isotherm, an adjustable parameter, equilibrium constant [ML^{-3}]	• A Langmuir-based isotherm, reduces to the Langmuir equation for D=1 • With the assumption of a continuous distribution of site affinities • Appropriate mostly for multilayer adsorption (Subramanyam, 2012) • "Possesses the correct Henry's law behavior" (Pikaar et al., 2006)
Freundlich isotherm model		$q_e = K_f {C_e}^n$	K_{Fr}: Freundlich capacity parameter $[MM^{-1}(ML^{-3})^{-1/n}]$ $\acute{n}$: Site energy heterogeneity factor or linearity factor [-] n: Freundlich exponent [-]	• For heterogeneous adsorbent sites (Gong et al., 2007) • Multilayer adsorption with non-uniform distribution of adsorption heat and affinities over the heterogeneous surface (Batzias et al., 2007; Shahbeig et al., 2013) • Describing non-ideal and reversible adsorption • "An infinite series of discrete Langmuir isotherms" (Pikaar et al., 2006)
Modified Freundlich isotherm (Khan et al., 1997/b)		$q_e = K_{Fr} C_e^n = K_{Fr} C_e^{n_1 + n_2 ln C_e}$	K_{Fr}: Freundlich capacity parameter n, n_1, and n_2: Model constants	• A second-order polynomial function is used for the Freundlich isotherm equation to compensate for the curvature on the logarithmic plot

Continued Table 2-5: Sorption isotherms of single component systems, C_e:Aqueous-phase equilibrium solute concentrations [ML^{-3}], q_e: Solid-phase equilibrium solute concentrations, [MM^{-1}]

Dubinin- Radushkevich (DR) isotherm model	$q_e = q_s e^{(-k_{ad}\varepsilon^2)}$ $\varepsilon = RTln\left[1+\frac{1}{C_e}\right]$ $E = \frac{1}{\sqrt{2B_D}}$	q_s: Theoretical isotherm saturation capacity [MM^{-1}] E: Energy of adsorption (kJ/mol) k_{ad}: Dubinin–Radushkevich isotherm constant (mol2/kJ2) ε: Dubinin–Radushkevich isotherm constant	• For the adsorption of trace constituents before saturation • Used to estimate the characteristic porosity and the apparent free energy of adsorption. If E is 8 -16 kJ/mol, the ion exchange can describe the adsorption type (Gunay et al., 2007; Subramanyam et al., 2012) • An empirical model (Foo et al., 2010) • Does not predict the Henry's law at low pressure (Foo et al., 2010)
Temkin model	$\theta = \frac{q_e}{q_s} = \frac{RT}{\Delta Q}\ln K_0 C_e$ $\Delta Q = -\Delta H$	R: universal gas constant (kJ mol−1K−1), T: Temperature [K] θ: Fractional coverage ΔQ: Variation of adsorption energy (kJ mol^{-1}) K_0: Temkin equilibrium constant [$M^{-1}L^3$] q_s: Theoretical isotherm saturation capacity [MM^{-1}]	• Considered the effect of adsorbent–adsorbate interactions (Foo et al., 2010; Subramanyam et al., 2012) • Characterized by a uniform distribution of binding energies. A good predictor of the gas phase equilibrium, but not suggested for liquid-phase adsorption isotherms
Redlich-Peterson (R-P) model	$q_e = \frac{K_R C_e}{1+a_R C_e^{\beta}}$ Linear forms: $\ln\left(K_R\frac{C_e}{q_e}-1\right) = lna_R + \beta\ln C_e$ $\frac{C_e}{q_e} = \frac{1}{K_R} + \left(\frac{a_R}{K_R}\right)C_e^{\beta}$	K_R: R-P isotherm constant (L/g) a_R: R-P isotherm constant (1/mg) β: the exponent which lies between 1 and 0	• Defines both Langmuir and Freundlich Isotherms. Can be applied in homogeneous and heterogeneous sites (Shahbeig et al., 2013; Gunay et al., 2007) • Having three parameters into an empirical isotherm • Approaches the Freundlich model at high concentration (Gunay et al., 2007) • When β= 1, it is the Langmuir isotherm equation (Wu et al., 2010)

Continued Table 2-5: Sorption isotherms of single component systems, C_e:Aqueous-phase equilibrium solute concentrations [ML^{-3}], q_e: Solid-phase equilibrium solute concentrations, [MM^{-1}]

Sips isotherm model, also known as Langmuir–Freundlich isotherm model	$q_e = \frac{q_m a_s C_e^m}{1 + a_s C_e^m}$	qm: monolayer adsorption capacity, the total number of binding sites [MM^{-1}] as: Sips constant related to energy of adsorption, related to the median binding affinity (K_0) via $K_0 = a^{1/m}$ [ML^{-3}]−1/n m: Sips isotherm model exponent, heterogeneity index, varies from 0 to 1	• A combination of the Langmuir and Freundlich isotherm models (Gunay et al., 2007), can model both homogeneous and heterogeneous sites (Umpleby et al., 2001). • Reduces for all systems to the Freundlich isotherm at the low concentrations (Umpleby et al., 2001) • The coefficients have physical meaning. For a homogeneous material, m=1. When m<1, the surface is heterogeneous (Umpleby et al., 2001) • Does not require a measure of the total number of binding sites (Umpleby et al., 2001)
Khan et al. (Khan et al., 1997/a; Khan et al., 2000)	$q_e = \frac{q_m K_L C_e}{(1 + K_L C_e)^b}$	K_L and b: Model constants q_m: Amount of q at full surface coverage	• Reduces to the Langmuir isotherm for $b = 1$ • Reduces to the Freundlich isotherm for high values of C_e
Koble–Corrigan isotherm model (Kumar et al., 2010)	$q_e = \frac{a C_e^n}{1 + b C_e^n}$	a, b and n: Model constants	• Combination of the Langmuir and Freundlich isotherm
Fritz–Schluender isotherm model (Kumar et al., 2006)	$q_e = \frac{q_m K_{FS} C_e}{1 + q_m C_e^m}$	q_m: Fritz–Schlunder maximum adsorption capacity [MM^{-1}] K_{FS}: Fritz–Schlunder equilibrium constant [L^3M^{-1}] m: Fritz–Schlunder model exponent	-
Fritz-Schluender isotherm model (Maurya et al., 2006)	$q_e = \frac{A_{FS} C_e^{\alpha_{FS}}}{1 + B_{FS} C_e^{\beta_{FS}}}$	A_{FS} and B_{FS}: Fritz–Schlunder equation parameters α_{FS} and β_{FS}: Fritz–Schlunder equation exponents	• Combination of the Langmuir and Freundlich isotherm, four parameters

Continued Table 2-5: Sorption isotherms of single component systems, C_e:Aqueous-phase equilibrium solute concentrations [ML^{-3}], q_e: Solid-phase equilibrium solute concentrations, [MM^{-1}]

Fritz-Schluender isotherm model (Maurya et al., 2006)	$q_e = \frac{K_1 q_{mFS} C_e^{m_1}}{1 + K_2 C_e^{m_2}}$	q_{mFS}: Fritz–Schlunder maximum adsorption capacity [MM^{-1}] K_1, K_2, m_1, and m_2 are the Fritz–Schlunder parameters	• Improvement over Langmuir and Freundlich empirical, five parameters
Flory–Huggins isotherm model (Vijayaraghavan el al., 2006)	$log\frac{\theta}{C_0} = \log K_{FH} + n_{FH}\log(1-\theta)$ $\Delta G^0 = -RTln(K_{FH})$	$\theta = 1 - \frac{C_e}{C_0}$: degree of surface coverage K_{FH}: Flory–Huggins model equilibrium constant n_{FH}: Flory–Huggins model exponent	-
Radke–Prausnitz isotherm models (Vijayaraghavan et al., 2006; Chern et al., 2001)	$q_e = \frac{a_R r_R C_e^{\beta_R}}{a_R + r_R C_e^{\beta_R - 1}}$	a_R and r_R:Radke–Prausnitz model constants β_R: Radke–Prausnitz model exponent	-
	$q_e = \frac{KNC}{(1+KC)^m}$	K, N, and m: Model constants	
UNILAN isotherm model (Quinones et al., 1996/a; Chern et al., 2001)	$q_e = \frac{N}{2s}\ln\left(\frac{1 + KC_e e^{s}}{1 + KC_e e^{-s}}\right)$ $\frac{q_e}{q_s} = \frac{1}{2\vartheta}\ln\left(\frac{C + C_e e^{\vartheta}}{C + C_e e^{-\vartheta}}\right)$	C: An adjustable parameter, which, in principle should be equal to 1 /K, where K is the low-pressure equilibrium constant or Henry constant ϑ: heterogeneity parameter, is also a parameter of the adsorption energy distribution	• Based on the assumption of a uniform distribution of the adsorption energies and a local Langmuir isotherm • ϑ can get negative values • Reduces to the Langmuir equation for values of ϑ=0, the homogeneous site
Weber and van Vliet isotherm model (Maurya et al., 2006/b; Van Vliet et al., 1980)	$C_e = a_1 q_e^{(a_2 q_e^{a_3} + a_4)}$	C_e: equilibrium solution concentration, [ML^{-3}] q_e: corresponding adsorption capacity, [MM^{-1}] $a_i (i = 1-4)$: coefficients determined by a multiple non-linear curve-fitting technique predicated on the minimization of the sum of squares of residuals	• Empirical

Continued Table 2-5: Sorption isotherms of single component systems, C_e:Aqueous-phase equilibrium solute concentrations [ML^{-3}], q_e: Solid-phase equilibrium solute concentrations, [MM^{-1}]

Jovanovic isotherm model (Quinones et al., 1996/a; Hossain et al., 2012)	$q_e = q_m(1 - e^{-K_J C_e})$	q_m, K_J: Model constants	• Monolayer adsorption, without lateral interactions on an homogeneous sites (Hossain et al., 2012; Quinones et al., 1996/a) • Considers the mechanical contacts between the adsorbing and desorbing molecules (Shahbeig et al., 2013),
Jovanovic–Freundlich isotherm model (Quinones et al., 1998)	$\frac{q_e}{q_s} = 1 - e^{-(aC)^{\vartheta}}$	ϑ: Heterogeneity parameter (with $0 < \vartheta \leq 1$) a: A constant, which characterizes the magnitude of the adsorbate–adsorbent interaction energy	• Semiempirical model for single component adsorption • a: Function of the temperature
Jossens model (Khan, 1997/b)	$C_e = \frac{q_e}{H} e^{(F q_e^p)}$	H, F, and p: The parameters of the equation of Jossens	• Described by distribution of energy • Reduces to Henry's law at low capacities • H and F depend only on temperature
Brouers–Sotolongo model (Altenor et al., 2009)	$q_e = q_{max}\left[1 - e^{-K_w C_e^{\alpha}}\right]$ $K_w = \frac{K_F}{q_{max}}$	q_{max}: Saturation value K_F: Freundlich constant, for a given temperature α: Exponent, a measure of the width of the sorption energy distribution	• q_{max}, K_w and α determined by a non-linear curve fitting procedure
Flory–Huggins model	$\frac{\theta}{C_0} = K_{FH}(1 - \theta)^{n_{FH}}$, $\theta = 1 - \frac{C_e}{C_0}$	K_{FH}: Flory–Huggins model equilibrium constant n_{FH}:Flory–Huggins model exponent	-
Hill model (Foo et al., 2010; Shahbeig et al., 2013)	$q_e = \frac{q_m C_e^n}{K_D + C_e^n}$	n: Hill cooperativity coefficient of the binding interaction q_m: Hill isotherm maximum uptake saturation [ML^{-3}] K_D: Hill constant	-

Continued Table 2-5: Sorption isotherms of single component systems, C_e:Aqueous-phase equilibrium solute concentrations [ML^{-3}], q_e: Solid-phase equilibrium solute concentrations, [MM^{-1}]

Polanyi-Dubinin-Manes (PDM) model (Kleineidam et al., 2002)	$q_e = V_0\rho_0 e^{\left[\frac{-RT(-ln\frac{C_e}{S})}{E}\right]^b}$ $E = E_0\beta$	*Vo*: Maximum volume of sorbed chemical per unit mass of sorbent [L^3M^{-1}] ρ_0: the compounds density [M L^{-3}], *R*, the ideal gas constant [$ML^2T^{-2}K^{-1}mol^{-1}$] T : the temperature [K] $\frac{C_e}{S}$: The equilibrium concentration in liquid normalized to the compounds solubility *S* [ML^{-3}], [$-$] *E*: The characteristic free energy of adsorption of a compound compared to that of a reference compound (*E0*) in a specific adsorbent [KJmol-1]	• Extended the Dubinin-Astakhov equation by Manes and co-workers to aqueous systems by defining the Polanyi adsorption potential $\epsilon_{SW} = RTln\left(S/C_W\right)$ [J mol-1]
The Brunauer-Emmett-Teller BET isotherm model (Aksu 2005; Khan et al., 1997/b;Parker et al., 1995)	$q_e = \frac{BQ^0C_e}{(C_s-C_e)\left[1+(B-1)\left(C_e/C_s\right)\right]}$	C_s: The saturation concentration of the adsorbed component B: A constant indicating the energy of interaction between the solute and the adsorbent surface Q^0: A constant indicating the amount of solute adsorbed forming a complete monolayer	• A special form of Langmuir isotherm which can account for multilayer adsorption onto a homogeneous surface • All the assumptions relating to the Langmuir isotherm • Considered as a representative of a generalisation of the Langmuir isotherm (Dąbrowski et al., 2001) • The first universal theory of physical adsorption (Dąbrowski et al., 2001) • Describe the whole processes of isotherm, monomolecular adsorption, polymolecular adsorption and capillary condensation, the last one is not satisfactory always (Dąbrowski et al., 2001)
Myers isotherm model (Parker et al., 1995)	$C = \frac{q}{K}e^{\alpha q^\eta}$	η: Exponent α: Heterogeneity or shape of isotherm parameters K: Strength of adsorption parameter q: Adsorption capacity (mg g-~)	• Gives the concentration as a function of capacity • Reduces to Henry's law at low concentration

Continued Table 2-5: Sorption isotherms of single component systems, C_e:Aqueous-phase equilibrium solute concentrations [ML^{-3}], q_e: Solid-phase equilibrium solute concentrations, [MM^{-1}]

Fowler isotherm model (Quinones et al., 1996/b)	$C_e = \frac{\theta}{K(1-\theta)} e^{-z\epsilon\theta/RT}$ $\theta = \frac{q_e}{q_m}$	K: Low-concentration equilibrium constant, the interaction energy between two molecules adsorbed on two nearest-neighbour sites z: Number of nearest-neighbour sites R: Universal gas constant T: Absolute temperature q_m: Monolayer capacity for the corresponding component	• The adsorbed molecules make a monolayer surface that are energetically homogeneous • The randomly interaction of adsorbed molecules with neighbour sites • $-z\epsilon\theta/RT$ is the average force field from the molecules in neighbour sites
Vacancy solution theory (VST) (Khan et al., 2000)	$C_e = \left[\frac{1}{b_0}\frac{\theta}{1-\theta}\right]\left[\Lambda_{12}\frac{1-(1-\Lambda_{21})\theta}{\Lambda_{12}+(1-\Lambda_{12})\theta}\right]$ $\exp\left[\frac{-\Lambda_{21}(1-\Lambda_{21})\theta}{1-(1-\Lambda_{12})\theta} - \frac{(1-\Lambda_{12})\theta}{\Lambda_{12}+(1-\Lambda_{12})\theta}\right]$, $\theta = \frac{q_e}{q_m}$	Λ_{12} and Λ_{21}: Wilson parameters b_0, q_m, Λ_{12} and Λ_{21}: Determined from non-linear regression of experimental data on C_e versus q_e	• Reduces to Langmuir isotherm for Λ_{12} and Λ_{21}=1 • Presented by Suwanayuen and Danner based on Wilson activity coefficient model for the non-ideality from Langmuir isotherm • Originally developed for gas adsorption isotherms
Unilin isotherm model (Khan et al., 2000)	$\frac{q}{q_2} = \frac{1}{2b_2}\ln\frac{a_2 + C\exp(b_2)}{a_2 + C\exp(-b_2)}$	$q2$, $a2$ and $b2$: Model constants	-
Frumkin isotherm model (Basar et al., 2006)	$\frac{\theta}{1-\theta}e^{-2a\theta} = kC_e$, $lnk = \frac{-\Delta G}{RT}$ $\theta = \frac{q_e}{q_m}$	θ: Fractional occupation q_m: Theoretical mono-layer saturation capacity (mg/g), (determined by D–R isotherm equation), and k: Related to adsorption equilibrium	• Considers the interaction between the adsorbed species

Table 2-6: The whole process kinetic models

Name of model		*Equation of model*		*Explanation/ Assumption/Remarks*
First-order mass transfer kinetic model, Noyes-Whitney equation (Dokoumetzidis, 2005)	*One compartment kinetic*	$\frac{dq_t}{dt} = k_{p1}(q_e - q_t)$ $q_t\ (0,0)=0$	$\frac{q(t)}{q(\infty)} = exp^{(-k_{p1}t)}$	-
	Two-compartment kinetic		$\frac{q(t)}{q(\infty)} = F_{rap}e^{-k_{rap}t} + F_{slow}e^{-k_{slow}t}$ $F_{rap} + F_{slow} = 1$	-
	Three-compartments		$\frac{q(t)}{q(\infty)} = F_{rap}e^{-k_{rap}t} + F_{slow}e^{-k_{slow}t} + F_{very\ slow}e^{-k_{very\ slow}t}$ $F_{rap} + F_{slow} + F_{very\ slow} = 1$	-
Second-Order Rate Equation or Hyperbolic	*Pseudo-second-order rate equation* (Ho, 2006)	$\frac{dq_t}{dt} = k_{p2}(q_e - q_t)^2$ $q_t\ (0,0)=0$ $\tau^{1/2} = {1}/{k_{p2}q_e}$	$\frac{t}{q_t} = \frac{1}{V_0} + \frac{t}{q_e},\ \ V_0 = k_{p2}{q_e}^2$	➢ The assumption of a pseudo-second order model is that chemical sorption is the rate limiting step (Ho, 2000) ➢ Half-adsorption time, $\tau^{1/2}$, is the time required for the adsorption to take up half of the equilibrium amount adsorbed (Cabal, 2009).
			$\frac{1}{q_t} = \frac{1}{tV_0} + \frac{1}{q_e}$	
			$q_t = q_e - \left(\frac{1}{k_{p2}q_e}\right)\frac{q_t}{t}$	
			$\frac{q_t}{t} = k_{p2}{q_e}^2 - kq_eq_t$	
	Typical second-order rate equation	$\frac{dC_t}{dt} = -k_2C_t^2$, *Ct (0,0)=0*	$\frac{1}{C_t} = k_2t + \frac{1}{C_0}$	-

Continued Table 2-6: The whole process kinetic models

Elovich's equation, semilogarithmic	$\frac{dq_t}{dt} = ae^{-bq}$ q_t *(0,0)=0*	$q = \frac{1}{b}\ln(1+abt) \quad or \quad q = \frac{1}{b}\ln(t+t_0) - \frac{1}{b}\ln t_0$ $q \to 0$ then $\frac{dq}{dt} \to \alpha$, α is the initial leaching rate, $t_0 = \frac{1}{ab}$ If $abt \gg 1 \rightarrow \quad q = \left(\frac{1}{b}\right)\ln(ab) + \left(\frac{1}{b}\right)\ln t$ If $abt\ is\ not \gg 1$, then a value of t_0 is chosen which results in a linear plot of q vs $\ln(t+t_0)$, with slope $\frac{1}{b}$ and intercept determined from $t_0 = \frac{1}{ab}$ (Havling, 1985)	-
Weibull's equation		$q = 1 - \exp\left(-\frac{t^m}{D}\right)$, $\quad \ln(-\ln(1-q)) = -lnD_w + mlnt$	-
Bangham equation	$\frac{dq}{dt} = \frac{q_t}{mt}$	$q_t = K_r t^{1/m}$, $\log q_t = \log K_r + \left(\frac{1}{m}\right)\log t$ K_r: rate constant of adsorption, q_t: amount of metal ions adsorbed at time *t* (mg/g), m: constant in relation to the adsorbent	➢ Bangham usually has a fast adsorption velocity, and it is slow in attaining sorption equilibrium (Yang, 2013)

2.5 Fenton Treatment

2.5.1 Fenton reaction

Among the different remediation processes for destroying the biorefractory organic compounds, advanced oxidation technique (AOT) uses oxidants such as ozone (O_3), hydrogen peroxide (H_2O_2), persulfate ($S_2O_8^{2-}$), and potassium permanganate ($KMnO_4$) (Neyens et al., 2003; Lu et al., 2010/b) to oxidise the contaminants. Each of them based on their properties is applicable in different situations. Sulphate free radical SO_4^{0-}, which is produced as an intermediate through the activation of persulfate, is stable and can diffuse further from the source (Usman et al., 2012). Among these oxidants, the radicals produced through Fenton reaction, hydroxyl, is the most studied oxidant. Fenton reaction is applicable for destruction of contaminants in aqueous waste, soils, and ground water (Neyens et al., 2003; Lu et al., 2010/b).

The definition of conventional Fenton reaction is adding dilute H_2O_2 slowly to a rapidly stirred, degassed iron II-substrate solution (Watts et al., 2005). Eq. (2-2) shows the Fenton reaction in a general way:

$$H_2O_2 + Fe^{2+} \rightarrow OH^0 + OH^- + Fe^{3+} \qquad k = 76\ M^{-1}s^{-1} \qquad Eq.(2-2)$$

The main produced radicals of the Fenton reaction are the hydroxyl radicals, which are produced by electron transfer of Fe^{2+} to H_2O_2, and the hydroxide anion. Hydroxyl radicals are very powerful, effective and non-specific oxidizing agents, second after fluorine in oxidizing power, with an estimated oxidation potential of $+2.8V$ in $pH = 0$ and $+2.0V$ in $pH = 14$ (Watts et al., 2005). As

hydroxyl radical is very reactive, the rate of the Fenton reaction is controlled by its diffusion rate in water, which is $\approx 10^{10}\mathrm{M}^{-1}\mathrm{s}^{-1}$; as a result, it becomes a diffusion-controlled reaction (Goi et al., 2006; Navalon et al., 2010). The radicals also have a very short life span as their reaction rates are faster than their generation rate (Chen et al., 2001; Watts et al., 2005).

Parallel reactions along with the original Fenton reaction can also take place between the reactants, such as those indicated in Eqs. (2-3) to (2-8) (Navalon et al., 2010). These reactions do not generate hydroxyl radicals thus they are considered as a wastage of H_2O_2 (Chen et al., 2001; Navalon et al., 2010).

$$Fe^{3+} + H_2O_2 \leftrightarrow Fe - OOH^{2+} + H^+ \qquad k_2 = 0.001 - 0.01\ M^{-1}s^{-1} \qquad Eq.(2-3)$$

$$Fe - OOH^{2+} \rightarrow HO_2^{\bullet} + Fe^{2+} \qquad Eq.(2-4)$$

$$Fe^{2+} + HO\bullet \rightarrow Fe^{3+} + HO^- \qquad k_3 = 3.2 \times 10^8\ M^{-1}s^{-1} \qquad Eq.(2-5)$$

$$H_2O_2 + HO\bullet \rightarrow H_2O + HO_2^{\bullet} \qquad k_4 = 3.3 \times 10^7\ M^{-1}s^{-1} \qquad Eq.(2-6)$$

$$Fe^{3+} + HO_2^{\bullet} \rightarrow Fe^{2+} + O_2 + H^+ \quad k_5 = 1.2 \times 10^6\ M^{-1}s^{-1}\ (\text{at pH} = 3) \qquad Eq.(2-7)$$

$$Fe^{2+} + HO_2^{\bullet} \rightarrow Fe^{3+} + HO_2^- \quad k_6 = 1.3 \times 10^6\ M^{-1}s^{-1}\ (\text{at pH} = 3) \qquad Eq.(2-8)$$

2.5.2 Possible pathways of hydroxyl radical's reactivity

It is reported that in the presence of sufficient Fenton reactants and continuous reaction, the organic matters can be completely converted to inorganic matters, CO_2, water or inorganic salts for substituted organics (Neyens et al., 2003). This process that is termed as "mineralisation" means that the organic substrate are converted to inorganic species.

Usman et al. (2012) reported the complete mineralisation (and probably vitalisation) of n-alkanes in a Fenton-like process with magnetite as the catalyst, at $\mathrm{pH} = 6.7 \pm 0.3$. This conclusion was based on the observation that no new compounds had been detected by the GC analysis. Through this process, the initial concentration of the soil 4000 mg/kg soil with the sum of 3200 µg/g n-alkanes reduced to 200 µg/g of the n-alkanes.

The main pathways of hydroxyl radicals with organic compounds can be classified as follows:

Electrophilic reaction: One possible reaction of hydroxyl radicals with organic matters is by reacting as an electrophile agent (Watts et al., 2005). The deficit of electron in the valence orbitals of the hydroxyl radical makes it an electrophile agent. In one possible route, it abstracts one electron from organic substrate, like hydrocarbons, or other species to form hydroxide anions, Eq. (2-9) (Chen et al., 2001; Watts et al., 2005).

$$\mathrm{OH^{o}} + \mathrm{S} \rightarrow \mathrm{HO^{-}} + \mathrm{S^{0+}} \qquad \text{Eq. } (2-9)$$

Another possible way is electrophilic substitution in which hydroxyl radicals attack multiple bonds, the π clouds of aromatic compounds, alkenes and other unsaturated organic compounds, and this represents the most common reaction of hydroxyl radicals (Chen et al., 2001; Watts et al., 2005; Navalon et al., 2010).

Hydrogen abstraction: For abstraction of one hydrogen atom by hydroxyl radicals, the bond energy of $\mathrm{O-H}$ should be more than the energy of the bond that hydroxyl radicals attacks, that are mostly $\mathrm{C-H}$. As the bond energy of $\mathrm{O-H}$ (109 $\mathrm{kcal.mol^{-1}}$) is higher than most of $\mathrm{C-H}$ bond energies, it is expected that hydroxyl radicals can overcome the required bond energy in most organic

compounds. The expected form of the reaction will be as shown in Eq. (2-10) (Neyens et al., 2003). Therefore, hydroxyl radicals by hydrogen abstraction from organics (RH) can oxidise them, and produce highly reactive organic radicals R^o that will be oxidised further (Chen et al., 2001; Neyens et al., 2003; Navalon et al., 2010).

$$RH + OH^o \rightarrow H_2O + R^o \rightarrow \text{furthur oxidation} \qquad \text{Eq. } (2-10)$$

Hydroxyl radicals usually react with saturated compounds such as alkanes in this way. The products of this reaction will be alkyl radicals and water (Watts et al., 2005; Chen et al., 2001). The generated alkyl, through the further oxidation processes, can give one electron to hydrogen peroxide and produces hydroxyl radical (Chen et al., 2001; Watts et al., 2005).

Other possible reactions are also proposed as follows (Chen et al., 2001):

$$2R^o \rightarrow \text{product(dimer)} \qquad \text{Eq. } (2-11)$$

$$R^o + Fe^{3+} \rightarrow Fe^{2+} + product \qquad \text{Eq. } (2-12)$$

$$R^o + Fe^{2+} \rightarrow Fe^{3+} + product \qquad \text{Eq. } (2-13)$$

Oxygen addition: The other defined way of reaction between hydroxyl radical and an unsaturated organic compound is the reaction to form a free radical that eventually transforms into an organic product, Eq. (2-14) (Chen et al., 2001; Xu et al., 2006):

$$RH + OH^0 \rightarrow ROH + H^+ \qquad \text{Eq. } (2-14)$$

2.5.3 Fenton-like System

To enhance radical formation, in the so-called modified Fenton system or Fenton-like reactions, researchers have used the addition of chemicals, such as chelating agents, changing the conventional Fenton reaction by applying peroxide in higher concentration, using iron sources other than Fe^{2+} like natural iron oxides such as goethite (Bandala et al., 2008; Ferrarese et al., 2008; Yeh et al., 2008), or applying chelating agents (Ma et al., 2018). Furthermore, cosolvents and surfactants have also been used to enhance the efficiency of Fenton reaction (Bogan et al., 2003/a).

In the modified Fenton reaction which is catalysed by high concentration of hydrogen peroxide (the different reported values: ≥2%, >0.3 M, or >1,000 mg/l), other reactive oxygen species and radicals as well as non-hydroxyl radicals will be produced (Watts et al., 2005). These different radicals and anions cause reactions apart from the conventional Fenton reaction. Among the produced species in the modified Fenton reaction with high peroxide concentration are hydroperoxide radicals (perhydroxyl radical) (HO_2^0), a relatively weak oxidant, superoxide anions (O_2^{0-}), a weak reductant and nucleophile in aqueous systems that cannot react with hydrocarbons, and hydroperoxide anions (HO_2^-), a strong nucleophile, but hydroxyl radicals are the strongest in comparison to all these (Chen et al., 2001; Watts et al., 2005; Goi et al., 2006; Ferrarese et al., 2008; Yeh et al., 2008). The relevant reactions which produce these species are shown in Eqs. (2-15) to (2-18):

$$H_2O_2 + OH^{\bullet} \rightarrow H_2O + HO_2^0 \qquad k = 2.7 \times 10^7 \quad M^{-1}s^{-1} \qquad Eq.(2-15)$$

$$HO_2^{\bullet} \leftrightarrow O_2^{\bullet -} + H^+ \qquad pK_a = 4.8 \qquad Eq.(2-16)$$

$$HO_2^{\bullet} + Fe^{2+} \rightarrow HO_2^- + Fe^{3+} \qquad k = 1.2 \times 10^6 \ \ M^{-1}s^{-1} \qquad Eq.(2-17)$$

$$R^{\bullet} + H_2O_2 \rightarrow ROH + OH^{\bullet} \qquad k = 10^6 - 10^8 \ \ M^{-1}s^{-1} \qquad Eq.(2-18)$$

Tsai et al. (2009) examined the oxidation rate of diesel TPH and fuel oil by high H_2O_2 concentration, 15%, and waste basic oxygen furnace slag (100 g/kg) as the catalyst. The results showed that 76% TPH of fuel oil and 96% of diesel oil had been removed after 40 h. The larger fuel oil molecules compared to diesel molecules have been explained as the reason behind their lesser destruction.

Another iron source for Fenton reaction is zero-valent iron. Zero-valent iron has been used widely for the remediation of water from heavy metals and organic pollutants such as halogenated methanes, ethanes, and ethenes and other halogenated compounds at ambient temperatures (Cundy et al., 2008). There exist some modifications to the zero-valent iron nanomaterials remediation method. Liao et al. (2007), for example, added H_2O_2 to the zero-valent iron nanomaterial to promote Fenton reaction. Meanwhile, Quinn et al. (2005) showed the applicability of nanoscale zero-valent iron for remediation of non-aqueous phase liquid (NAPL). Varanasi et al. (2007) applied iron nano-particles to remediate polychlorinated biphenyls (PCB) contaminated soil. They reported 38% of destruction at room temperature which was lower than the reported value for destruction of PCB in water, i.e. 90%. They attributed the lower efficiency to the lower diffusion of PCB from soil to the catalyst surface. It was demonstrated that adding a solvent to the Fenton reaction could increase the removal efficiency. The solvent dissolved the adsorbed pollutants into the liquid phase thus enhancing the efficiency of the reaction.

2.5.4 Related variables to Fenton and Fenton-like Reaction

The variables which affect the Fenton reaction efficiency include all site-specific and contaminant-specific variables. The organic matter content, oxide content, H_2O_2 concentration, initial concentration of contaminants, octanol-water partition coefficient, temperature, specific surface area, and the age of the contamination all have been shown to impact the degradation of TPH (Watts et al., 2005; Yeh et al., 2008). The most studied variables are discussed in this section.

The effect of acidity (pH): The reported effect of pH on hydrogen peroxide oxidation efficiency mostly depends on the used catalyst, Fe^{2+} or Fe^{3+} (Watts et al., 2005; Yeh et al., 2008). In Fenton reaction, acidic range is favourable because Fe^{2+} is soluble in acidic range, $pH = 3 - 4$, and will precipitate in higher pH range (Watts et al., 2005). By using goethite as the catalyst, natural $pH = 7$ has been reported to have higher efficiency than acidic pH (Kanel et al., 2003; Yeh et al., 2008).

In pH above 7, the efficiency is reduced as hydrogen peroxide decomposes into H_2O and O_2 and hence there would not be any hydroxyl radicals to react with the organic matters (Kanel et al., 2003). As a result, Eq. (2-19) would proceed:

$$H_2O_2 \rightarrow {}^{1}/_{2}\, O_2 + H_2O \qquad \text{Eq.}\,(2-19)$$

$$2Fe(OH)_2 + 1/2\, O_2 + H_2O \rightarrow 2Fe(OH)_3 \qquad \text{Eq.}\,(2-20)$$

Other species such as feryl ion (FeO^{2+}) has also been recognised for its role of increased efficiency at neutral pH (Ojinnaka et al., 2012) as shown by:

$$Fe^{2+} + H_2O_2 \rightarrow FeO^{2+} + H_2O \qquad \text{Eq.}(2-21)$$

$$FeO^{2+} + H_2O_2 \rightarrow Fe^{2+} + H_2O + O_2 \qquad \text{Eq.}(2-22)$$

Ojinnaka et al. (2012) examined the efficiency of Fenton reaction in three different pH ranges, acidic, neutral and basic, for PAH and aliphatic hydrocarbons. Based on the reported results of this research, PAH and aliphatic hydrocarbons showed the most reduction at the acidic pH followed by basic and neutral conditions. The different pathways in acidic and neural conditions via hydroxyl radical and non-radical feryl ion, respectively, have been explained as the reason behind this difference.

Effect of hydrogen peroxide concentration: The effect of hydrogen peroxide dosage on the Fenton reaction efficiency should be analysed in parallel with the sorption rate, dissolution rate, the contaminant $\log K_{ow}$, and scavengers of produced radicals through the Fenton reaction (Watts et al., 2005).

As discussed in the previous sections, the high concentration of hydrogen peroxide has been applied to increase the Fenton reaction efficiency, and the process is named as Fenton-like reaction. Kong et al. (1998) reported an increase in the reaction and TPH removal efficiency with increasing hydrogen peroxide concentration from 0 to 35 wt% (0,1, 7, 15 and 35 wt%).

There are some results related to the decrease in the removal efficiency due to the increase in the hydrogen peroxide concentration; in some cases, no changes have also been reported (Ferrarese et al., 2008; Yeh et al., 2008). For instance, it is stated by Yeh et al. (2008) that hydrogen peroxide dosage was not an effective variable in the reaction efficiency of octachlorodibenzo-*p*-dioxin due

to strong sorption of contaminants. Ferrarese et al. (2008) reported a decrease in Fenton reaction efficiency in removal of PAHs and TPH (aliphatic hydrocarbons) by increasing the hydrogen peroxide dosage.

The existence of an optimum concentration for hydrogen peroxide has been suggested to describe the effect of hydrogen peroxide concentration on reaction efficiency. In this sense, based on Goi et al. (2006)'s work, the degradation efficiency increased with increasing the hydrogen peroxide dosage before this optimum concentration. After this optimum value, the reaction efficiency decreased or did not change with increasing hydrogen peroxide dosage. Competition between hydrogen peroxide and organic matters for hydroxyl radicals and the lesser contact between the oxidant and pollutants because of rapid reactions at high reactant dosage were given as the reasons for this observation.

SOM: Inorganic matters such as carbonates and natural organic matters (NOM) are reported as the main hydroxyl radical scavengers (Watts et al., 2005). The reactions of hydroxyl radicals with NOM are more complex than their reactions with inorganic anions (Watts et al., 2005). The effects of the organic matter on Fenton reaction may be a function of the organic material state (e.g. soluble or sorbed), the hydrophobicity and reactivity of the probe compound or contaminants, the nature of the used catalyst and many other factors (Watts et al., 2005).

SOM are considered as a determinative factor in the sorption-desorption processes (Lindsey et al., 2000). FA and HA are the most effective fractions of SOM that participate in sorption reactions (Lindsey et al., 2000). Two possible

yet contradictory ways for participation of SOM in the Fenton reaction have been reported. FA and HA can participate in Fenton reaction by binding with metals and performing the role of metal chelates, and reducing Fe^{3+} to Fe^{2+} (Lindsey et al., 2000). Alternatively, they can decrease the Fenton reaction efficiency by the consumption of hydrogen peroxide thereby playing the role of competitors for hydroxyl radicals (Lindsey et al., 2000; Goi et al., 2006; Romero et al., 2009; Fan et al., 2013; Sherwood et al., 2014). The reported data regarding the final result of this positive effect (reducing of $Fe^{3+}$to Fe^{2+}) and negative effect (consumption of hydroxyl radicals) are different. Fan et al. (2013) reported that organic matters could increase the degradation rate of methomyl in Fenton reaction. Contrarily, Romero et al. (2009) reported a higher decomposition rate of hydrogen peroxides in the soil with higher SOM percent in natural pH. The low stability constant of HA–Fe^{3+}, 2.8, at circum-neutral pH makes SOM a great metal chelate (Sherwood et al., 2014). This is significant when compared to EDTA-Fe^{3+} stability constant of 27.7 (Lindsey et al., 2000).

Thus, the effect of the Fenton reaction on SOM and the effect of SOM on the Fenton reaction need to be considered in the analysis of oxidation of contaminants. However, insufficient information related to the effect of oxidation on the physical and chemical properties of soil is available (Sedlak et al., 1994; Sirguey et al., 2008). Among the reported results in this area, the research of Leifeld et al. (2001) for the reaction of SOM with hydrogen peroxide could be mentioned. Based on their experiment, the depletion of aliphatic carbons in the reaction is less than the aromatic carbons.

In another study, Voelker et al. (1996) have studied the effect of different ligands in the rate of Fenton reaction. They mentioned that carboxylate ligands, which can be found in abundance in FA, could enhance the Fenton reaction rate. Carboxylate ligands by making the complexes with Fe^{2+} that has the higher reactivity potential in comparison with aqua complexes can increase the oxidation rate. This effect was reported to be obvious at pH=5 whereas no considerable changes at pH=3 were observed due to the increase in FA.

In the study by Goi et al. (2006) on determining the effect of peat on destruction of transformer oil by hydrogen peroxide, they reported that the an optimum H_2O_2 to transformer oil weight ratio of 4:1 in peat, which was high in organic matter. Increasing the ratio from 1.6:1 to 4:1 increased the removal efficiency from 22% to 47%, and increasing from 4:1 to 8:1 decreased the efficiency from 47% to 0%. Meanwhile, increasing the ratio from 0.04:1 in sand changed the efficiency marginally from 82% to 87%.

Considering the changes in soil properties solely due to the reaction with hydrogen peroxide was considered in the experiments carried out by Romero et al. (2011). They reported the following results after treatment of the soil with hydrogen peroxide without monitoring the pH in natural pH: reduction in surface area, more hydrophilic regions created, no considerable changes in organic carbon and carbon contents, and a small increase in SOM due to the addition of oxygen. Reduction in desorption ability could be predicted as the result of hydrophilic regions.

Effect of soil slurry volume, L/S: Watts et al. (1996) studied the effect of soil slurry volume by keeping the hydrogen peroxide concentration at a constant

level in the values from 0.15 to 1.5 M, but applying different liquid volumes from 1.5 to 5 ml per 5 g soil. The effectiveness of the reaction in view of the amount of consumed hydrogen peroxide and the diesel removal efficiency has been argued. The efficiency increased by increasing the liquid volume to a maximum value at 3.5 ml whereas by increasing to more than 3.5 ml to achieve the same diesel removal, higher hydrogen peroxide concentration was required (Watts et al., 1999). The increase in the efficiency has been attributed to the increase in the soil and liquid contact (Watts et al., 1999). In contrast, the decrease in the effectivity of the reaction has been explained by the non-effective contact between liquid and solid which meant that the produced hydroxyl radicals were not in close contact to the sorbed contaminants (Watts et al., 1996).

2.5.5 Combination of Fenton Reaction with Other Remediation Methods

As mentioned before, various in-situ remediation technologies such as soil vapour extraction, thermal treatment, bio-venting, surfactant flushing, and chemical oxidation using Fenton reagent, permanganate, and ozone have been considered to remediate soils and aquifers contaminated with petroleum hydrocarbons (Yu et al., 2007). Fenton reaction and other oxidation reactions are among the most studied methods. Nonetheless, one or two studies have reported unsuccessful results with regard to applying Fenton oxidation for petroleum-contaminated soils. For example, Ferguson et al. (2004) studied the application of several oxidative treatments (Fenton reagent, hydrogen peroxide, and sodium hypochlorite) to remediate petroleum-contaminated soil at Old Casey Station, East Antarctica. The results showed that the methods applied at this site, where contamination occurred over a decade ago, did not significantly

reduce the petroleum hydrocarbon concentrations, and that this process could hinder biodegradation through the destruction of subsurface microbial communities.

To achieve complete or almost complete soil remediation, from one point of view, we need to consider at least two major processes. First, the contaminants should be desorbed from the soil matrix. This involves all desorption, dissolution, and diffusion processes. Second, the process of destruction of the desorbed or dissolved matters including oxidation occurs. The most reported limiting factors in Fenton oxidation processes are related to the first step; in other words, the contaminants bound to the soil are more resistant to the oxidation than the soluble contaminants in the solution (Watts et al., 1996; Watts et al., 2005; Yeh et al., 2008; Wu et al., 2013b). This problem is more prominent for systems with low hydrogen peroxide concentration (Bogan et al., 2003/a). It is also possible that direct oxidation of sorbed contaminants occur.

Combining the Fenton reaction and Fenton-like reactions with other remediation methods have been studied widely (Bogan et al., 2003/a Ferguson et al., 2004; Lundstedt et al., 2006; Lu et al., 2010/a). Combing different processes, which focuses on different parts of the sorption-desorption processes, and the oxidation process, could effectively improve the efficiency of the remediation process. The combination of Fenton reaction with surfactants and solvents for increasing the solubility (Isosaari et al., 2001; Bandala et al., 2008), and with bioremediation process (Rivas et al., 2006; Lu et al., 2010/a) could be mentioned as the examples.

In some reported studies, ET (Lundstedt et al., 2006) and EL (Yap et al., 2012/a) are applied as co-solvents to increase the desorption rate. Lundstedt et al. (2006) used an ET pre-treatment to enhance the depletion of all PAH in the soil by facilitating their desorption from the soil matrix. However, some PAH, especially anthracene, benzo[a]pyrene and perylene, were more extensively depleted than other PAH with fewer or equal numbers of fused rings, indicating that the hydroxyl radicals reacted faster with these PAH than with other kinds. The ET present in the slurry also appeared to influence the relative reactivity of the PAH.

In another study, Yap et al. (2012/a) examined the influence of EL-based Fenton treatment for soils contaminated with PAH, and the remediation efficiency achieved by this mixture was compared with ET/water mixture. It was reported that EL/water system had a greater desorption capacity than ET/water system. The efficiency of the treatment was mainly attributed to the enhanced solubility and desorption. The positive laboratory results indicated the potential of this technique, firstly, to treat soil with high contamination level and, secondly, to destruct the contaminant mass in-situ, both of which were difficult to achieve by conventional methods.

Vegetable oil has also been applied to increase the solubility of the contaminants by Bogan et al. (2003/a). It was explained that vegetable oil could act like synthetic chemical surfactants, and its effectivity increased by applying it as a microemulsion of vegetable oils. The results showed an increase in the oxidation rate of PAH (phenanthrene and pyrene). Whilst Fenton reaction was unable to

decrease the contaminant level significantly, especially for higher molecular weight PAH, adding vegetable oil could remove them almost completely.

Increasing the solubility of HOC in organic solvents is not just because of their higher dissolution rate in solvents than in water, but the desorption rate also increases by dissolving SOM, which are the main adsorbents of HOC in solvents (Gong et al., 2005/b). Table 2-7 compiles reported studies on application of Fenton, Fenton-like and modified Fenton reactions for soil remediation. The reported data in this table mostly is related to the organic pollutants and the reagents used in the Fenton, modified Fenton, and Fenton-like and the removal efficiency are summarized in the table to compare the efficiency with the reagents percentages. The data in the table is also important to give a general view of the studied contaminants in this area.

Table 2-7: Selected Fenton, Fenton-like and modified Fenton remediation studies

Fenton reaction			
Pollutants	**Reagents**	**Removal efficiency**	**Reference**
2,4-dimethylphenol	H_2O_2/pollutant weight ratios used were 182 and 364	75% and 86%	Romero et al., 2009
Trichloroethylene	H2O2:Fe2+= 57.1:1, 54.9:1	90–100%	Chen et al, 2001
2-methylnaphthalene, n-hexdecane and diesel fuel	-	2-methylnaphthalene: 36%, n-hexadecane: 12.5%, and diesel fuel :14% at pH=7	Chen et al., 1998

Continued Table 2-7: Selected Fenton, Fenton-like and modified Fenton remediation studies

Oil hydrocarbons	Equivalent of utilized H_2O_2=0.71	98.50%	Yousefi et al.,2012
Perchloroethylene (PCE)	6.0 g soil and 6.0 ml liquid after addition of 1 ml of H2O2 (50, 150, 300, and 600 mM) and 1 ml of Fe catalyst (0, 2, 5, and 10 mM)	In Warsaw soil: 44–49% decrease in PCE	Kang et al. , 2006
Diesel fuel	H2O2/diesel/Fe2+ weight ratio: 0.03:1:0.005 and 0.06:1:0.01. H2O2/Fe2+ =10:1	70% and 83%	Goi et al.,2006
PAHs: naphthalene, acenaphthylene, acenaphthene, fluorene, anthracene, pyrene, benz[*a*]anthracene, benzo[*k*]fluoanthene, benzo[*g*,*h*,*i*]perylene, fluoranthene	soil to liquid (S/L) ratio of 1:3. 10 ml of 10mM iron sulphate and 20 ml of 15% hydrogen peroxide	PAHs with two and three rings: 89 and 59% and PAHs with four, five, and six rings: between zero and 38%	Jonsson et al., 2007
Benzo[a]pyrene	H_2O_2=15M iron(II)=6.6mM	BaP mineralization: 85%	Watts et al., 2002
Phenanthrene and pyrene	4, 6 or 8mL of H2O2 50% ; 0.9, 1.3, 1.8mL of FeSO4	Pyrene: 56.4%, Phenanthrene: 93.8%	Silva et al., 2009
Petroleum	H2O2:Fe2+=0.5:1 to 50:1	up to 97%	Millioli et al.,2003
TPH; BTEX; and PAH	H_2O_2: 50 ml and $FeSO4{\cdot}7H_2O$: 5 ml	PAH: 96%, BTEX:99%, and some TPH complete disappearance	Ojinnaka et al.,2012

Continued Table 2-7: Selected Fenton, Fenton-like and modified Fenton remediation studies

Modified Fenton and Fenton-like reaction				
		Removal efficiency	**Combined effect**	**Reference**
benzo[a]pyrene, dibenz[a]; [h]anthracene, benzo[g; h; i]perylene and indeno[c; d]pyrene	-	5% (average removal efficiency)	Palm kernal oil (PKO)	Bogan et al., 2003/a
Transformer oil	15 g of sand and 15 ml of liquid (twice-distilled water + H2O2 solution)	At H2O2/transformer oil= 4:1: 47%	Biodegradation	Goi et al., 2006
BTEX	Fe(II) or Fe(III); 2, 5, and 10 mM, H2O2; 30, 150, 300 mM	>90% removal after 15 min and 95% removal after 3 h	Metal chelating agents (L-ascorbic acid, gallic acid, or N-(2-hydroxyethyl)imino diacetic acid)	Kang et al., 2005
1-indanone, 9-fluorenone, anthracene-9,10-dione, 2methylanthracenedione, 7H benz[de]anthracen-7-one,benz[a]anthracene-7,12-dione and naphthacene5,12-dione	Fe^{2+} solution: 5 mM and 15% H_2O_2:20 ml		Fenton oxidation preceded by ethanol treatment	Lundstedt et al., 2006
carbon tetrachloride and chloroform	H_2O_2: 2M and iron(III)-chelate: 5mM	74%	Chelation, hexaketocyclohexane (HKCH)	Smith et al., 2006
Creosote, seven compounds—fluoranthene (Flu), phenanthrene (Ph), fluorene (Flu), pyrene (P), triphenylene (TPh), benz(a)anthracene (B(a)A) and chrysene (Chr)	H2O2/soil/Fe^{2+}= 0.043:1:0.007 to 0.086:1:0.014	73.5 to 80%	Biodegradation	Kulik et al., 2006
TPH	0.3 pore volumes of 17.5% H2O2 solution flushing for 15 days	63.5%	Biodegradation	Kim et al., 2012
PAHs	Oxidant dosages about 100 mmols per 30 g sediment sample	52% to more than 90%	Chelation, catechol	Ferrarese et al., 2008

Continued Table 2-7: Selected Fenton, Fenton-like and modified Fenton remediation studies

Petroleum	accumulative H_2O_2 dosage: 2.45 mol/ kg	Reduce from 14,800 to 2300mgkg−1	Ferric ion chelated with EDTA	Lu et al., 2010/b
2,4-dimethylphenol	H_2O_2/KH2PO4:5:1 and 40:1, an initial H_2O_2: 0.29 and 0.58 M	90% of 2,4-DMP for 50 mM of EDTA and 90% for 50 mM of CITRt	Natural Fe species present in soil, and chelating agents (EDTA, sodium citrate 2-hydrate (CITRt)	Vicente et al., 2011
Petroleum-contaminated	Optimum molar ratio of H2O2 and Fe3+: 300/1	Decrease from 32,400 to 21,800 mg kg_1 soil,	Combining Fenton-like pretreatment with biodegradation	Lu et al., 2010/a
Fenton-like reaction				
Pollutants	**Reagents**	**Removal efficiency**	**Different variables from Fenton reaction**	**Reference**
Trichloroethylene		71.6%	Natural silica sand	Yeh et al.,2003
Benzo[a]pyrene (BaP)	H_2O_2:15M and iron(II) concentration:6.6mM	Complete within 24 h and 85% mineralization	High H_2O_2 concentration	Watts et al., 2002
TPH	Fe(0): 1 and 2 g and H_2O_2:250 mg/l	More than 90%	Zero-valent iron [Fe(0)]	Oh et al., 2014
Petroleum hydrocarbons (e.g., fuel oil and diesel)	H_2O_2:15% and BOF slag:100 g/ kg	Fuel oil: 76%, Diesel:96%	Waste basic oxygen furnace slag (BOF slag)	Tsai et al., 2009
Diesel	H_2O_2:1.5 M	99%	Iron 3 perchlorate, and Iron 3 nitrate	Watts et al.,1996
Diesel and/or kerosene	H202: (0, 1, 7, 15, and 35wt%) and iron mineral contents (0, 1, 5 and l0wt%).	10% magnetite: C/C0=40% 15% H2o2:C/C0=50%	Naturally-occurring iron minerals, goethite and magnetite,	Kong et al., 1998
oil hydrocarbons	Oxidant:Fe/ H2O2 molar ratio: 10/1	Approximately 70–80%	Magnetite catalyzed Fenton-like oxidation	Usman et al., 2012
Diesel	Fe3+:720 mg/l	Injection test: 30% diesel removal	Ferrous salts application	Xu et al., 2006

2.5.6 Fenton Reaction with NAPL and Sorbed Phase

The main problem in degradation of contaminants in soil is with the ones existing in the sorbed and NAPL forms (Watts et al., 1996; Watts et al., 2005). The water-soluble forms could be effectively decreased by Fenton reaction as the hydroxyl radicals mainly react with dissolved species much faster than with the organic matters in NAPL or sorbed forms. The reason is that for reacting with the sorbed and NAPL forms, the hydroxyl radicals have to cross the two phase interfaces, liquid-solid and liquid-liquid (aqueous-NAPL), that pose mass transfer limitations (Sedlak et al., 1994; Watts et al., 1996; Watts et al., 2005).

Yeh et al., (2006) showed that the high hydrogen peroxide concentration could directly oxidise the sorbed and particulate phases of hexachlorobenzene. This conclusion was drawn based on the comparison of the dissolution rate of hexachlorobenzene and Fenton reaction rate. Degradation of NAPL by high hydroxyl concentartion has also been reported (Watts et al., 1994; Watts, 2005; Yeh et al., 2008). Yeh et al. (2008) evaluated Fenton-like reaction of five chlorinated ethylenes and three aromatic hydrocarbons using goethite as the catalyst. The reaction efficiencies and rate constants of these compounds in NAPL and dissolved forms were compared. According to the results, the removal efficiencies of 0.02 mmol NAPL-formed contaminants were 26-70% less than the dissolved form of these contaminants in water. The measured rate constants were in the order of $10^9 M^{-1} s^{-1}$ for dissolved chlorinated ethylenes and aromatic hydrocarbons, and the rate constant were 25-60% less for their NAPL forms. However, the NAPL form of petroleum hydrocarbons could also be effectively oxidized by Fenton-like process. These results strongly indicated

that in addition to the dissolution and reaction mechanisms, direct interaction between Fenton radicals and NAPL is also possible.

The produced radicals, hydroperoxide radicals (HO_2^0), superoxide anions (O_2^{0-}), and hydroperoxide anions (HO_2^-), through the use of high concentration hydrogen peroxide has been reported to be capable of increasing the oxidation of sorbed contaminants (Watts et al., 1996; Ferrarese et al., 2008). These radicals are known as the only radicals that participate in the DNAPL destruction of carbon tetrachloride (Watts et al., 2005). Watts et al. (1994) studied the Fenton-like oxidation of hexachlorobenzene in silica sand and natural soil, and reported that the aggressive Fenton-like reaction conditions in high hydrogen peroxide concentration by perhydroxyl radicals could alter the hexachlorobenzene sorption characteristics and increase its desorption rate, as well as promote the desorption of hydrophilic organic compounds from solid surfaces.

2.5.7 The Effects of Fenton Reaction on Aliphatic and Aromatic Reduction

The reaction of hydroxyl radical with alkenes and aromatics with reported second-order rate constants of $10^9 - 10^{10}\ M^{-1}S^{-1}$is considered as a fast reaction (Lindsey et al., 2000). Some studies have compared the oxidation of the aliphatic compounds with aromatic compounds or TPH totally. The greater resistance of alkanes towards oxidation has been mostly reported along with the greater reduction of aromatic TPH in the treatment of unleaded gasoline as compared to the aliphatic fraction (Watts et al., 2000; Leifeld et al., 2001; Lee et al., 2002; Mater et al., 2006,). For example, in Mater et al. (2006)'s work, the

lesser consumption of iron and H_2O_2 for the oxidation of the aromatic compounds than the oxidation of the aliphatic compounds were reported.

Watts et al. (2000) reported greater than 95% recovery of benzene, toluene and mixed xylene (BTX) at near-neutral pH using 2.5% H_2O_2 and 12.5 mM Fe^{3+}, while only 37% nonane, 7% decane, and 1% dodecane oxidation was achieved under the same conditions. In another study, Lee et al. (2002) compared the removal efficiency of normal alkanes with the removal efficiency of diesel by using ozone oxidation. The efficiency and the rate of alkanes removal were lower than that of the diesel removal. The low removal efficiency of diesel (40%) was attributed to the normal alkanes in diesel that were considered as a major part of diesel. Inconsiderable differences between the aromatic and aliphatic reduction results have also been reported in another study (Ojinnaka et al., 2012). Leifeld et al. (2001) studied the effect of H_2O_2 treatment, hydrogen peroxide 15% followed by hydrogen peroxide 30%, on soil $< 20\mu m$ on removal of organic carbon. The results showed that the alkyl C had a higher resistance to peroxide oxidation in comparison with O-alkyl C and aromatic C.

2.6 Soil Column

Soil columns have been used for over three centuries in the study of hydrogeological properties. In the dynamic column procedure, a fixed amount of soil is eluted by a fluid flowed by gravity (Lewis et al., 2010; Reemtsma et al., 1997). Column experiments make it possible to study some specific soil physical, chemical, and hydrodynamic properties that are required for understanding and determining the time dependent release of contaminants, and modelling the contaminants transport and fate in the soil whereby most of them

cannot be achieved through batch tests. The ability of the column set-ups to stipulate the field condition by flowing the fluid through the column represents a good opportunity for modelling the fate and transport of the contaminants in the real situations. The determinative effects in migration of contaminants, hydrodynamic effects (such as dispersion, colloidal transport, low liquid to solid ratio, chemical heterogeneities), which cannot be examined in batch tests, and chemical phenomena (like multiple species, reversibility, etc.) can be studied in column set-ups (Weber et al., 1996; Reemtsma et al., 1997; EPA 402-R-99-004A, 1999; Kalbe et al., 2007; Lewis et al., 2010).

Soil columns may be classified either according to their level of saturation, saturated or unsaturated, or according to the method of their construction, packed columns or monolithic columns (Lewis et al., 2010). Packed soil columns result in a better reproducibility while monolithic columns use undisturbed samples that would lead to results that can represent the field conditions better, but with less reproducibility (Lewis et al., 2010). The effects of variables such as bulk density and scaling effects on dispersivity are required to be evaluated appropriately for using the experiments results (Lewis et al., 2010). Achieving reproducible results, between different laboratories and even different columns, is one of the major advantages of column set-ups. For comparing the results from different columns with different dimensions, contact time can be calculated from the flow rate and bulk density (Kalbe et al., 2007).

Comparing the results of batch and column experiments has been the aim of many researchers. Some contaminants such as anions give the same

concentration results, and some such as HOC lead to different results in batch and column experiments (Kalbe et al., 2007; Grathwohl et al., 2009).

The involved processes in desorption of the contaminants have been given as the reason behind these discrepancies. Based on the explanation of Kalbe et al. (2007), when the responsible processes for desorption are solubility and availability of the contaminants, as for anions such as sulphate and chloride, column and batch experiments provide the same cumulative concentration. When adsorption/desorption processes play the dominant role, like leaching of PAH, differences in batch and column experiments will be observed (Grathwohl et al, 2009). Kalbe et al. (2007) reported that this difference is decreasing by increasing the molecular weight of the PAH.

The other sources of differences between column and batch experiments are the contact of the soil with the same liquid during the batch experiment, and renewing the liquid through the column experiments (Delay et al., 2007). In column tests, at the start of the experiment, the effluent concentration is at the equilibrium condition, for strongly adsorbed contaminants, this state will exist for a longer time (Grathwohl et al., 2009). By extending the time of the experiment, the effluent concentration will decrease and the non-equilibrium condition will be observed (Grathwohl et al., 2009). This change can be recognised by a sudden drop in the concentration followed by the tailing in the effluent concentration (Grathwohl et al., 2009).

For comparing the non-equilibrium conditions (the prominent case in column experiments), which are to be expressed in time, and the equilibrium conditions (the final conditions in batch experiments), a variable applicable in both

conditions is required. The ratio of the liquid to solid, L/S, is used for comparing the results between these two set-ups (Al-Abed et al., 2008). At fixed flow rate, the L/S is proportional to the contact time. Grathwohl et al. (2009) who studied the modelling of aqueous leaching in a column percolating test showed that the curve of concentration against L/S is a good approach for comparing the batch and column percolation. In applying this variable (L/S), a caution about the time when the tailing appears is necessary. After tailing appears, the results in different columns versus L/S will not be similar (Grathwohl et al., 2009). The contaminants release kinetic, grain size, and flow velocity will affect the time when the equilibrium condition will change to the non-equilibrium in column experiments (Grathwohl et al., 2009).

The problem associated with this variable is that batch experiments in equilibrium conditions are supposed to have the same results in all L/S, but this is not usually observed (Reemtsma et al., 1997). Therefore, another way for comparing the results of these two designs, batch and column experiments, have been proposed by Delay et al. (2007). They suggested calculating the concentration by achieving the total percolated amount in the elution agent.

Reemtsma et al. (1997) reported that the short-term column experiments could be representative of the spontaneously desorbed part of PAH, and not the diffusing part. The observation of Grathwohl et al. (2009) related to the comparable results of batch and column tests for strongly adsorbed compounds or at very early times might be explained by this. Therefore, batch and column set-ups can each be designed in a way that each of them represents different transport mechanism, advection, or diffusivity.

2.7 Concluding Remarks

Due to the limitation of conventional Fenton reaction, research on modified Fenton reaction combined with different methods are being developed considerably for treatment of petroleum hydrocarbons-contaminated soil. Combination of conventional Fenton reaction with a solvent has shown promising results in a number of soil remediation studies. One of the major concerns regarding the application of a solvent in soil remediation is how it affects the soil. Therefore, the application of an environmentally friendly solvent will resolve this issue and represents further development in this area. Whilst there are numerous studies on petroleum hydrocarbons contaminated soil, based on the author's best knowledge, research on the aliphatic fraction of petroleum hydrocarbons with the applied green solvent in this study, EL, has not been considered. The response of aliphatic fraction of petroleum hydrocarbons to the combination of a biodegradable solvent, such as EL, with Fenton reaction is important in making decisions in finding an applicable process for contaminated soil treatment. Examining the effects of different variables, especially HA, on Fenton reaction is also equally important in determining optimum conditions for remediation.

CHAPTER 3: MATERIALS AND METHODS

3.1 Introduction

As the analytical methods applied in any research represent an essential prerequisite to successful data collection and analysis, they need to be adhered to carefully. This chapter summarizes all the materials, tools and analytical techniques used in this study. These methods include the ones used for soil spiking and soil characterization, H_2O_2 concentration, quantification of the amount of diesel in soil, GC analysis and quantification. The methods are adopted from standards established by agencies such as US EPA and other related published works.

3.2 Reagents and Chemicals

N-hexane (98.0%, for gas chromatography ECD & FID), EL (99.0% for analysis), and silica gel 60 (0.063-0.200 mm) were supplied from Merck. R&M chemicals supplied dichloromethane (DCM 99.5%, analytical reagent), iron (II) sulphate heptahydrate ($FeSO_4.7H_2O$), H_2O_2 (30%), potassium iodide solution (KI2, 99.0%), ammonium molybdate tetrahydrate ([NH4]6 Mo7O24•4H2O), sodium thiosulfate solution ($Na_2S_2O_3$), and starch solution (10.00 g/l) (soluble). Diesel was supplied form Shell gas station, Semenyih. HCl (37%), mercury (II) chloride ($HgCl_2$, >99%) and H_2SO_4 (95%-97%) were supplied by Sigma Aldrich. Silica gel for column chromatography was pre-heated up to 160°C before usage and sodium sulphate was activated by heating up in a furnace at

420°C. Standards n-nonane (C9, 99.5%), n-docosane (C22, 99.5%), and n-octacosane (C28, 99.5%) were supplied by Dr Ehrenstofer GmH Germany, and n-hexadecane (C16, 99.5%) from Merck. To prepare the standards for calibration, they were dissolved in different concentrations in n-hexane.

3.3 Soil Collection, Characterization and Spiking

3.3.1 Soil collection

Surface soil samples (0-10 cm) were collected in December 2014 from a forest located in Cameron Highlands, Malaysia. The soil sample was air-dried at ambient temperature (25-28^{o}C) for 2 days. Fibrous materials were removed. After drying, the soil was passed through a 2 mm sieve and was stored at ambient temperature (25-28^{o}C).

For soil spiking, the predetermined amount of diesel and soil were calculated to give three initial contamination levels of 3500 mg/kg, 5000 mg/kg, and 10000 mg/kg. The determined amount of diesel was dissolved into n-hexane solvent to enable faster dissolution and penetration into the soil samples. Then, the diesel dissolved in n-hexane was mixed with the appropriate amount of soil. After mixing, the solvent was evaporated under the fume hood, and the soil was kept in closed containers before usage.

3.3.2 Soil characterization

There are a few of characteristics related to soil that are usually reported in papers and studied attributed to the soil remediation processes as they are capable of affecting the results and also for the sake of comparison with the results of different studies.

3.3.2.1 Iron Content

The environmental available native Fe is of importance because it can act as a catalyst in Fenton reaction and also can play as an oxidant scavenger, it also can be the reason of clay swelling due to the redox reactions (Yap, 2012/b). Iron content was determined following the US EPA Method 3050B, which is based on digestion by nitric acid (HNO_3, 65%, Merck, Germany) and then quantification by atomic absorption spectrometry (AAS). The procedure was as follows: 2.00 g of soil (wet weight) was transferred to a digestion vessel. 10 ml of 1:1 HNO_3:water was added to the soil, and the vessel was covered with a watch glass. The slurry was heated to 95ºC ± 5ºC and refluxed for 10 to 15 min without boiling. After cooling the sample, 5 mL of concentrated HNO_3 was added. The vessel was covered and heated for 30 min. No generation of brown fume indicated complete sample oxidation by HNO_3.

By heating the solution at 95ºC ± 5ºC without boiling for 2 h and removing the watch glass, the volume of the solution was reduced to approximately 5 mL. After cooling the slurry, 2 mL of water and 3 mL of 30% H_2O_2 (30% R&M) were added to the solution. The vessel was covered and warmed up to accelerate the reaction of H_2O_2 until the effervescence subsided. After cooling the vessel, 30% H_2O_2 in 1-mL aliquots was added until the effervescence was minimal. The solution volume was reduced to 5mL by heating at 95ºC ± 5ºC without boiling for 2 h.

By adding 10 mL HCl to the sample and heating at 95ºC ± 5ºC for 15 min, the sample was ready for AAS analysis (Perkin-Elmer Analyst 400). The digestate was passed through a Whatman No. 41 filter paper, the filtrate was collected in

a 100-mL volumetric flask, and by adding deionized water until the volume reached 100 mL. By preparing and using the 5-point calibration curve (1, 2, 5, 10 and 100 ppm), the concentration of the sample solution was determined.

3.3.2.2 Soil Moisture

Soil moisture is also measured because it can affect the Soxhlet extraction. The moisture of the air-dried soil was measured by the oven method. In summary, 1.000 g of the moist soil was put in the oven at 105°C for 24 h. The weight loss in this process was measured and the moisture content was calculated by Eq. (3-1):

$$\text{Moisture}\left(\frac{\text{W}}{\text{W}}\%\right) = \frac{\text{W}_{t2} - \text{W}_{t3}}{\text{W}_{t3} - \text{W}_{t1}} \times 100 \qquad \text{Eq.}\,(3-1)$$

Where W_{t1} is the weigh of the container [M], W_{t2}denotes the weight of moist soil and the container [M], W_{t3} is the weight of dried soil and the container [M]

3.3.2.3 Soil Texture

The texture of soil can be determinative in the composition and physical properties of the soil like the porosity, so it can be determinative in the sorption/desorption processes. As the clay is one of the most important adsorbents of pollutants in soil, its percentage needs to be calculated. The percentage of sand, silt and clay in the inorganic fraction of soil was measured by the hydrometer method. The method uses Stoke's Law in calculating the rate of sedimentation of particles. As the soil used in this project had more than 5% organic matter, the amount of organic matter was firstly reduced by reaction with H_2O_2.

50 g of fine-textured material with 50 g of water were added to a 1 L beaker. 50 ml of H_2O_2 was slowly added to the mixture. After stirring the mixture, the beaker was covered and set aside for 24 h. Then, 10 mL of H_2O_2 was added to the suspension and heated up to 80°C until no foams appeared. After cooling, 400 mL water was added to the beaker. By heating up the suspension for 2 h, the remaining H_2O_2 was removed.

Once the sample reached ambient temperature, 100 mL of 5% dispersing solution, sodium hexametaphosphate, was added to the suspension. Subsequently, the suspension was mixed for 1-2 min, and was transferred to a 1000 mL cylinder. The cylinder was filled up to 1000 mL. After mixing the suspension thoroughly, a thermometer and a hydrometer were inserted into the cylinder. The hydrometer was read at 40 s, 52 min and 6 h. The suspension was transferred to a 0.063 mm sieve, and after drying the sand, its weight was recorded.

3.3.2.4 SOM Content

Organic matters in soil is the factor that can affect the Fenton reaction efficiency directly. SOM was determined by two methods, weight loss on ignition (LOI), and thermogravimetric analysis (TGA).

- ***SOM by LOI***

The weight LOI method was conducted as follows: a 50 mL beaker was weighed and 5 cm^3 of air-dried, 2-mm sieved soil was scooped into the beaker. The soil was dried for 2 h at 150°C ±5°C. The soil and beaker were weighed after the temperature reduced to 100°C. Then, the soil was heated to 550±5°C for 24 h.

The beaker and soil were weighed after the temperature reduced to 105°C. The reported LOI% as percent organic matter was calculated based on the Eq. (3-2):

$$\text{Percent weight loss on ignition LOI\%} = \frac{\text{Soil}_\text{d} - \text{Soil}_\text{a}}{\text{Soil}_\text{d}} \times 100 \quad \text{Eq. } (3-2)$$

Where:

Dried Soil (Soil_d) = (weight of the beaker + weight of soil at 150°C) - Weight of the beaker

Ashed Soil (Soil_a) = (weight of the beaker + weight of soil at 550°C) - Weight of the beaker

- ***SOM by TGA***

In another method, the SOM content in the soils was determined by TGA using METTLER thermogravimetric analyser, DSC1, Switzerland. 17.1717 mg of the sample was heated from 150°C to 550°C at a rate of 20 °C/min under the flow of oxygen with a flow rate of 20 mL/min. The sample was then heated at 550°C for 2 h. The mass loss within the interval from 150°C to 550°C from the thermogravimetric curve was determined based on the applied method by Romero et al. (2009) which was considered to be the organic carbon content of soil.

3.3.3 Extraction of humic acid

15.00 g of soil material were stirred in 100 ml of 0.1 M NaOH for 24 h. The slurry was centrifuged at 5500 rpm for 25 min. The supernatants from this extraction contained the HA and FA fractions, and the residue contained the humin. The supernatant was acidified by 6 M HCl to pH ≤ 2. The suspension was left to stand for 16 h, and then was centrifuged at 5500 rpm for 25 min. The

precipitated part contained the HA. The HA fraction was dissolved by adding 0.1 M KOH with periodic shaking for 2 h. The purpose of this step was to remove fine mineral particles such as clay silicates. The HA was re-precipitated by adding 6 M HCl and acidifying to pH ≈1 allowing the suspension to settle for 16 h. HA was separated by centrifuging at 5500 rpm for 25 min. HA was frieze-dried for 16 h and finely ground prior to Fourier-Transform Infrared Spectroscopy (FT-IR) (Perkin-Elmer, FTIR/FIR spectrometer, Frontier, USA) analysis.

3.4 Analytical Methods

3.4.1 TPH extraction

The diesel in the soil was extracted by Soxhlet extractor (Gerhardt, SOXTHERM®, Germany), one beaker in the extractor is represented in figure 3-1.

Figure 3-1: A beaker of the used Soxhlet extractor

Before extraction using an extraction thimble (Advantec, ID (84) 33 mm × 80 mm, Japan), the soil was mixed with activated sodium sulphate at a ratio of 2:1 (w/w) soil:sodium sulphate, (10 g sodium sulphate for 5 g soil) to remove the remaining water. The extraction solvent used was DCM with Soxhlet extraction conditions of 2.15 h hot extraction and 1 h extraction with 9 evaporating intervals in 2 evaporating steps. The solvent of the extract was exchanged to hexane before purification and separating the aliphatic fraction of the TPH, i.e. diesel range, by silica gel column chromatography prior to running GC analysis.

3.4.2 Column chromatography

For preparation of the samples before injection into the GC, the soil extract was fractionated to separate the aliphatic phase, which was the main concern in this study, by column chromatography. 5 g of silica gel, plus 1 g of sodium sulphate on top of silica gel comprised the chromatography column. Columns were firstly conditioned by adding 25 mL of n-hexane. Then, the extract was added and eluted by 20 mL of n-hexane; this process resulted in the separation of the aliphatic fraction. The solvent of the separated aliphatic fraction was evaporated until the volume was less than 2 mL. For analysis, TPH were divided into three fractions. Figure 3-2 shows the column used for chromatography.

Figure 3-2. Column chromatography

3.4.3 Preparation of external standards for GC-FID calibration

For quantification of the aliphatic part of diesel and TPH, four alkanes, nonane (C9), hexadecane (C16), docosane (C22), octacosane (C28), have been chosen as the markers. For calibration purpose, a 5-point calibration curve for each of four alkanes, individually and in the mixture with the equal weight of these four n-alkanes in n-hexane were prepared.

For the individual n-alkanes, the required amount of the standard was dissolved in n-hexane to make the desired concentrations of 50 ppm, 100 ppm, 200 ppm, 500 ppm, and 1000 ppm. Two replicates for each measurement were carried out by GC analysis on two different days. The prepared solutions were transferred to sealed vials prior to GC analysis. The retention time of each n-alkane markers was determined by these five concentrations. The correlation coefficients, R^2, of peak areas against standard solution concentrations for the individual n-alkanes and the mixture solutions were > 0.99.

To analyse the results, all peaks between C9-C28 were divided into three fractions of C9-C16, C16-C22, and C22-C28. Fraction 1 included all peaks within C9-C16 range plus half of C16 peak and the peak of C9. For fraction 2, C16-C22, all peaks between C16-C22 range plus half of C16 peak and half of C22 peak were considered. Finally, fraction 3 comprised all peaks between C22-C28 plus half of C22 peak and peak of C28. The aliphatic groups included alkanes, alkenes, and cycloalkanes. The reported peaks could possibly include Fenton reaction products as reported by Yu et al. (2007). The TPH was the summation of all peaks settling into the aliphatic part of diesel between C9 to C28.

3.4.4 GC Analysis

For determining the concentration of TPH, GC has been used. GC is a technique to separate semi-volatile compounds like TPH. The TPH concentration was measured by a GC (Perkin-Elmer, model Clarus 680, Beacons Field, UK) equipped with a flame ionisation detector (GC-FID), using an Agilent DB-TPH capillary column (30m × 0.25 mm × 0.25 μm). The injected volume into the GC was 1 μL. The oven temperature program was as follows: the initial temperature was held at 35°C for 2 min, and then was increased to 300°C with a rate of 15°C/min, and the temperature was held at 300°C for 2 min. The injector temperature was set at 310°C. Helium was used as a carrier gas with its pressure set at 14 psi. The detector temperature was set at 315°C. The GC conditions are summarised in Table 3-1.

Table 3-1: GC-FID (Perkin-Elmer, model Clarus 680, Beacons Field, UK) analytical conditions

Column	30m × 0.25 mm × 0.25 μm , Agilent DB-TPH capillary column
Sampler	1 μL injection, autosamler
Injection port temperature	310°C
Detector temperature	315°C
Oven temperature program	35°C for 2 min 15°C.min^{-1} to 300°C , holding for 2 min
Carrier gas	Helium
Total run time	21 min

TPH concentrations are defined as the sum of all peaks detected on gas chromatograms in the given retention time. Thus, an estimate of TPH includes not only various diesel components such as normal-, iso, cyclo-alkanes and aromatics, but also potential degradation products from oxidation reactions as long as they are detectable under the GC conditions used (Yu, 2007).

The identity of each marker was determined by comparison with the retention time of each n-alkane. For each alkane, the retention time window was defined as the absolute retention times plus or minus three times the standard deviation.

A retention time window was also considered for extractable petroleum hydrocarbons between the markers. In this project, the aliphatic hydrocarbons were divided into three parts, between the four markers of C9 (n-nonane), C16 (n-hexadecane), C22 (n-docosane), and C28 (n-octacosane), as listed in Table 3-2.

Table 3-2: n-Alkane markers

Hydrocarbon Range	Beginning Marker	Ending Marker
C9-C16 Aliphatic Hydrocarbons	Apex of n-Nonane	Apex of n-Hexadecane
C16-C22 Aliphatic Hydrocarbons	Apex of n-Hexadecane	Apex of n-Docosane
C22-C28 Aliphatic Hydrocarbons	Apex of n-Docosane	Apex of n-octacosane

The n-alkane markers on the chromatogram of a diesel sample after passing a silica chromatography column are shown by arrows on Figure 3-1.

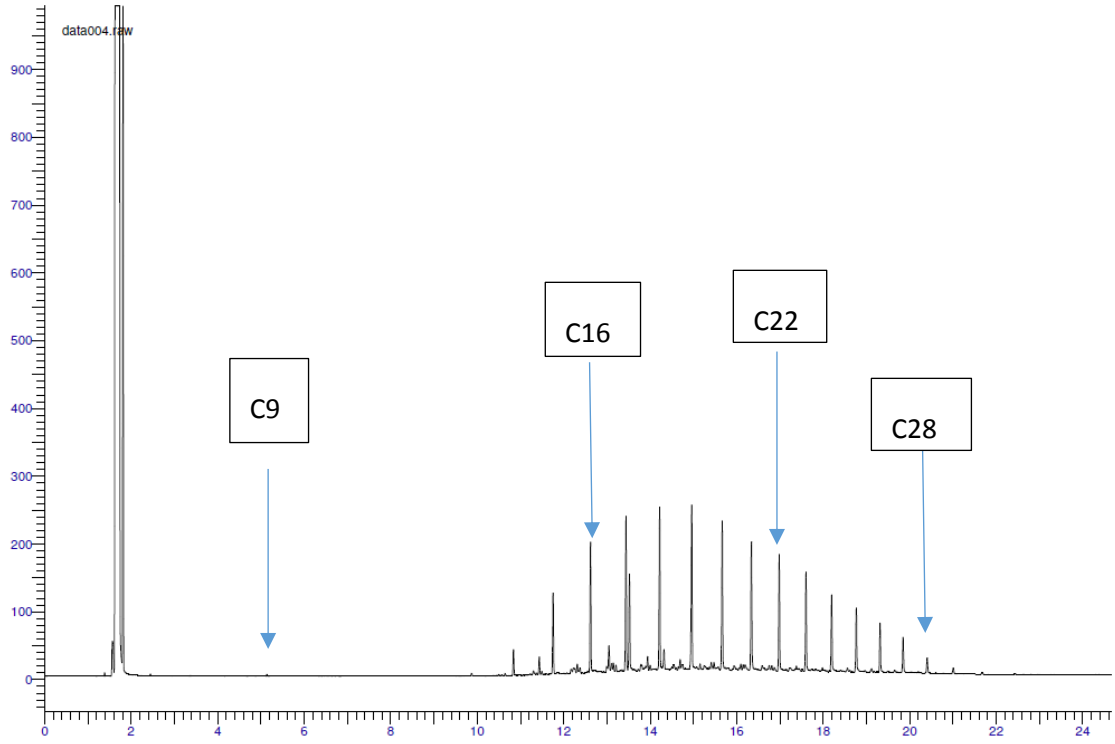

Figure 3-1: n-Alkane markers on the mixture chromatogram

For calculation of the concentration in the sample, a response factor (RF) for each hydrocarbon standard alkanes (nC9, nC16, nC22, nC28) within each of the 5-point calibration curve was calculated by Eq. (3-3). Then RF_{ave} would be achieved by Eq. (3-4).

$$RF = \frac{A_{n-alkane}}{C_{n-alkane}} \qquad \text{Eq. } (3-3)$$

Where:

$A_{n-alkane}$ is the area under the individual n-alkane peak, and $C_{n-alkane}$ denotes the concentration of the individual n-alkane standard

$$RF_{ave} = \frac{sum\ of\ individual\ RF\ values}{number\ of\ RF\ values\ used} \qquad \text{Eq. } (3-4)$$

The concentration of extractable petroleum hydrocarbons in the sample was calculated based on Eq.s (3-5), (3-6), and (3-7), as described in the reference method in the Canada wide standard for petroleum hydrocarbons (CCME).

$$C9-C16\ hydrocarbons\ \left(\frac{mg}{kg}\right) = \frac{A_{C9-C16} \times Vol}{RF_{ave} \times W_d} \qquad \text{Eq. } (3-5)$$

$$C16-C22\ hydrocarbons\ \left(\frac{mg}{kg}\right) = \frac{A_{C16-C22} \times Vol}{RF_{ave} \times W_d} \qquad \text{Eq. } (3-6)$$

$$C22-C28\ hydrocarbons\ \left(\frac{mg}{kg}\right) = \frac{A_{C22-C28} \times Vol}{RF_{ave} \times W_s} \qquad \text{Eq. } (3-7)$$

Where A_{C9-C16} is the integration of all area counts from the apex of the C9 peak to the apex of the nC16 peak, $A_{C16-C22}$ denotes the integration of all area counts from the apex of the C16 peak to the apex of the nC22 peak, $A_{C22-C28}$ shows the integration of all area counts from the apex of the C22 peak to the apex of the nC28 peak, Vol is final volume of the sample extract (mL), RF_{ave} is the average response factor, W_s is weight of sample taken (g).

3.4.5 H_2O_2 concentration assay

The H_2O_2 concentration was quantified by iodometric titration (Yap, 2012/b). Briefly, 3.00 g of sample was added to 200 ml of distilled water, and then 20.00 ml of potassium iodide solution and 25.00 ml of the acid mixture, were added in a 500 mL Erlenmeyer flask. The acid mixture was prepared by adding 0.18 g of ammonium molybdate tetrahydrate in 750 ml distilled water, then the addition of 300 ml of H_2SO_4. The sample in the Erlenmeyer flask was then

mixed and left to stand for 5 min. The mixture was titrated with standardized 0.1 N sodium thiosulfate solution until the brown triiodide colour changed to a light straw colour. A few drops of starch solution were added which changed the solution colour to blue and the titration was continued until the solution colour changed from blue to colourless. A blank sample was also passed through all the described steps above. H_2O_2 in the sample was calculated by Eq. (3-3).

$$\text{Hydrogen eroxide } \%\,{}^{W}/_{W} = \frac{(A-B)(0.1N)(1.7007)}{\text{sample weight}} \qquad \text{Eq. (3-3)}$$

Where A denotes titration volume for sample [L^3], B is titration volume for blank [L^3], and N is normality of $Na_2S_2O_3$. The results were reported as residue of H_2O_2, as shown in Eq. (3-4):

$$\frac{C}{C_0} = \frac{H_2O_2 \text{ concentration at time t (\% W/W)}}{H_2O_2 \text{ concentration at time 0 (\% W/W)}} \qquad \text{Eq. (3-4)}$$

3.5 Fourier-transform infrared spectroscopy

Fourier-transform infrared spectroscopy was performed to determine the functional groups in samples and analyses were performed to compare the functional groups in the HA extracted, soil, and the separated part of soil treated with EL. The separated fraction of treated soil is the collected part of EL treated soil that was on top of the soil sample after contact with EL for 2 h. Infrared spectra were recorded in frequency ranges in a wave number range of 4000 to 400 cm^{-1} by a FT-IR. The required amount of the sample was pulverized and located on the detector part.

3.6 Desorption experiments methodology

3.6.1 Extraction solvent tests

Choosing the best solvent is the first step and is considered as a preliminary step in sorption/desorption and Fenton experiments. Three commonly used solvents, dichloromethane (DCM), n-hexane, and acetone, were examined to choose the best solvent for use in an automated Soxhlet extractor (Gerhardt, SOXTHERM®, Germany) for extraction of TPH. 14-days contaminated soil, which was prepared at an initial concentration of 5000 mg/kg soil, was extracted using the Soxhlet extractor with the same method explained in Section 3.4.1 with the three different solvents specified above. To investigate the effects of aging on desorption and availability of TPH, the contaminated soil was extracted by DCM on 54, 82 and 262 days of contamination. To evaluate the effect of pre-treatment of soil by EL, one 82-days contaminated soil sample was directly extracted by DCM, and another 82-days contaminated soil sample was pre-treated by EL=10% for 10 min and then extracted by DCM. TPH in HA and humin parts were extracted following the method of Yang et al. (2010). The extract was passed through the silica gel column for fractionation and analysed via GC, as explained previously in Section 3.2.2 and 3.3.4. To compare the recoveries, the results of the extracted TPH were compared with fractionated diesel from column chromatography. All experiments were carried out twice and standard deviations were determined for results presentation in all figures.

3.6.2 Desorption experiments

Batch desorption experiments were carried out by placing 5 g of 14-days contaminated soil in a 50 mL beaker and adding 10 mL of distilled water

(L/S=2). Mixing was carried out by using a magnetic stirrer (Cole-Parmer, USA) at a speed of 350 rpm. The solutions were prepared by mixing 25%, 50%, and 75% by volume of EL with water and one solution of EL%=100%. The experiments were stopped at predetermined times until equilibrium had been achieved. Separation of soil and liquid was accomplished by centrifuging at 1700 rpm for 15 min. The soil portion was analysed to determine the remaining amount of diesel as described in Sections 3.2.1, 3.2.2, and 3.2.4 for TPH extraction, chromatography column fractionation and GC analysis. Batch desorption experiments for examining the effect of initial contamination level on desorption kinetic were conducted with three levels of initial contamination of 3500 mg/kg soil, 5000 mg/kg soil, and 10000 mg/kg soil at L/S=2, EL=25%, and mixing speed of 350 rpm. To examine the effect of L/S, batch desorption experiments were carried out at L/S=1, 2 and 4 at EL= 25%, and mixing speed of 350 rpm and soil with 5000 mg/kg soil initial contamination level. All experiments were repeated twice and standard deviations were determined for results presentation in all figures.

3.6.3 Kinetic modelling

Desorption of TPH from soil with different EL% was modelled by pseudo-second order rate equation. Typical second order rate equation is written based on the concentration in solution. Analogous to Ho (2006a/b) work, in utilizing the pseudo-second order rate equation for the desorbed amount in solution, the underlying assumption for desorption is that desorption rate is proportional with the driving force and capacity of solvent in desorbed contaminants. The equations used in modelling the desorption are shown by:

$$\frac{dq_{Lt}}{dt} = k_{p2}(q_{Le} - q_{Lt})^2 \quad \text{Eq. (4-1)}$$

Initial condition: $q_{Lt}(0)=0$

$$\frac{t}{q_{Lt}} = \frac{1}{V_0} + \frac{1}{q_{Le}}t \quad \text{Eq. (4-2)}$$

$$V_0 = k_{p2}{q_{Le}}^2 = \lim_{t\to 0}\frac{q_{Lt}}{t} \quad \text{Eq. (4-3)}$$

where t is time [T], q_{Lt} is the desorbed amount in solution at time t [M], V_0 is the initial desorption rate [MT^{-1}], k_{p2} is the psoudo-second-order rate constant [$M^{-1}T^{-1}$], and q_{Le} is equilibrium desorbed amount in solution [M]. Based on Eq. (4-2), $\frac{t}{q_{Lt}}$ is linear versus t. It was proven by Azizian (2004) that k_{p2} is a complex function of initial concentration of solute, equilibrium molar concentration of solute, and the coverage fraction.

3.7 Fenton reaction methodology

3.7.1 EL-Fenton reaction and reaction with zero-valent iron nanomaterials

EL-Fenton reaction was carried out batchwise in a 50 ml beaker by placing H_2O_2, EL and water solution at the predetermined L/S (V/W) and EL% conditions, at natural pH=2.7, which was measured. Fe^{2+} was supplied by weighing and adding the required amount of $FeSO_4.7H_2O$ to provide the predetermined Fe^{2+} molarity in the solution. Then, 5 g of 5000 mg/kg 1-month aged contaminated soil was added first followed by 0.1% $HgCl_2$ solution to stop biological degradation. Then, the slurry was mixed with a magnetic stirrer (Cole-Parmer, USA) at a speed of 350 rpm. The reaction was stopped at different times by adding H_2SO_4 to lower the pH to less than 1 (Lee et al., 2001) to determine the remaining TPH in soil at a specific time to study the reaction

kinetic. Finally, the mixture was separated by centrifuging. The solid phase was separated to analyse the amount of TPH, as it is explained in sections 3.2.2 and 3.2.4.

To examine the effect of L/S, EL%, and H_2O_2, experiments were carried out by keeping two of the variables constant and changing the third variable. For each set of experiments Fe^{2+} was kept constant. Experiments for constant H_2O_2=4 M, Fe^{2+}=0.05M, and L/S=2 were conducted at different EL%=0%, 25%, and 50%. Constant EL%=25%, Fe^{2+}=0.05M, and L/S=2 were accompanied by different H_2O_2=0.1 M, 0.5 M and 2 M. Changes in L/S=1, 2 and 5 were tested at fixed H_2O_2=0.5 M, Fe^{2+}=0.05M, and EL%=25%.

Reactions with zero-valent iron were carried out as described above with the exception of adding zero-valent iron nanomaterial (with Fe^{2+}=0.28g/gsoil and 0.14g/gsoil) at 0, 0.02, 0.05, 0.1 mg/gsoil, H_2O_2=0.5 M and L/S=2. All experiments were conducted twice and standard deviations are presented for data in all figures.

3.7.2 Fenton reaction with HA

HA solutions were prepared by dissolving the appropriate amount of HA in distilled water. The pH of the solution was adjusted by adding 0.1 M NaOH. Afterwards, the solution in each reaction was brought to the predefined pH by adding 1 M, 0.2 M H_2SO_4 or 0.1 M NaOH. The Fenton reactions at different HA dosages and with and without EL were conducted in a batchwise manner. The Fenton reaction was performed with H_2O_2=0.5M and Fe^{2+}=0.05M for all experiments. The pre-calculated amounts of HA with H_2O_2 and water, with EL in cases with this solvent, comprised the liquid phase. Fe^{2+} was added to this

liquid phase and subsequently, a 1.5-month aged contaminated soil at 5000 mg/kg soil contamination level was added at L/S=2. To stop biological degradation, 0.1% $HgCl_2$ solution was added to the reactor. The pH was adjusted whenever it was required. At predetermined times, the reaction was terminated by adding H_2SO_4 solution to bring the pH lower than 1. The amount of remaining diesel in soil was determined following the method explained in sections 3.2.2 and 3.2.4.

3.7.3 EL-Fenton reaction kinetic modelling

The power law kinetic and pseudo-first order kinetic equations for Fenton reaction were used to model the kinetic data obtained from the experiments. The power law equation is as follows:

$$q_t = K_p t^{-m} \qquad \text{Eq.(5-12)}$$

where K_p is rate constant of reaction, q_t(mg) is the amount of hydrocarbon in soil at time t (min), and m is a constant.

The pseudo-first order reaction is defined in Eqs. (5-13) and Eq.(5-14), with the initial condition of $q_t = q_0$ at t=0.

$$\frac{dq_t}{dt} = -k(q_t - q_e) \qquad \text{Eq. (5-13)}$$

$$q_t = q_e + (q_0 - q_e)e^{-kt} \qquad \text{Eq. (5-14)}$$

where k, (min^{-1}) is the pseudo-first order kinetic constant, q_e, (mg), is the amount of hydrocarbon in the solid phase, soil, at equilibrium, and q_0, (mg), is the initial amount of hydrocarbon in the solid phase.

3.8 Methodology of optimization using RSM

For RSM design, the results from the parametric batch study described earlier and information from the literature were used. Based on the studied variables, L/S=2 was chosen as the fixed value because it had a high removal efficiency. The value of H_2O_2 was fixed at 0.5 M as it was shown that an increase in H_2O_2 of more than 0.5 M had not increased the removal efficiency considerably. EL% was considered as one of the variables for the RSM analysis, because it is the main focus of this study and determining its interactions with other variables are important. The range of pH was chosen based on the reported values in papers and as discussed before, Fenton reaction with Fe^{2+} is possible in acidic range, pH=3-5, and by adding HA, the range of the pH increases. The EL% range was based on the results within the range of 10%-60%. The chosen HA range corresponded to the values that were more or less than the case without HA.

The removal efficiency of Fenton reaction was analysed and optimised by RSM. A central composite design (CCD) with three independent factors was used to measure the effect of variables on the Fenton reaction removal efficiency. The three factors were HA (A), EL % (B), and pH (C). The number of experiments was 20, (2^k+2k+ 6) where k is the number of factors and equals 3. The responses of different fractions were formulated by linear, quadratic, and interaction terms. The overall equation and the related formula are described in Appendix 1. The Design-Expert 7.1 software was used to analyse and plot response surface and experimental data.

3.9 Column set-up methodology

Column experiments were carried out with 150 g 1.5 month aged soil at 5000 mg/kg contamination level using column with a height of 25 cm and 2.5 cm inner diameter. The experiments were initiated by adding Fenton reagents solution in water with EL and 0.05 M iron solution, and 0.1% $HgCl_2$ to the top of the column. Sufficient time was given such that all mobile liquid phase eluted from the column. After finishing experiments, the soil inside the column was divided into 5 equal sections with numbering from the top as the first section, and HCl was added to each section to bring the pH below 1 to quench the reaction. From each section, sampling was carried for extraction and GC analysis of remaining TPH in the soil according to Section of 3.2.1 and 3.2.4.

The studied variables were EL%, overall L/S (instead of the contact time), and H_2O_2 at constant Fe^{2+} concentration. By keeping two of three variables constant, the remaining variable was changed. At constant L/S, Fe^{2+}=0.05 M, and EL%, H_2O_2 values were 0.1 M, 0.5 M, and 2 M. L/S values were 1/3, 1/2, 1 at Fe^{2+}=0.05 M, H_2O_2=0.5 M, and EL=10%. Values of Fe^{2+}=0.05 M, H_2O_2=0.5 M, and L/S=1/2 accompanied the change in EL% with values of 0%, 10%, 25%, and 50%. All experiment were conducted two times, in the wet laboratory of University of Nottingham. The ranges of H_2O_2 and EL% have been chosen based on the results in batch experiments. L/S was chosen based on preliminary experiments, and as will be discussed later, an increase in L/S from 1/2 to 1 had not changed the results considerably. Hence, L/S=1 was determined as the maximum value in its range.

3.10 Concluding remarks

This chapter has outlined all the analytical methods crucial to the research work. Soil characteristics have been determined prior to starting the main experiments. Properties such as soil texture, iron content, SOM %, moisture, and acidity were determined according to methods from organisations such as US EPA, or other mentioned scientific papers in each relevant section. The results of GC calibration with high R^2, coefficient of correlation, showed the credibility of the applied analysis for TPH. The procedures will be used to obtain data for subsequent desorption, batch and column studies.

CHAPTER 4: DESORPTION OF TOTAL PETROLEUM HYDROCARBONS FROM SOIL USING ETHYL LACTATE

4.1 Introduction

One approach for soil treatment is dissolving the contaminants in a solvent. Among different decontamination methods, solvent extraction is considered as an effective way for remediation of oil-contaminated soil (Gong et al., 2007). Solvent extraction applies a solvent or mixture of solvents for removing hazardous and harmful pollutants from soil. Determining desorption rate is important for predicting the transport of the contaminants in the field and its bioavailability (Birdwell et al., 2007). Desorption and kinetic rate of aromatic hydrocarbons like PAH in soils have been widely studied in the last two decades (Connaughton et al., 1993; Ghosh et al., 2001; Loehr et al., 2003; Shor et al., 2003; Gong et al., 2005 a/b; Haddadi et al., 2009; Yang et al., 2013; Barnier et al., 2014). However, the aliphatic part has been lesser studied.

This chapter aims to examine the applicability of EL as a green solvent for desorption of diesel range of TPH and to determine the associate desorption kinetics. Most commonly used organic solvents are volatile with known effects on global warming (Aparicio et al., 2009/b). EL which is a clear and colourless liquid of low volatility and complete miscibility with water and most organic solvents is considered as a green solvent. To date, to the authors' best knowledge, the potential of EL to desorb aliphatic part of diesel fractions from contaminated soil has not been reported. In this phase of study, the effect of

sequestration on diesel removal from soil as well as a comparison between different solvents in desorption of diesel from soil were firstly carried out. Subsequently, batch desorption experiments were conducted as the main focus of this chapter to evaluate the effect of increase in EL% on TPH desorption. The effect of EL%, initial soil contamination level, and liquid to solid ratio (L/S (v/w)) on initial desorption rate as defined by pseudo-second order kinetics equation was also examined.

4.2 Results and Discussion

4.2.1 Soil characteristics

Table 4-1 lists the properties of the model soils. The texture of soil was determined as sandy loam. The iron content in soil was more than the typical range of 0.5-5% (Yap, 2012/b). The amount of iron, 63.1 mg/g soil, was also more than most reported values between 17.3 mg/g soil (Kawaraha, et al. 1995) and 45 mg/g soil (Kong et al., 2005). The measured amount of SOM was considered high. As there are controversial arguments regarding the importance of SOM in soil remediation process, which will be discussed later in Chapter 5, the high value of SOM provided the opportunity to study the effect of SOM, or its fraction. The high percentage of SOM leads to higher diffusion of contaminants into the soil which affect their accessibility especially with aging. The high Fe content in this sample can be due to the mining activities which were done nearby, it was noticed in that area, as it was also reported by Koranteng – Addo, et al. (2011).

Table 4-1 Soil sample physicochemical properties

Properties	Values[a]
Sand (%)	68
Silt (%)	13.1
Clay (%)	18.9
Iron content (mg/g soil)	63.1±0.01
Moisture (%)	4.2±0.06
(pH_{H2O}) pH in water at 23±0.1°C	5.1±0.03
(pH_{CaCl2}) pH in 0.01 M CaCl2 at 23±0.1°C	4.3±0.02
SOM, loss on ignition (%)	10.32±0.009
SOM, TGA (%)	11.8

[a]Average of two determinations with standard deviation

4.2.2 Calibration results

The retention time windows of four alkanes are shown in Table 4-2.

Table 4-2: Retention time window of individual n-alkanes

Compound (n-Alkane)	Retention Time Window (min)
	Single Calibration
n-Nonane (C9)	5.15±4.26 [a] %
n-Hexadecane (C16)	12.58±5.5 [a] %
n-Docosane (C22)	16.91±5.94 [a] %
n-Octacosane (C28)	20.33±0.36 [a] %

a: absolute retention time±3 times the standard deviation

The calculated RF for each n-alkane and the average value are tabulated in Table 4-3.

Table 4-3: RF and RF_{ave} values

n-alkane Compound	*RF*
C9 (n-Nonane)	359.4
C16 (n-Hexadecane)	368.8
C22 (n-Docosane)	290.84
C28 (n-Octacosane)	250.3
Average RF_{ave}	318.1

4.2.3 Extraction solvent

A comparison between the most commonly used organic solvents for extraction of TPH was carried out to choose the most favourable solvent with the highest recovery of analytes. Figure 4-1 shows the comparison of extracted amount of aliphatic diesel fractions (C9-C16, C16-C22, C22-C284, TPH) from soil using three different solvents with diesel. The TPH reported in Figure 4-1 is the summation of solvent extractable TPH via Soxhlet extraction and TPH in humin since the TPH in HA and FA were not detectable by GC. As can be deduced from the data, DCM had the highest desorbed recovery followed by n-hexane, and finally acetone with the least desorbed values. The difference in recovery between acetone and n-hexane was mainly because of fraction 2. Similarly, the same fraction was responsible for the main difference between DCM and n-hexane. This trend of fraction 2 >fraction 3 >fraction 1 was the same for all three solvents as well as diesel.

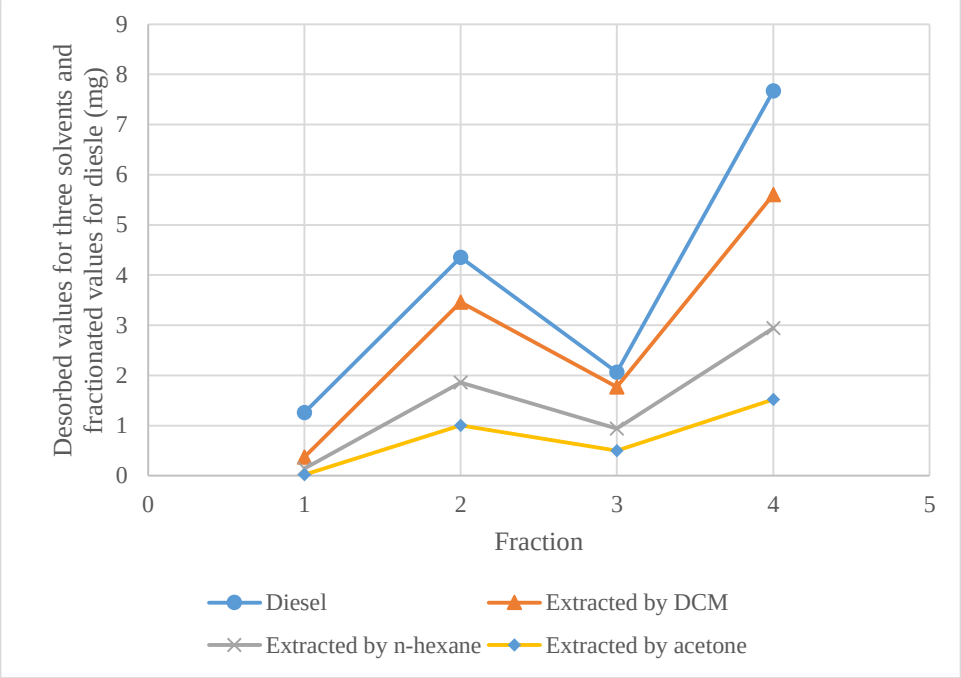

Figure 4-1. Comparison of extracted amount of aliphatic diesel fractions from soil using three different solvents with diesel (Fraction 1: C9-C16, Fraction 2: C16-C22, Fraction 3: C22-C284, Fraction 4: TPH)

The percentage extraction of aliphatic diesel from soil by these solvents were compared with the fractionated diesel used. Table 4-4 tabulates the results of the comparison. With a TPH extraction of 73.03% of initial diesel used for contamination, DCM had the highest extracted value in comparison with n-hexane and acetone with 38.39% and 19.79%, respectively. Therefore, DCM was chosen as the solvent for Soxhlet extraction. The difference between 86.84% and complete recovery was likely caused by analyte losses on the walls of the container, evaporation, or biodegradation.

Table 4-4: Percentage of aliphatic diesel fractions and TPH extraction by different solvents

	(DCM/diesel)%	(n-Hexane/diesel)%	(Acetone/diesel)%
Fraction 1	29.64	11.15	1.46
Fraction 2	79.42	42.77	23.00
Fraction 3	86.00	45.77	24.19
TPH	73.03	38.39	19.79

The solvent extractable fraction by DCM and the fraction diffused in humin are reported in Table 4-5. After Soxhlet extraction by DCM, the remaining TPH on humin fraction was 2.455% of the solvent extractable part for 14-days contaminated soil. This small value had been neglected in analysing the TPH.

Table 4-5: Aliphatic diesel and TPH in solvent extractable and humin fractions of DCM extracted soil for 14-days contaminated soil

	Solvent extractable (mg)	Humin (mg)	Humin/Solvent extractable%
Fraction 1	0.675	0.003	0.403
Fraction 2	3.305	0.053	1.602
Fraction 3	1.400	0.076	5.455
TPH	5.380	0.132	2.455

Figure 4-2 illustrates the solvent extractable fraction from soil by DCM with different contamination age. With passing time, the solvent extractable fractions decreased. This loss could possibly be attributed to TPH diffusion into organic matter (FA, HA, and humin) (He et al., 2008; Yanng et al., 2010), or biodegradation.

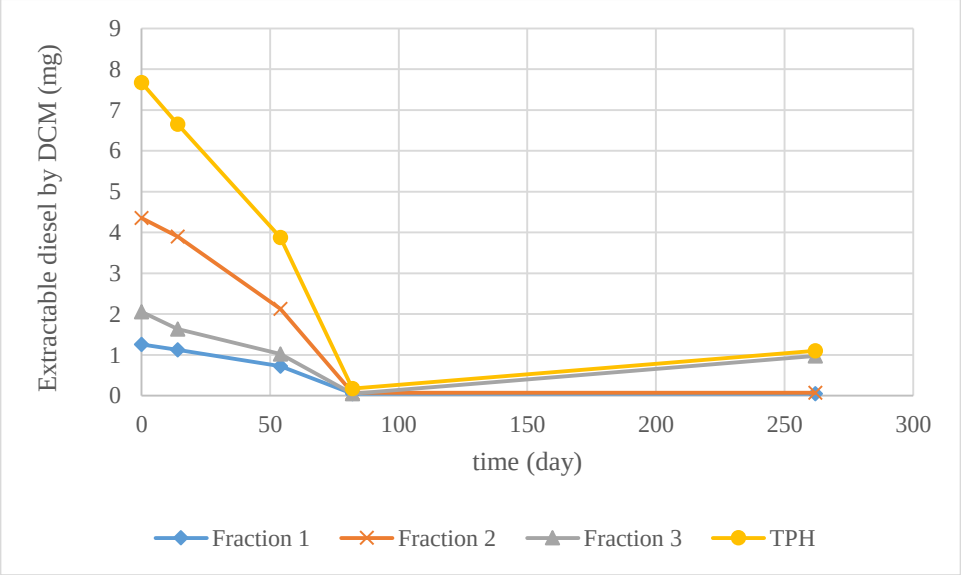

Figure 4-2: Solvent extractable fraction from soil by DCM with different contamination age

The effect of EL on desorption from 82-days aged soil was also evaluated by pre-treating the contaminated soil with EL=10% solution for 10 min, and subsequently extracting with DCM. The results were compared with direct soil extraction using DCM and are summarized in Table 4-6. As can be seen, the desorbed value from 10 min pre-treated soil by solution of EL%=10% was 1.993 mg while DCM could desorb 1.104 mg of TPH from soil with the same contamination age. This indicated that diesel had diffused into the organic part of soil which reduced the availability of the pollutant (Barnier et al., 2014), and formed non-extractable fractions by binding with recalcitrant organic matters such as HA (He et al., 2008). With passing time and aging, the extractability of TPH had decreased. This agrees with the findings of Ncibi et al. (2007) and Northcott et al. (2001) who observed that aging had decreased the availability of PAHs. This observation was probably because contact with EL=10% solution for 10 min disintegrated a part of the soil, or diffused into that part of soil that DCM was not able to extract via Soxhlet extraction. The separated black part of

soil accumulated on top of the soil after treatment with EL=10% solution indicated the separation of humic matter which was a sign of the possibility of organic matter breakdown which was accessible after treatment with EL. As it is reported by Kosaka et al. (1961) that some organic solvents can dissolve humic matter, it is possible that EL can dissolve or separate some part of organic matter. Therefore, it is likely that EL has the ability to access to parts of soil that is inaccessible by DCM. This shows the potential of EL as a desorption solvent for TPH in contaminated soils.

Table 4-6: Effect of soil pre-treatment by EL on Soxhlet extraction efficiency using DCM for aged soil

	Day	Fraction 1	Fraction 2	Fraction 3	TPH
Soxhlet extraction of soil using DCM (mg)	82	0.241	0.715	0.148	1.104
Soxhlet extraction of 10 min pre-treated soil by 10% EL using DCM (mg)	82	0.254	1.327	0.412	1.993

4.2.4 EL and desorption process

In examining the effect of increase in EL% from 25% to 100%, batch desorption experiments were carried out with soil at 5000 mg/kg soil initial contamination level. Figure 4-3 depicts the removal efficiency of diesel or TPH remaining in soil. As can be observed, desorption of TPH was characterized by a very fast initial stage followed by a much slower stage until equilibrium. The slow stage and equilibrium is usually attributed to organic matter diffusion or diffusion through the hydrophobic micropores (Cornelissen et al., 1998). The very fast initial stage of desorption demonstrated the high desorbing ability of EL for TPH in soil. For solutions of EL%=25% (which was very close to EL=0%) and EL%=100%, 35.78% and 82.45% of TPH desorption were achieved in 30 min, respectively. Meanwhile, the TPH equilibrium desorption values for EL%=25% and EL%=100% were 49.98% and 94.79%, respectively. This meant that 71.60% for EL%=25% and 86.98% for EL%=100% of TPH equilibrium values were achieved in 30 min. The other point that could be deduced from the experimental data is that by increasing the EL%, the equilibrium value of removal efficiency of TPH in soil had increased. This could be linked to the increasing EL% enabling more available solvent desorption ability.

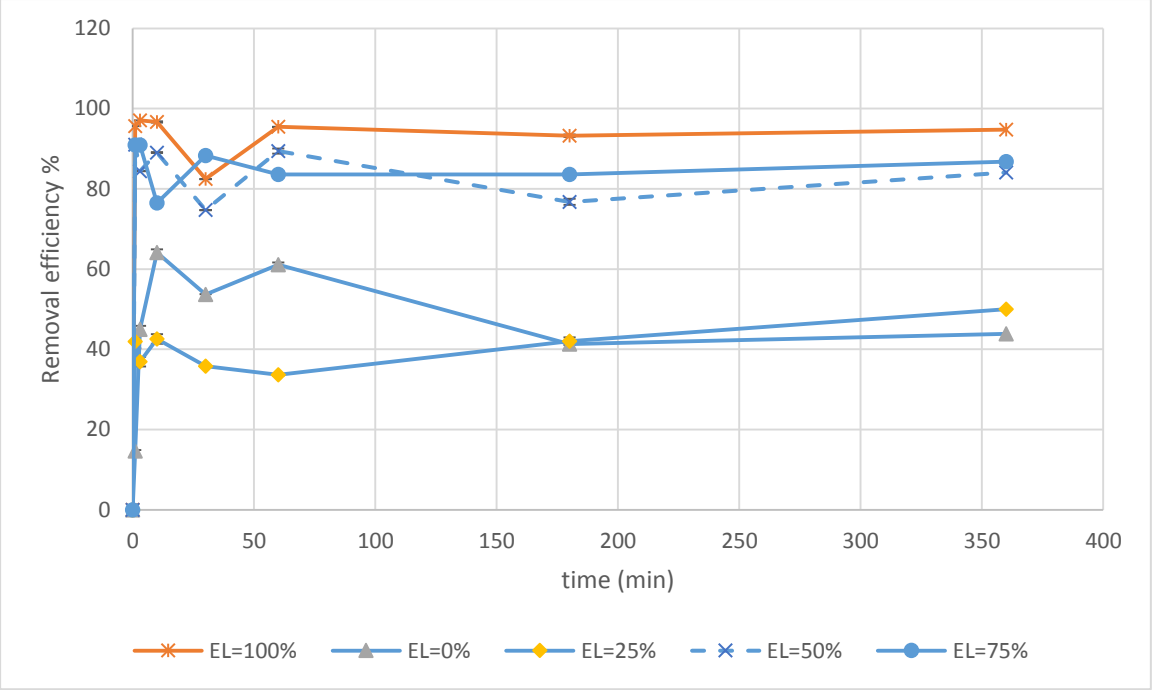

Figure 4-3: Desorption experimental data for 5000 mg/kg soil at L/S=2 with different EL%

It could be observed that desorption process experienced fluctuations as shown in Figure 4-3. The observed fluctuations indicated a dynamic adsorption-desorption processes. This meant that the desorbed amount from the soil in the solvent was partially adsorbed again by soil, which indicated that the driving force for desorption was not high enough to inhibit the re-adsorption onto the soil (Johnson et al., 2001). This process could be related to the high adsorption capacity of soil due to its high organic content which is considered as the fraction of soil which provides uptake potential of hydrophobic hydrocarbons (He et al., 2006). The observed data could also be explained by different compartments within the soil with different contaminant sorption affinity. When a part of TPH in soil is not accessible to solvent, it is likely that the contaminant level in the soil is close to zero whereas the amount in solution is higher than the amount in soil. Mass transfer would then be towards the soil instead of the

solution hence diesel would be adsorbed onto the soil until a point at which the direction of mass transfer and driving force changes. Each cycle will end when another compartment becomes accessible. The cycles will continue until equilibrium is reached. Thus, it can be concluded that EL is recyclable as soil can re-adsorb the TPH.

The experimental kinetic data were modelled using pseudo-second order rate equation for three aliphatic diesel fractions and TPH. The obtained results for the three fractions and TPH for different EL% are presented in Figure 4-4. For all fractions and all EL%, the pseudo-second order model fitted the experimental desorption data well with good correlation coefficient values of R^2 between 0.8899-0.9999.

4.2.5 Effect of EL%, initial contamination level, and L/S on initial desorption rate on each fraction

Table 4-7 lists the calculated variables from the pseudo-second order kinetic modelling by curve fitting with Excel 2013. The results were fitted with Elovich equation and first-order rate equation as1 well, but correlation coefficients were not satisfying. By increasing the EL% from 25% to 100%, the initial desorption rate for TPH increased which could be explained by the increased desorption ability of the solvent in the solution. q_{Lt} had increased from the EL=25% to EL=100%.

The effect of initial contamination level on the initial desorption rate at L/S=2 and EL=25% can be seen in Figure 4-5. The data obtained showed that 3500 mg/kg soil had the highest initial desorption rate. In contrast, further increase from 3500 mg/kg to 5000 mg/kg resulted in a decrease in initial desorption rate

from 4.75 mg/min to 0.30 mg/min for TPH. However, further increase from initial contamination level of 5000 mg/kg soil to 10000 mg/kg soil had led to a slight decrease to 0.12 mg/min. It is plausible that the TPH solution concentration for 3500 mg/kg soil was less than 5000 mg/kg soil which led to the higher capacity of the solution for desorbing TPH. Conversely, an increase from 5000 mg/kg soil to 10000 mg/kg soil did not change the capacity of solution for desorbing the contaminants. This could be due to the accessible fraction of contaminates for the solvent. Fraction 3 of all three initial contamination levels had very close initial desorption rates which was followed by fraction 1 and finally fraction 2 which had the most difference between the 3500 mg/kg soil and 5000 mg/kg soil. The reason why fraction 1 had a lower initial desorption rate than fraction 2 despite its lowest molecular weight could be because of the small number of hydrocarbons that were classified in this group. Although aliphatic hydrocarbons between C9-C16 had been considered in this group, after desorption experiment and Soxhlet extraction, only aliphatic hydrocarbons between C14-C16 were detectable by GC. In addition, as initial desorption rate was representative of the desorbed amount per unit time, the amount was significant in addition to how fast it desorbed. Fraction 2 had a higher initial desorption rate than fraction 3, which could be attributed to its lower molecular weight.

Figure 4-6 illustrates the effect of L/S on the initial desorption rate of 5000 mg/kg soil using EL=25%. As depicted, the initial desorption rate at L/S=2 was the lowest in comparison to L/S=1 and L/S=4. It could be expected that with the increase in L/S, the increase in liquid amount would lead to more solution ability to desorb and contain the contaminants, as observed by the increase in L/S from

2 to 4. However, at L/S=1, fractions 1, 2, 3 and TPH had the highest initial desorption rate (0.132 mg/min, 2.496 mg/min, 6.930 mg/min and 4.550 mg/min, respectively). The equilibrium time of batch desorption experiment at L/S=1 was 30 min. For L/S=2 and L/S=4, the equilibrium time was 60 min. The results here indicated that apart from molecular weight of contaminant and solvent desorption ability, the initial desorption rate was a function of equilibrium time as well. The difference between L/S=1 and L/S= 2 and 4 increased with increase in molecular weight from fraction 1 to 3.

	Fraction 1	Fraction 2	Fraction 3	TPH
a.	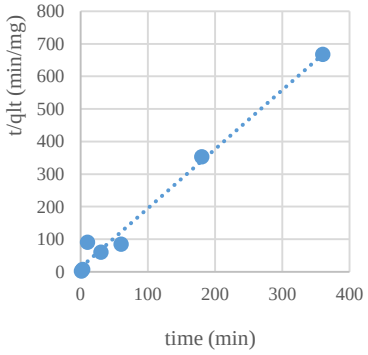	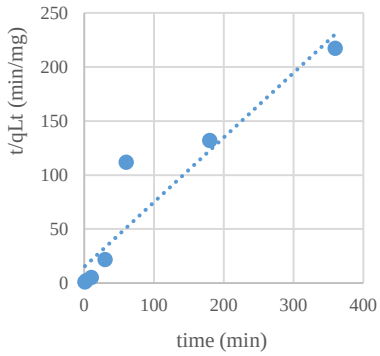	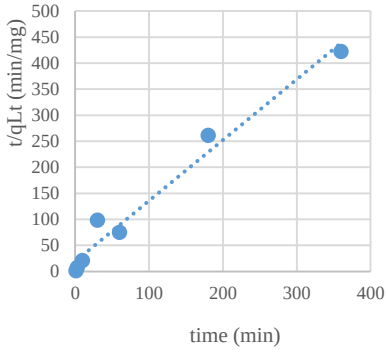	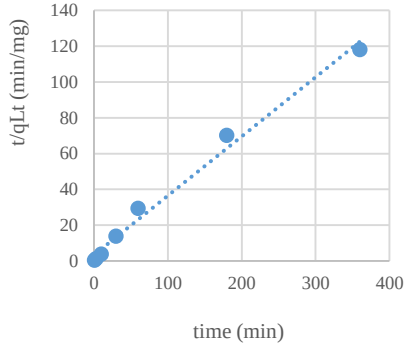
b.	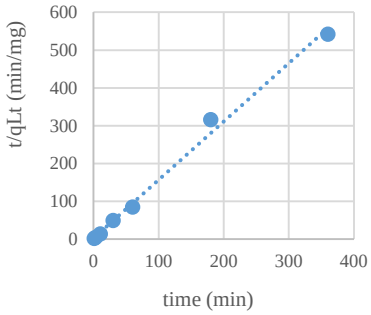	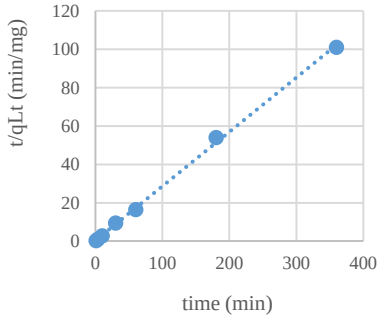	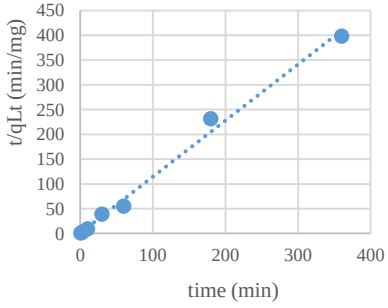	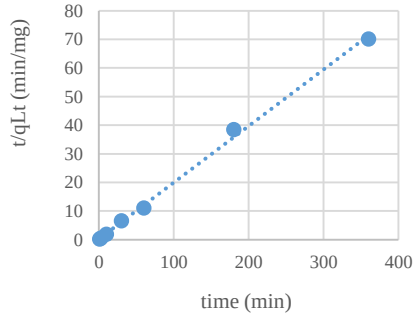

Figure 4-4: Pseudo-second order kinetic models for desorption experiments for 5000 mg/g at L/S=2; a) 25% EL, b) 50% EL, c) 75% EL, d) 100% EL

c.	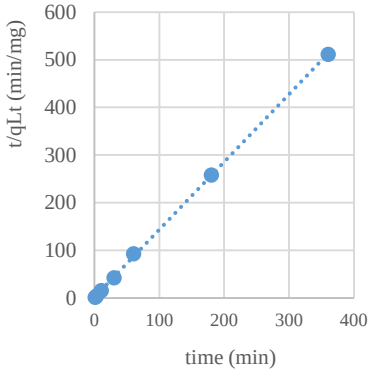	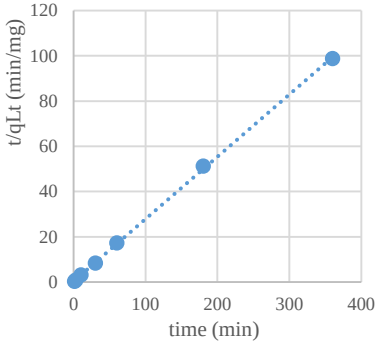	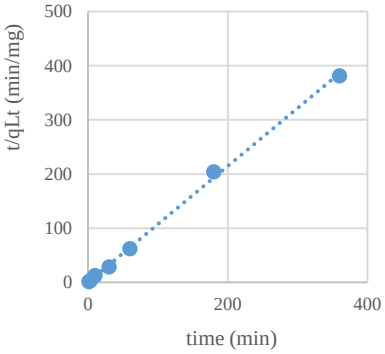	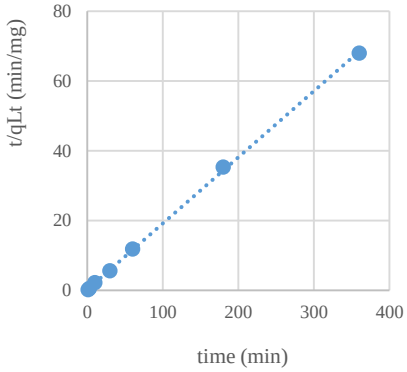
d.	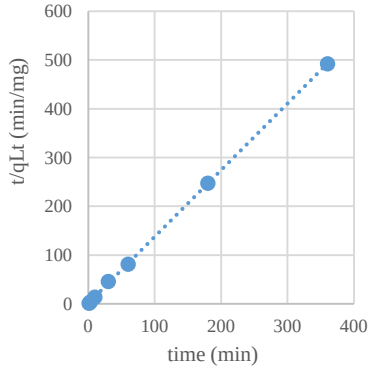	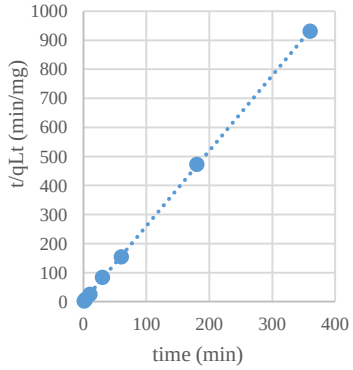	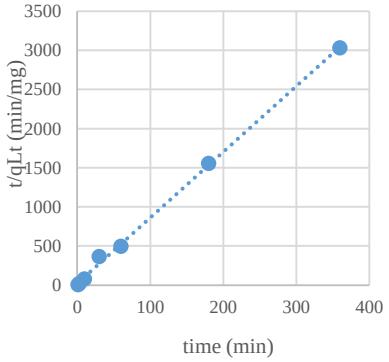	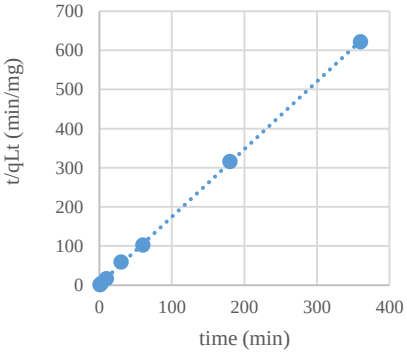

Continued Figure 4-4: Pseudo-second order kinetic models for desorption experiments for 5000 mg/g at L/S=2; a) 25% EL, b) 50% EL, c) 75% EL, d) 100% EL

Table 4-7: Calculated parameters and variables from the pseudo-second order kinetic modelling for 5000 mg/kg soil at L/S=2; a) 25%, b) 50, c) 75%, d) 100%

EL%	Parameters and variables	Fraction 1	Fraction 2	Fraction 3	TPH
a) 25%	**Vo (mg/min)**	0.076	0.066	0.052	0.297
	q_{Le} (mg)	0.550	1.671	0.858	3.020
	k_{p2} ((mg.min)$^{-1}$)	0.250	0.024	0.071	0.033
	R^2	0.9848	0.8899	0.9724	0.9885
b) 50%		**Fraction 1**	**Fraction 2**	**Fraction 3**	**TPH**
	Vo (mg/min)	0.427	2.836	1.021	4.428
	q_{Le} (mg)	0.633	3.533	0.882	5.064
	k_{p2} ((mg.min)$^{-1}$)	1.064	0.227	1.313	0.173
	R^2	0.9936	0.9988	0.9925	0.9976
c) 75%		**Fraction 1**	**Fraction 2**	**Fraction 3**	**TPH**
	Vo (mg/min)	0.645	2.943	4.475	5.274
	q_{Le} (mg)	0.704	3.635	0.933	5.271
	k_{p2} ((mg.min)$^{-1}$)	1.300	0.223	5.135	0.190
	R^2	0.9998	0.9997	0.9986	0.9996
d) 100%		**Fraction 1**	**Fraction 2**	**Fraction 3**	**TPH**
	Vo (mg/min)	1.067	0.596	0.047	0.608
	q_{Le} (mg)	0.732	0.386	0.119	0.578
	k_{p2} ((mg.min)$^{-1}$)	1.990	3.997	3.292	1.818
	R^2	0.9990	0.9999	0.9985	0.9998

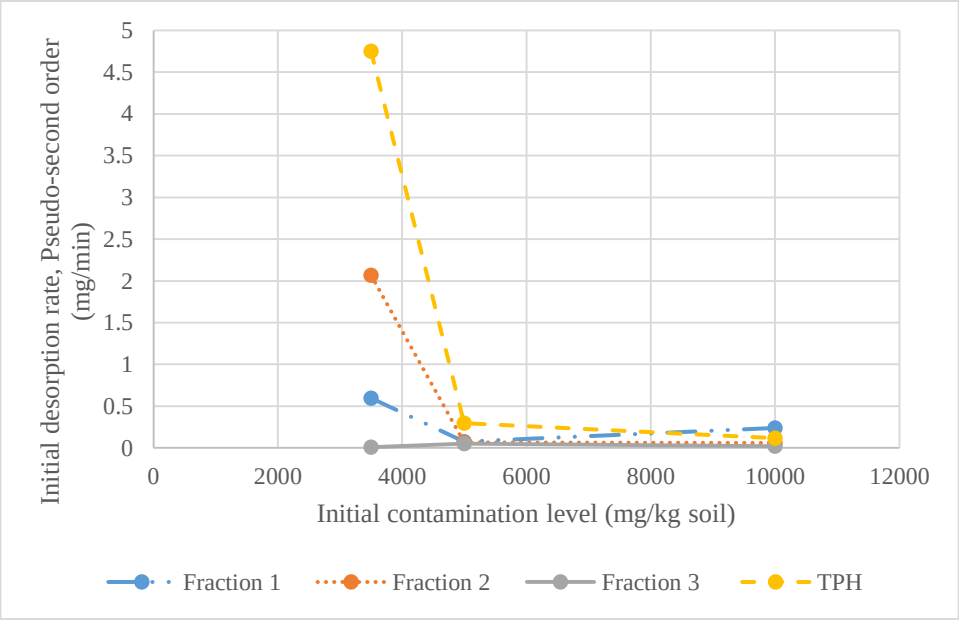

Figure 4-5: Effect of L/S on initial desorption rate at EL=25% for 5000 mg/kg soil

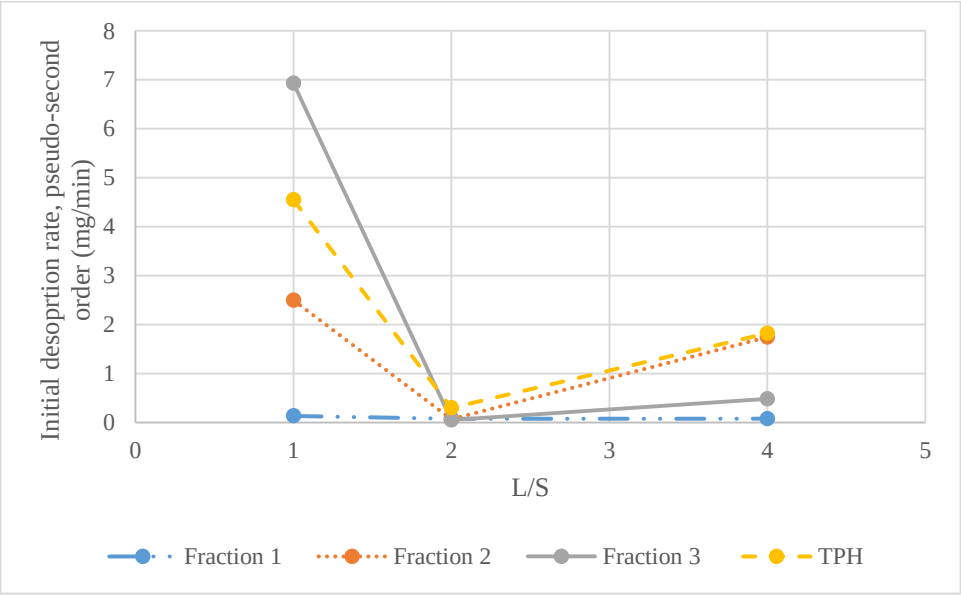

Figure 4-6: Effect of initial contamination level on initial desorption rate at L/S=2 and EL=25%

4.3 Concluding Remarks

This chapter has evaluated the effect of EL on desorption of aliphatic diesel fractions and TPH from contaminated soil. An increase in EL% increased the desorption of TPH from contaminated soil. Desorption was characterised by a very fast initial stage followed by the slower stage till equilibrium. In 30 min, EL=25% desorbed 63% of TPH while EL=100% desorbed 81% of TPH from soil. The desorption ability of EL shown by the very fast initial desorption indicated its feasibility for treatment of diesel contaminated soil. Desorption kinetics were well described by pseudo-second order model. The initial desorption rate increased from 1.625 mg/min to 3.368 mg/min for TPH with an increase in EL % from 25% to 100%, respectively. EL also showed the potential of accessing TPH which has diffused into organic matter in aged soil. In summary, the potential of EL as a green solvent for desorption of TPH from contaminated soil has been demonstrated.

CHAPTER 5: ETHYL LACTATE-FENTON BATCH STUDIES FOR REMEDIATION OF TPH-CONTAMINATED SOIL

5.1 Introduction

Contamination of soil by petroleum hydrocarbons has long been recognised as a health and environmental problem. Oxidation of TPH by O_3 and H_2O_2 is one of the most successful soil remediation approaches that have been reported in the literature (Lee et al., 2002; Yu et al., 2007; Wu et al., 2013; Sui et al., 2014). In particular, several researchers have highlighted Fenton reaction as a highly effective and efficient remediation method for destruction of hydrocarbons by oxidation (Watts et al., 1996; Watts et al., 2000; Neyens et al., 2003).

Combining different processes, which focus on different parts of the sorption-desorption processes, as well as the oxidation process could effectively improve the overall efficiency of the remediation process. The combination of Fenton reaction with surfactants to increase the solubility (Isosaari et al., 2001; Bandala et al., 2008), and with bioremediation process (Rivas et al., 2009; Lu et al., 2010) are specific examples of this combined approach. Combining Fenton reaction with solvent extraction is now recognized as a successful soil remediation strategy (Lundstedt et al., 2006; Jalilian et al., 2017). This is because destroying adsorbed contaminants is more difficult than destroying contaminants in solution (Bogan et al., 2003). By applying a solvent, the dissolution rate of contaminants will increase. In dissolved form, destruction of contaminants by Fenton reaction will be more efficient.

In light of the developments in combining Fenton reaction and solvent extraction, EL is the solvent of interest to be used in conjunction with Fenton reaction in this study. As the aim of soil remediation is to decrease contaminants levels and their environmental side effects, a green solvent such as EL is suitable. This chapter describes the batch experiments carried out in order to determine the effects of H_2O_2, liquid phase volume to soil weight ratio (L/S), and EL% on aliphatic fraction of TPH removal efficiency after soil treatment. The experimental kinetic data obtained were analysed by the ability law and pseudo-first order equations. Furthermore, tests were carried out to investigate how HA affects the removal efficiency of Fenton reaction in the absence and presence of EL. Response surface method (RSM) was finally used to determine the interactions between the involved variables after fixing L/S and H_2O_2 based on the parametric studies.

5.2 Results and Discussion

5.2.1 The removal efficiency of Fenton reaction

5.2.1.1 Effect of H_2O_2 concentration on removal efficiency

In Figure 5-1, the effect of H_2O_2 concentration on removal efficiency results has been depicted. With increasing H_2O_2 from 0.1 M to 0.5 M, the removal efficiency for TPH increased significantly from 68.41% to 85.76% after 4 h. In contrast, an increase in H_2O_2 from 0.5 M to 2 M increased the removal efficiency from 85.70% to 89.23% only from 85.76% to 90.21% for TPH after 4 h. Hence, increasing H_2O_2 from 0.5 M to 2 M, a four-fold increase, had not improved the removal efficiency considerably; Xu et al. (2006) have also reported similar

results. This observation could be linked to an excess of H_2O_2 at concentration above 0.5M for Fe^{2+}=0.05M which was not practically involved in the reaction.

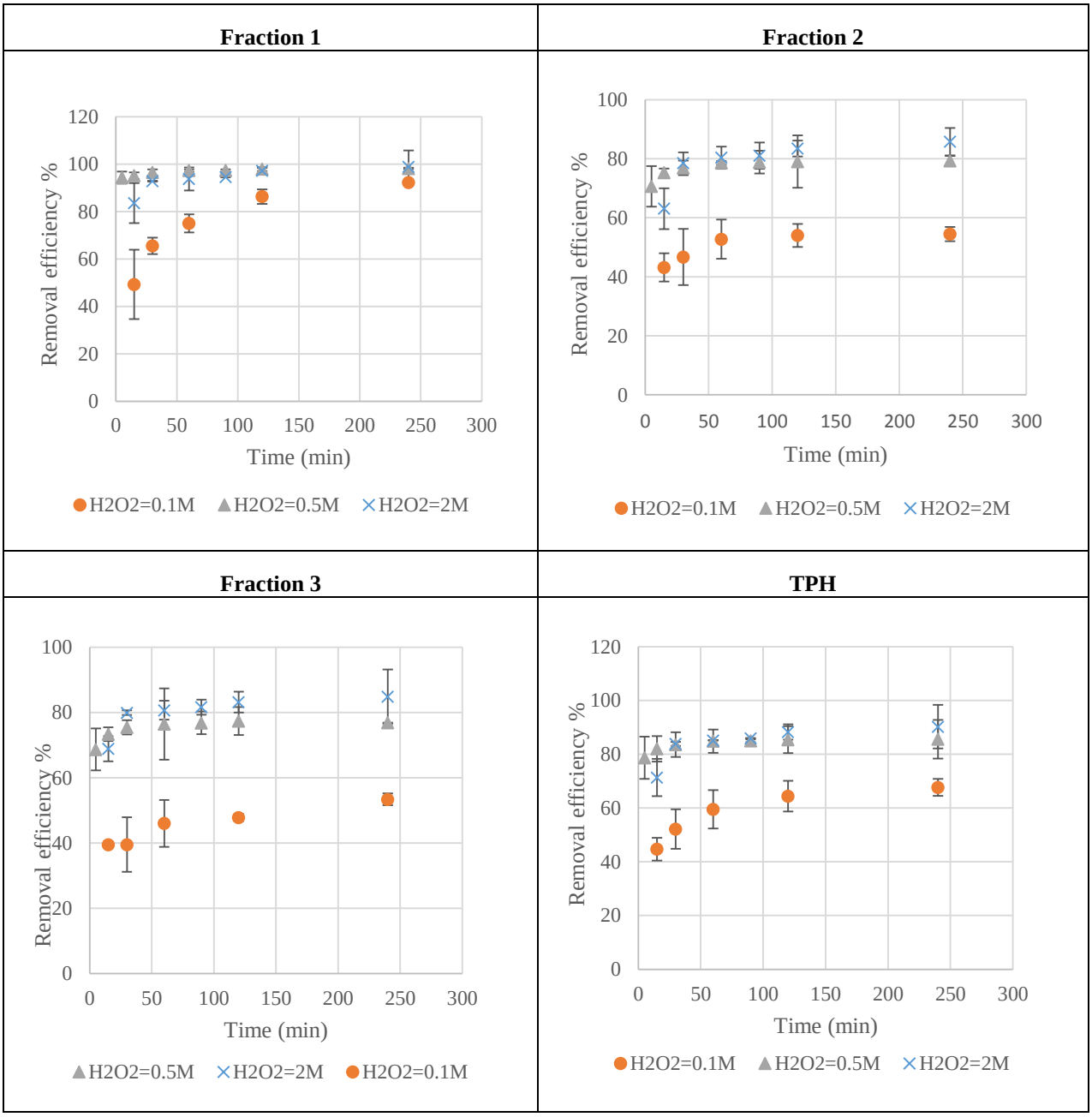

Figure 5-1: Removal efficiency at H_2O_2= 0.1M, 0.5M, and 2M at constant Fe^{2+}=0.05 M, EL=25%, and L/S=2, fraction 1, fraction 2, fraction 3 and TPH

5.2.1.2 Effect of soil slurry volume, L/S, on removal efficiency

Figure 5-2 shows the effect of L/S on removal efficiency. As can be observed from the figure, L/S=1 and 2 had higher removal efficiencies than L/S=5. As the

reaction progressed, the removal efficiencies of the three L/S values for the most experiments became closer to that of L/S=1 which had a removal efficiency of 85.77% for TPH after 4 h. For L/S=2 and 5, the removal efficiency for TPH in soil after 4 h were 85.57% and 85.61%, respectively. For all three fractions too, L/S=5 had the lowest removal efficiencies. The difference in removal efficiency between L/S=1 and 2, and L/S=5 at the beginning of most of the experiments could possibly be attributed to better contact of Fenton reagents with the sorbed contaminants at smaller L/S values (Watts et al., 1996).

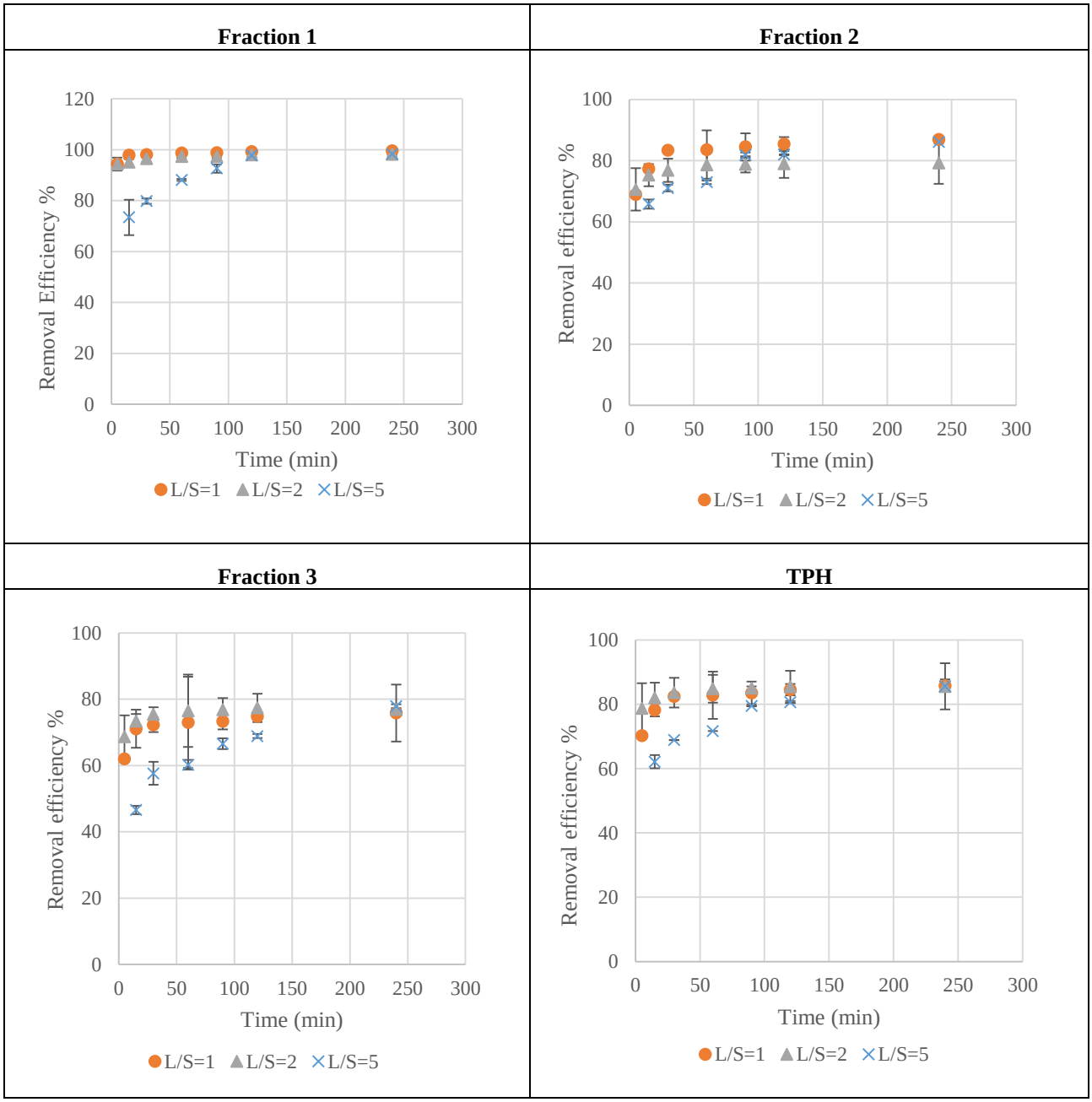

Figure 5-2 Removal efficiency at L/S=1, 2, and 5, at constant H_2O_2=0.5 M, Fe^{2+}=0.05M, EL=25%, fraction 1, fraction 2, fraction 3 and TPH

5.2.1.3 Effect of EL% on removal efficiency

Figure 5-3 shows the change in removal efficiency as EL% was varied. From Figure 5-3, EL=25% and 50% had higher removal efficiencies than EL=0% until 2 h. The removal efficiencies for EL=25% for fractions 1, 2, and 3, and TPH were also higher than those of EL=50%. This observation could be due to

the ineffective reaction of Fenton in solution with higher EL%, as discussed in the subsequent paragraph.

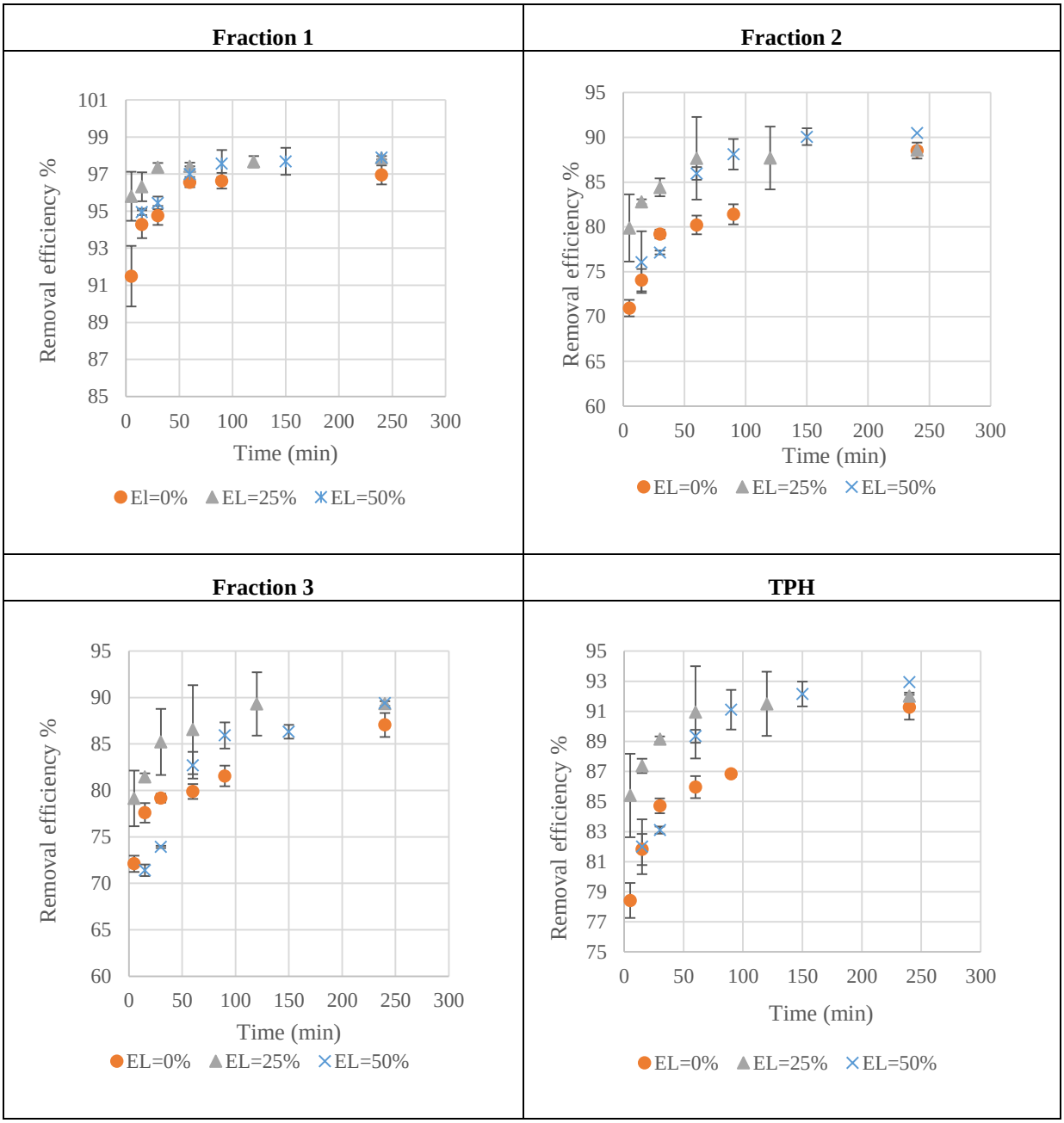

Figure 5-3: Removal efficiency at EL%= 0%, 25%, and 50% at constant H_2O_2=4 M, Fe^{2+}=0.2M, and L/S=2, fraction 1, fraction 2, fraction 3 and TPH

To further evaluate the effect of increase in EL% on removal efficiency, the reactions were conducted for EL%=10%, 25%, 50% and 68% for 4 h. The results for the alkanes and the three fractions along with TPH are illustrated in

Figure 5-4. The results obtained for the three fractions and TPH depicted the highest removal efficiency for EL=10%, with 96.74% for TPH. Decrease in removal efficiency for higher EL% was observed with the lowest value of 89.6% for TPH at EL=68%. The three fractions followed the same pattern as TPH. This observation could be explained by the possible effects of EL and water on Fenton reaction. By increasing the EL%, the water% in the solution would decrease. $FeSO_4.7H_2O$ is almost insoluble in EL. For EL% lower than 10%, the effect of increase in solubility of hydrocarbon contaminants in EL was greater than the insolubility of $FeSO_4.7H_2O$. Increasing EL% to above 10% likely caused the insolubility of $FeSO_4.7H_2O$ to dominate over other effects leading to slower Fenton reaction. This study has shown that a low amount of EL (10% in this case) could increase the removal efficiency by increasing the solubility of diesel compounds. In addition, as the H_2O_2 is decomposed and only iron is present, and the desorbed contaminants are mineralized by Fenton reaction, the spent EL can be reused.

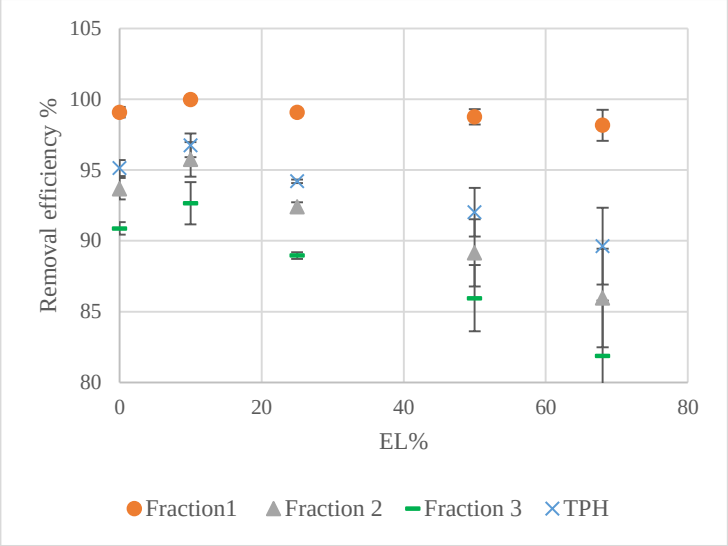

Figure 5-4 Effect of increase in EL% from 0% to 68% on removal efficiency, fraction 1, fraction 2, fraction 3 and TPH

5.2.1.4 Effect of Fenton reaction on distribution of the three fractions

In this section, the percentages and the changes in percentages of three fractions in TPH are examined. In diesel, TPH consisted of 42.98% of fraction 1, 40.55% of fraction 2, and 16.47% of fraction 3. After Fenton reaction, the percentage of fraction 1 of remaining diesel in soil decreased to 8.46%, while the percentages of fractions 2 and 3 increased to 68.97% and 23.56%, respectively for H_2O_2=0.1M, Fe^{2+}=0.05M, L/S=2, EL=25% after 4 h. The same trend was observed for all other experiments. Figure 5-5 shows the percentages of the three fractions at H_2O_2=0.1M, Fe^{2+}=0.05M, L/S=2, EL=25% and H_2O_2=4M, Fe^{2+}=0.2M, L/S=2, EL=25%. As can be seen, fraction 1 had the most significant changes or decreases in percentage of TPH, followed by fractions 2 and 3 with less significant changes or increases in percentage of TPH. The lower molecular weight of fraction 1 caused faster desorption and possibly faster degradation that led to the biggest changes in TPH percentages.

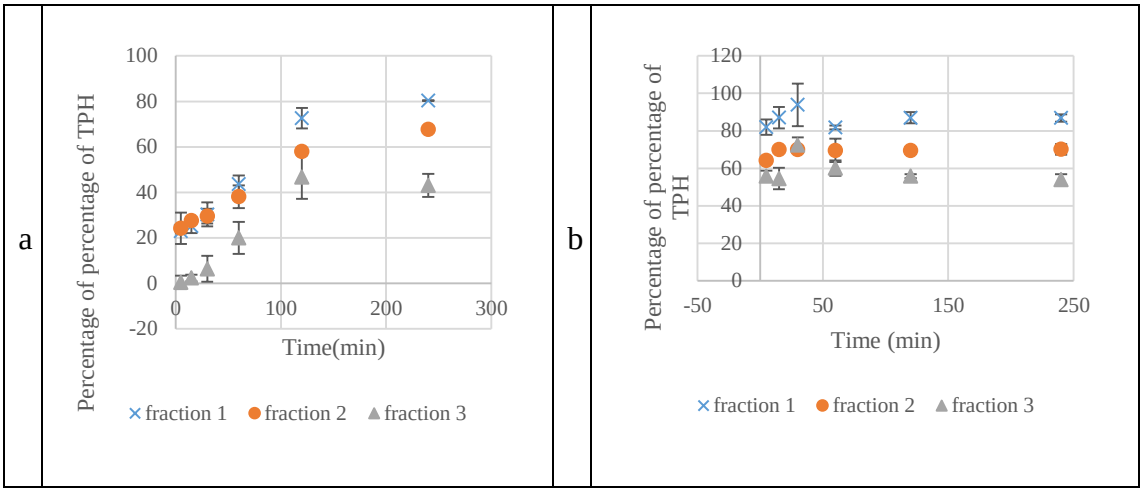

Figure 5-5: Percentages of three fractions in a: H_2O_2=0.1M, Fe^{2+}=0.05M, L/S=2, EL=25%, and b: H_2O_2=4M, Fe^{2+}=0.2M, L/S=2, EL=25%

5.2.1.5 Kinetic of EL-Fenton reaction

The results were fitted to three kinetic models, power law equation, pseudo-first order equation, and pseudo-second order equation. The results of power law equation and pseudo-first order equation are reported and the results of correlation coefficient of pseudo-second order rate equation are reported in Appendix 3. The coefficients of power law equation are reported in Table 5-1 while the coefficients of the pseudo-first order equation are reported in Table 5-2. As can be seen from these tables, the coefficient of correlation, R^2, values were all close to 1 which indicated a good fit of data to both models. q_e in pseudo-first order kinetic model had the highest value for fraction 2 followed by fraction 3 and fraction 1.

Table 5-1: Coefficients of two constant power law equation for fraction 1, fraction 2, fraction 3, and TPH for kinetic of combined EL-Fenton

Experimental Conditions				Fraction 1			Fraction 2			Fraction 3			Total		
H_2O_2,M	EL%	L/S	Fe^{2+},M	K_p	m	R^2	K_p	m	R^2	K_p	m	R^2	K_p	m	R^2
0.1	25	2	0.05	12.85	0.65	0.9862	3.91	0.08	0.9434	1.46	0.08	0.9286	10.85	0.20	0.9910
0.5	25	2	0.05	0.42	0.31	0.9651	1.81	0.09	0.9115	0.65	0.08	0.8697	2.81	0.10	0.9360
2	25	2	0.05	6.96	0.85	0.9156	4.12	0.31	0.8850	0.99	0.23	0.8625	7.53	0.35	0.9078
4	0	2	0.2	0.52	0.28	0.9366	2.54	0.22	0.8997	0.73	0.18	0.9142	3.78	0.22	0.9450
4	25	2	0.2	0.23	0.18	0.9287	1.44	0.15	0.9504	0.56	0.19	0.9604	2.23	0.17	0.9736
4	50	2	0.2	0.55	0.35	0.9431	4.00	0.38	0.9417	1.58	0.37	0.9595	6.12	0.38	0.9527
0.5	25	1	0.05	0.06	0.58	0.9647	0.99	0.22	0.9370	0.37	0.10	0.8726	1.37	0.18	0.9340
0.5	25	5	0.05	2.97	1.08	0.8978	1.59	0.27	0.8922	1.08	0.30	0.9504	3.87	0.35	0.9580

Table 5-2: Coefficients of pseudo-first order kinetic model of Fenton reaction for fraction 1, fraction 2, fraction 3, and TPH, for kinetic of combined EL-Fenton

Experimental Conditions				Fraction 1			Fraction 2			Fraction 3			Total		
H_2O_2,M	EL%	L/S	Fe^{2+},M	q_e	k	R^2	q_e	k	R^2	q_e	k	R^2	q_e	k	R^2
0.1	25	2	0.05	0.54	0.05	0.9829	2.77	0.28	0.9585	1.05	0.28	0.9286	4.22	0.07	0.9837
0.5	25	2	0.05	0.12	0.72	0.9992	1.23	0.47	0.9977	0.46	0.46	0.9979	1.82	0.54	0.9985
2	25	2	0.05	0.17	0.13	0.9976	0.96	0.10	0.9969	0.33	0.12	0.9982	1.48	0.11	0.9975
4	0	2	0.2	0.17	0.62	0.9992	1.08	0.41	0.9809	0.36	0.44	0.9906	1.61	0.48	0.9925
4	25	2	0.2	0.11	0.83	0.9998	0.77	0.52	0.9961	0.26	0.49	0.9932	1.14	0.59	0.9979
4	50	2	0.2	0.12	0.25	0.9995	0.71	0.12	0.9858	0.29	0.11	0.9837	1.15	0.15	0.9924
0.5	25	1	0.05	0.00	0.62	0.9998	0.40	0.34	0.9918	0.24	0.37	0.9960	0.63	0.37	0.9948
0.5	25	5	0.05	0.05	0.33	0.9326	0.56	0.32	0.9445	0.33	0.67	0.8569	0.94	0.36	0.9282

5.2.2 Effect of adding zero valent nanomaterial

Figure 5- shows the results of removal efficiency versus time at different nano concentration with comparison with two concentrations of Fe^{2+}. As it can be seen from the graphs with increasing the concentration of nano the removal efficiency increased. And in comparison with Fe^{2+}, Fe^{2+}=0.14g/gsoil has the lowest removal efficiency and with increase to the two times, Fe^{2+}=0.28g/gsoil, the removal efficiency is almost equal to nano=0.1g/gsoil. It shows that almost 28 times in concentration of Fe^{2+} needs to reach the same removal efficiency of the reaction with nano.

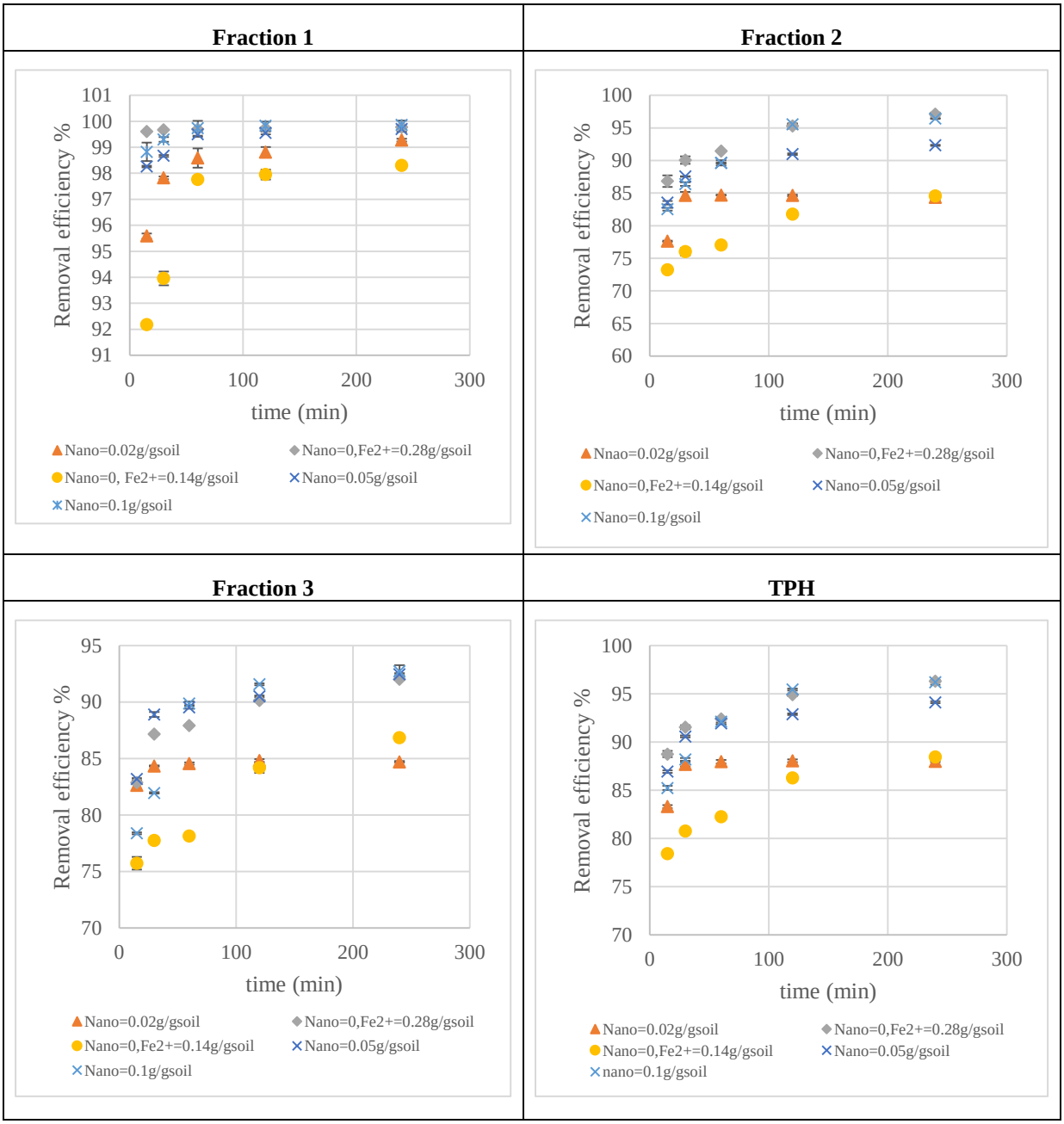

Figure 5-6: Fenton reaction with Fe^{2+} and zero valent nanomaterial, Fe^{2+}=0.14g/gsoil, Fe^{2+}=0.28g/gsoil, nano=0.02g/gsoil, nano=0.05g/gsoil, nano=0.1 g/gsoil

5.2.3 Effect of HA on Fenton reaction

5.2.3.1 Characterization of derived HA, soil, and soil treated with EL

Figure 5-6 shows the FTIR spectra for HA. H-bonded OH groups of alcohols, phenols and organic acid as well H-bonded NH groups were represented at

3400-3330 cm^{-1}, conjugated carbonylic C=O was detected at a small shoulder at 1726 cm^{-1}, C=O conjugated and C=C in aromatic structure could be detected at 1630 cm^{-1}; a small shoulder at 1550-1570 cm^{-1} was attributed to amide and carboxylate C=O and a peak at 1430 cm^{-1} showed the C–H deformation of CH_2 or CH_3 groups (Castaldi et al., 2005). There are contradictory results related to the role of aromatic and aliphatic fraction in sorption/desorption processes. Chefetz et al. (2000) reported tha the attraction of nonionic compounds to the aromatic moieties is higher than the attraction to the aliphatic functional groups. On the other hand, based on the study done by Eriksson et al. (2004), aliphatic carbon plays a more significant role in hydrophobic partitioning.

Single C–O bond in carboxylic acids, esters and ethers could be detected at approximately 1200 cm^{-1}(Castaldi et al., 2005). Carboxylic groups play important roles in the acidic nature of HA and it will affect the Fenton reaction and without pH adjustment it can favour the Fenton reaction. But it is reported that HA structure does not change with Fenton oxidation (Sun et al., 2007).

The peaks at 1006–1122 cm^{-1} belonged to C–O stretching. The peaks at 1000–1100 cm^{-1} were assigned to the characteristics of P–O=R esters and the peak at 1014–1024 cm^{-1} showed the characteristics of C–O–C/C–O (Liu et al., 2015). The peak at 740–779cm^{-1} was interpreted as C–O–C or C–H stretching vibrations. The strong peak at 484–534 cm^{-1} was attributed to P–Cl and the peak at 469–457 cm^{-1} was associated with C–X (halogen) stretching (Liu et al., 2015).

HA rearranges itself in this way that its hydrophilic moieties, such as carboxyl, phenols and hydroxyl groups, are outward which will form micelle formation

that have detergency properties, also are the best sequestrating agents (Salati et al., 2011).

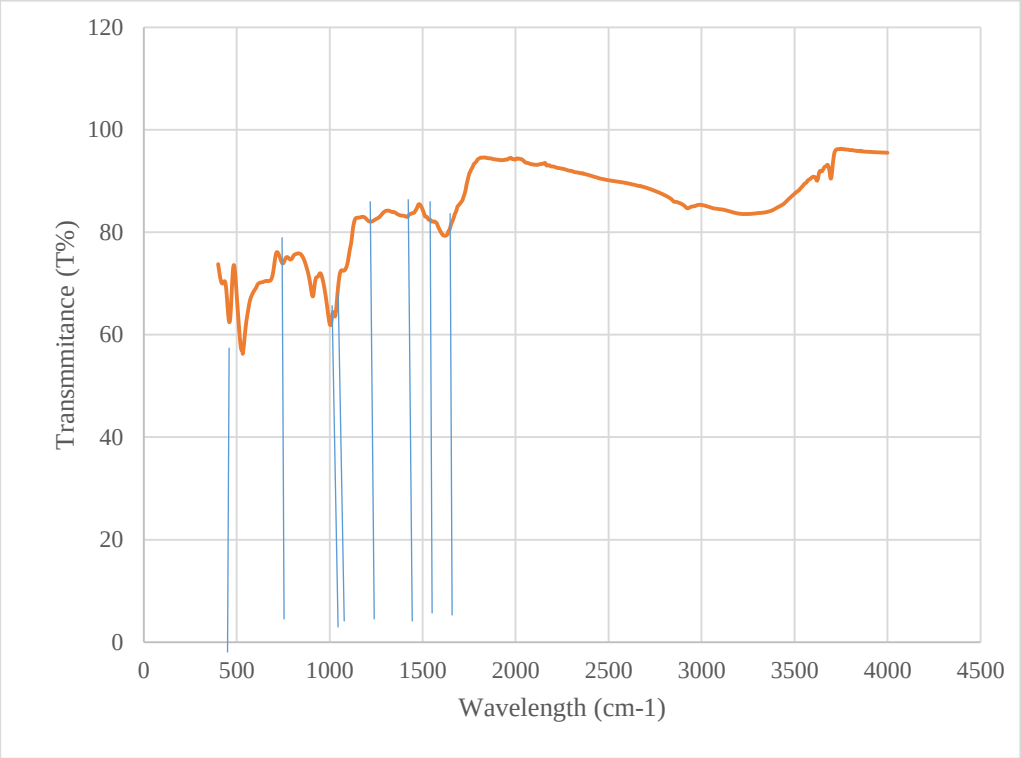

Figure 5-6: Fourier transform infrared (FTIR) spectra of HA

The FTIR spectra of soil, soil after reaction with EL and the spectra of HA are illustrated in Figure 5-7. It should be noted that the spectra of soil in comparison with the other two cases had lower intensities and by displaying all of them on the same axes, not all peaks could be observed in detail. As shown in Figure 5-7, the separated part had the same peaks as the original soil, but with higher intensities. It could be deducted that EL could separate the organic matter of the soil after contact, and among different fractions of organic matters, it seemed that the HA was the main fraction or at least part of the organic matter with the same functional groups as the HA. Among the absent functional groups of HA

in the contacted soil with EL and soil, was the peak at 3100-3650 cm^{-1} which belonged to H-bonded OH groups.

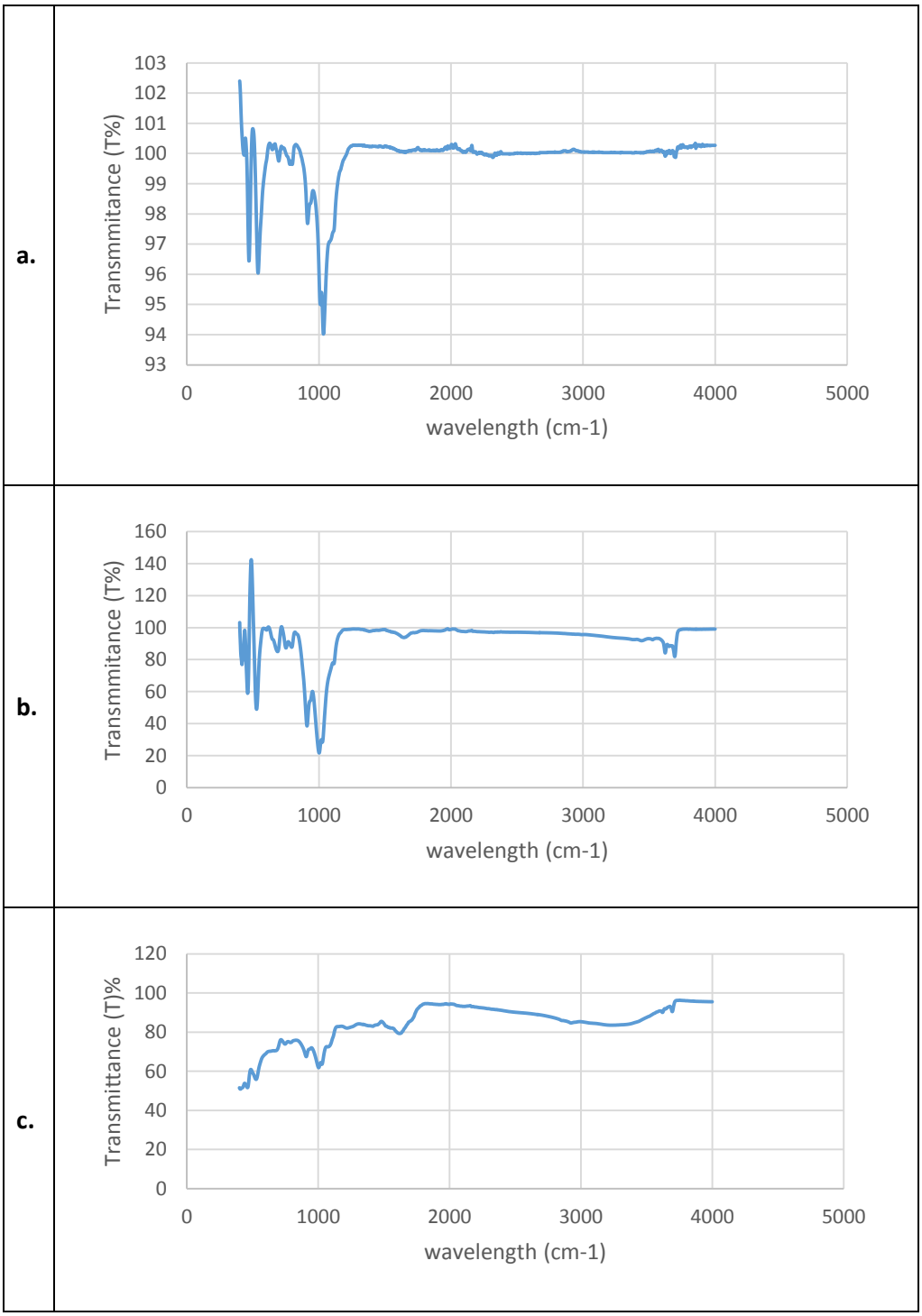

Figure 5-7: FTIR spectra of a: soil, b: soil after treatment with EL, c: HA

5.2.3.2 Effect of HA dosage on removal efficiency

The effect of HA, which is one of the main fractions of SOM, dosage on removal efficiency of the three fractions and TPH was monitored at four dosages of 10 mg/l, 50 mg/l, 100 mg/l and 150 mg/l at pH=2.7. Figure 5-8 presents the changes in removal efficiency versus time at different HA dosages. As explained earlier in Chapter 2, there are two opposing effects on Fenton reaction in the presence of HA. First is the consumption of hydroxyl radicals by HA and second is the reduction of Fe^{3+} to Fe^{2+} by HA. For the case of HA=10 mg/l, the removal efficiency for fractions 2, 3 and TPH was lower than at HA=0. The efficiency was also lower than all other cases with higher HA values. Meanwhile, for fraction 1, the efficiency at HA=10 mg/L was higher than at HA=0 and lower than higher HA dosage.

The observed results implied that for fraction 1, at HA=10mg/l, the effect of reducing Fe^{3+} to Fe^{2+} was the dominant factor. Thus, the removal efficiency increased from 96.26% for fraction 1 at HA=0% to 97.54% at HA=10% after 4 h. By increasing the dosage of HA to 50 mg/l, 100 mg/l and 150 mg/l for fraction 1, the effect of reducing Fe^{3+} to Fe^{2+} played a more significant role than the consumption of hydroxyl radical. As a result, the removal efficiency increased. The difference in efficiency between HA=50 mg/l and HA=100 mg/l was larger than the difference between HA=100 mg/l and HA=150 mg/l.

For fractions 2 and 3, the effect of hydroxyl radical consumption was more important. For fraction 2, in the case of HA=150 mg/l, its removal efficiency was higher than at HA=0. For fraction 3, HA=0 had the biggest removal efficiency although the value of HA=150 was very close to HA=0. It could be

deducted that the two effects of consumption of hydroxyl radicals and reduction of Fe^{3+} to Fe^{2+} were offset at HA=0 for fraction 3. With an increase in the molecular weight of the three fractions, the negative effect of consumption of H_2O_2 became more significant than for the lighter fractions. For TPH, the results reflected the summation of the effects of all three fractions. Here, the case of HA=150 mg/l had the highest removal efficiency and HA=100 mg/l had values with insignificant differences to that of HA=0. The results indicated that the positive effect of HA increased with an increase in its dosage. Based on the results discussed here, it could be deduced that there is an optimum value for HA in exerting an overall positive effect on Fenton reaction, which is dependent on the soil properties, pollutants and possibly the H_2O_2 and Fe^{2+} initial concentration.

Figure 5-9 illustrates the effect of HA on the removal efficiency at pH=5. Experiments were carried out at pH=5 with and without HA. It could be observed that by addition of HA=10 mg/l led to an increase in the removal efficiency for fractions 1, 2 and TPH, but resulted in a decrease in the removal efficiency for fraction 3. Similar to the cases at pH=2.7, an increase in the molecular weight led to a decrease in the positive effect of HA.

For evaluating the effect of pH, the results for HA=10mg/l in figure 5-8, 5-9. As it can be deducted from the graphs the removal efficiency at pH=2.7 is higher than pH=5, as it was explained before, the Fenton reaction with Fe^{2+} is more active at lower pH values because Fe^{2+} is soluble in acidic range and it is likely to precipitate in higher pH range (Watts et al., 2005).

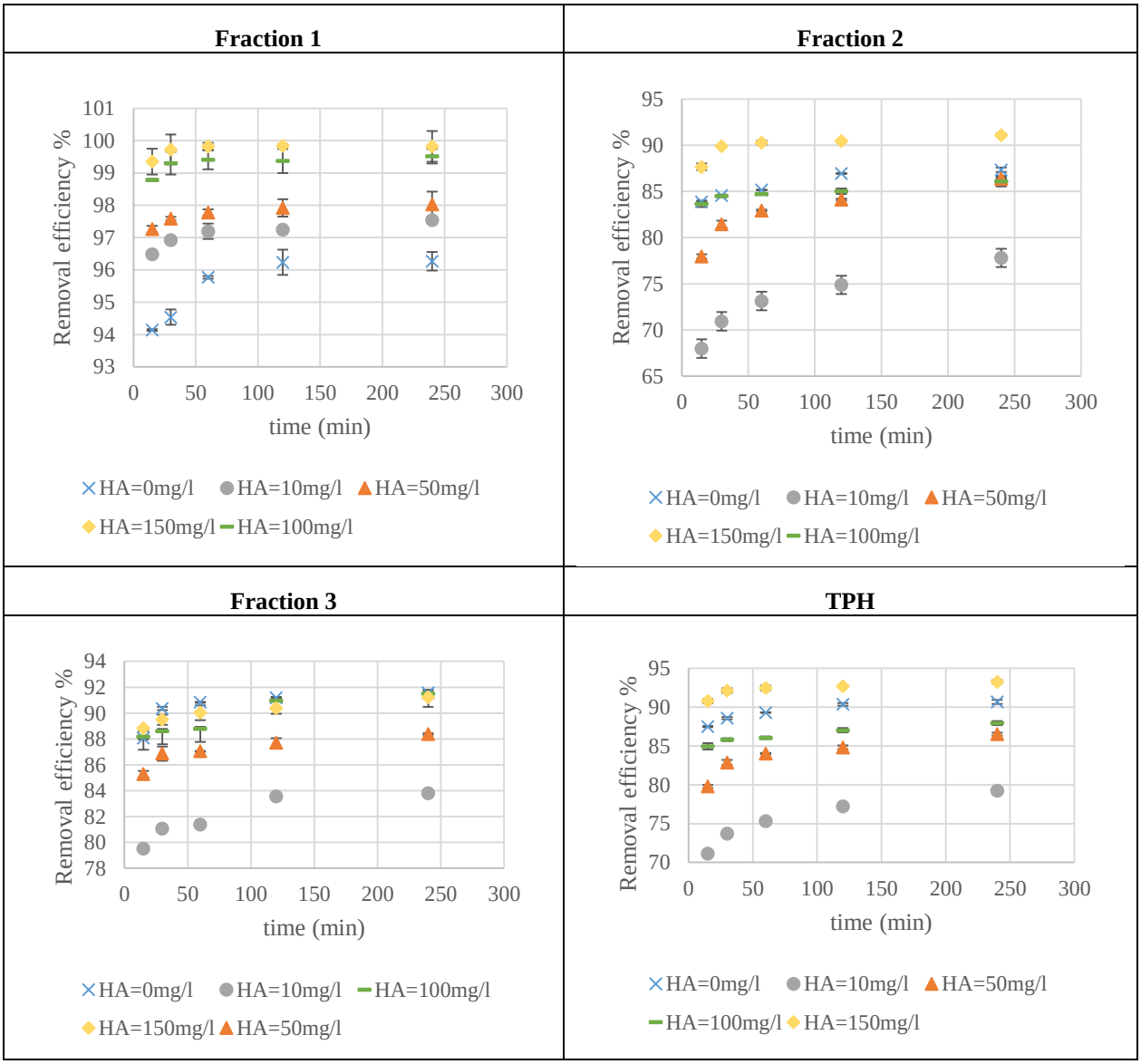

Figure 5-8: Removal efficiency at H_2O_2= 0.5M, at constant Fe^{2+}=0.05 M, LS=2, fraction 1, fraction 2, fraction 3 and TPH

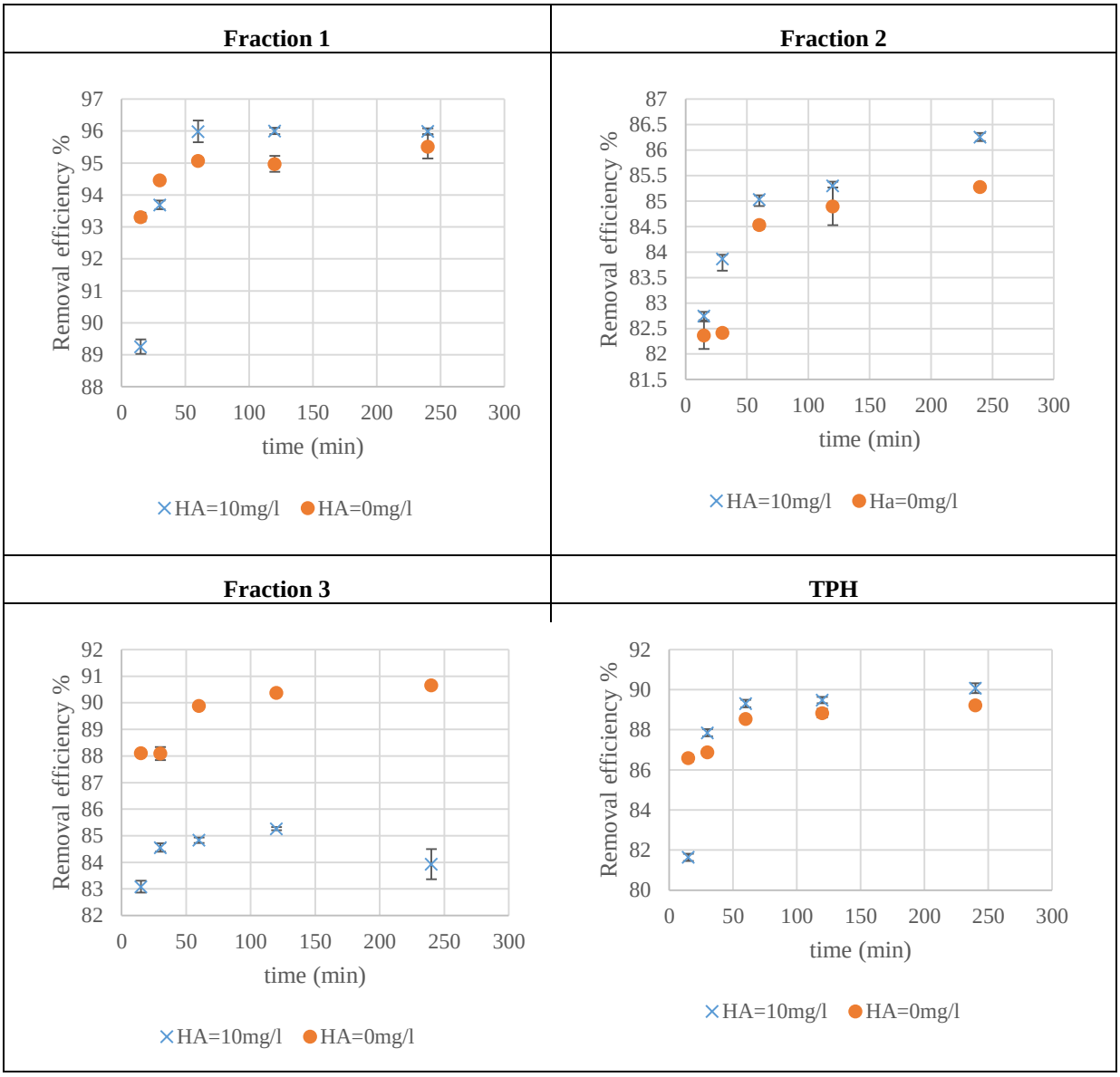

Figure 5-9: Removal efficiency at pH=5 with and without HA, at H_2O_2= 0.5M, at constant Fe^{2+}=0.05 M, LS=2, fraction 1, fraction 2, fraction 3 and TPH

5.2.3.3 Effect of EL% on removal efficiency for Fenton reaction in HA

The effect of adding EL=10% to HA=50 mg/l was compared to the case without EL in Figure 5-10. The aim of this section was to investigate whether EL could affect the Fenton reaction in the presence of HA. The results indicated that similar processes occurred as for the cases without HA. As can be seen in Figure 5-11, the removal efficiency decreased from 86.51% without EL to 81.48% with

EL=10% for TPH at 4 h. As previously explained, EL could hinder the Fenton reaction at high concentrations. However, in the case without HA, the optimum EL% was 10%. The results showed that HA led to the change in this optimum value. It has been reported in the literature that adsorption of pollutants by organic matters could hinder their engagement in Fenton reaction (Lindsey et al., 2000; Georgi et al., 2007).

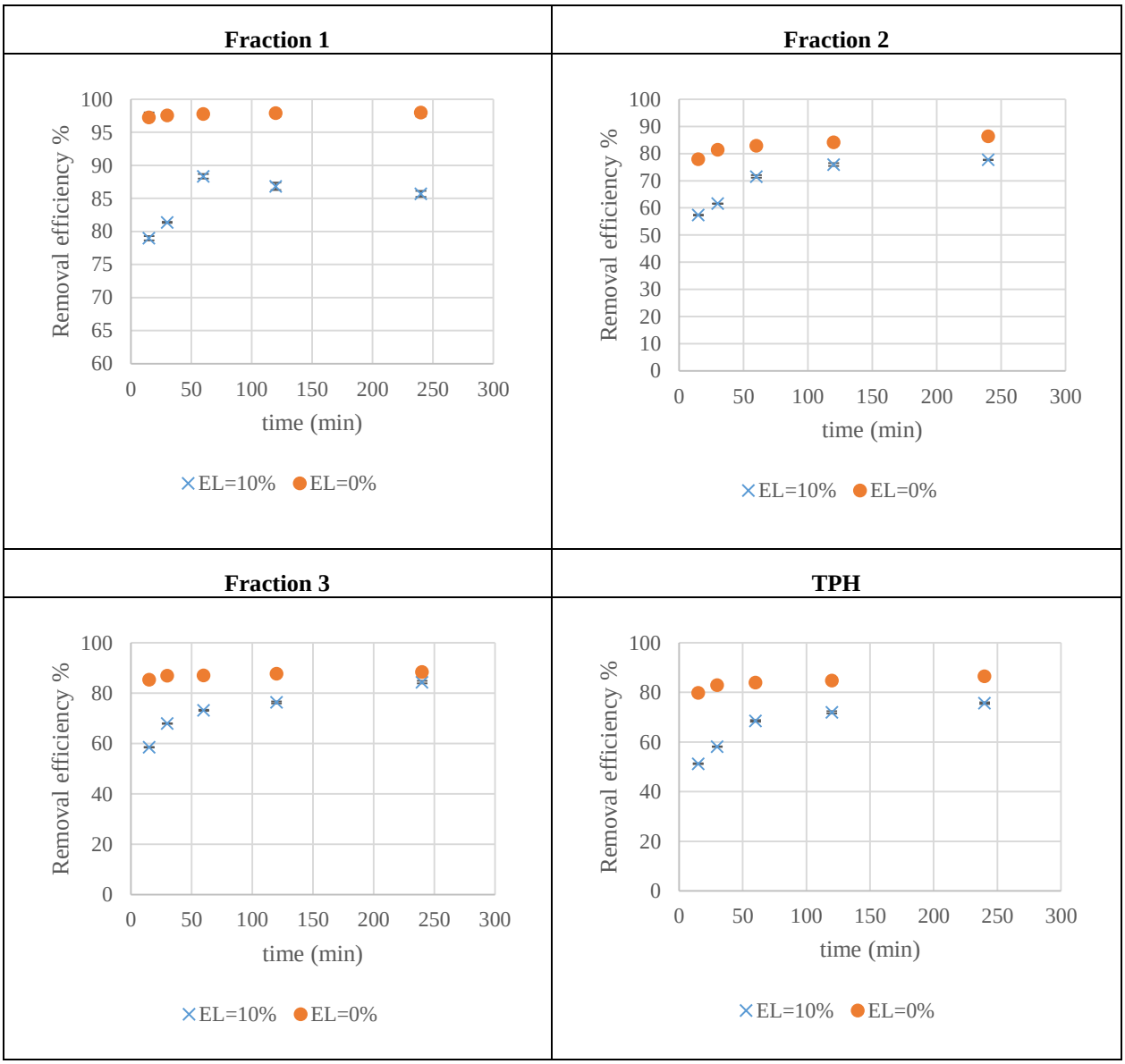

Figure 5-10: Effect of EL on removal efficiency with HA=50mg/l, at H_2O_2= 0.5M, at constant Fe^{2+}=0.05 M, LS=2, fraction 1, fraction 2, fraction 3 and TPH

5.2.3.4 Kinetic of Fenton reaction

Two kinetic models have been used for modelling the kinetic data, the power law kinetic and pseudo-first order kinetic equations based on Eqs (5-12),(5-13) and (5-14). Second order kinetic equation was fitted but the correlation coefficient was low, the results are reported in Appendix 3. Table 5-3 lists the coefficients of the power law equation while Table 5-4 lists the coefficients of the pseudo-first order equation which were determined by curve-fitting. The close values of coefficient of correlation, R^2, to 1, indicated a good fit of data to both models. As can be seen from Table 5-4, by increasing the HA dosage, the q_e decreased for all three fractions and TPH, as was expected. Meanwhile, the first order reaction constant, *k*, for TPH increased from HA=10 mg/l to HA=150 mg/l. K_p values for all sets of experiments had the biggest value for fraction 2, followed by fraction 3 and were lowest for fraction 1. q_e reported from the pseudo-first order kinetic model had the biggest value for fraction 2, followed by fraction 3 and finally, fraction 1.

Table 5-3: Coefficients of two constant power law kinetic model of Fenton reaction for fraction 1, fraction 2, fraction 3, and TPH, for kinetic of Fenton in different HA dosages

Experimental Conditions	Fraction 1			Fraction 2			Fraction 3			TPH		
HA	m	K_p	R^2	m	K_p	R^2	m	K_p	R^2	m	K_p	R^2
0	0.184	0.069	0.9131	0.094	0.309	0.9489	0.113	0.130	0.8394	0.109	0.507	0.9809
10	0.107	0.072	0.9965	0.127	0.662	0.9906	0.088	0.222	0.9397	0.115	0.953	0.9967
50	0.116	0.026	0.9703	0.162	0.489	0.9758	0.077	0.152	0.9367	0.134	0.654	0.9613
100	0.282	0.016	0.7895	0.052	0.275	0.9222	0.129	0.150	0.8784	0.075	0.430	0.9588
150	0.521	0.015	0.8846	0.103	0.225	0.8350	0.083	0.120	0.9788	0.100	0.354	0.9062

Table 5-4: Coefficients of pseudo-first order kinetic model of Fenton reaction for fraction 1, fraction 2, fraction 3, and TPH, for kinetic of Fenton in different HA dosages

Experimental Conditions	Fraction 1			Fraction 2			Fraction 3			TPH		
HA	q_e	k	R^2	q_e	k	R^2	q_e	k	R^2	q_e	k	R^2
0	0.031	0.70	0.9997	0.205	0.24	0.9991	0.077	0.23	0.9999	0.312	0.22	0.9993
10	0.045	0.29	0.9998	0.374	0.16	0.9952	0.150	0.22	0.9990	0.585	0.18	0.9961
50	0.015	0.34	0.9997	0.236	0.17	0.9981	0.107	0.24	0.9998	0.357	0.19	0.9989
100	0.004	0.34	0.9998	0.218	0.27	0.9998	0.086	0.26	0.9990	0.309	0.25	0.9995
150	0.001	0.36	0.9989	0.140	0.23	0.9999	0.083	0.27	0.9998	0.224	0.26	0.9999

5.2.4 Result and discussion of optimization by RSM

5.2.4.1 Design of experiments by RSM

The relationship between the removal efficiency of TPH and the three independent variables, HA, EL and pH, were studied. The three factors were coded in 5 levels as reported in Table 5-5. The experimental design and the values of removal efficiency for each run are summarised in Appendix 2.

Table 5-5: variables and their coded and actual values

Variables	Units	Coded values				
		-1.633	-1	0	+1	+1.633
HA	mg/l	18.35	50	100	150	181.65
EL	%	10.50	20	35	50	59.49
pH	-	2.05	3	4.5	6	6.95

5.2.4.2 Regression model and statistical analysis

The correlation of response for the removal efficiency of TPH with the three independent variables based on a polynomial equation in terms of coded values is expressed as Eq. (5-18).

$$TPH=79.53-1.74*A-5.87*B+2.07*C-1.10*B^2+1.46*A*C-2.23*B*C \quad \text{Eq. (5-18)}$$

Analysis of variance (ANOVA) evaluation of this model is shown in Table 5-7. For evaluation of how well this equation could describe the results, the F-value, R^2, p-value and lack of fit were calculated. The significance of each term was determined by p-value test. When the p-value is smaller than 0.05, it means that the term is significant. The linear value of A, B, and C, quadratic value of variables B and interaction of AC and BC were significant. The F-value of

quadratic term of B had a smaller F-value than the corresponding linear term of B. The lack of fit for F-value was 4.23 implying that the lack of fit was not significant relative to pure error.

Table 5-7: Analysis of variance table [Partial sum of squares]

Source	**Sum of Squares**	**DF**	**Mean square**	**F value**	**Prob > F**	
Block	3.14	1	3.14			Irrelevent
Model	629.10	6	104.85	82.58	*< 0.0001*	*Significant*
A	40.39	1	40.39	31.82	*0.0001*	Irrelevent
B	458.90	1	458.90	361.45	*< 0.0001*	Irrelevent
C	56.93	1	56.93	44.84	*< 0.0001*	Irrelevent
B^2	16.02	1	16.02	12.62	0.0040	Irrelevent
AC	17.02	1	17.02	13.41	0.0033	Irrelevent
BC	39.83	1	39.83	31.37	0.0001	Irrelevent
Residual	15.24	12	1.27			Irrelevent
Lack of fit	13.62	8	1.70	4.23	0.0901	*Not significant*
Pure Error	1.61	4	0.40			Irrelevent
Cor Total	647.47	19				Irrelevent

Whether the distribution of residuals, the deviation between predicted and actual values, followed a normal distribution was analysed to determine the adequacy of the model. If the distribution of the model followed a normal distribution, this meant that the experimental error was random. By normalizing the residuals with respect to their standard deviations, the studentiszed residuals was obtained and a normal distribution function was fitted to them. This predicted studentized residuals by the best-fit distribution were plotted against the experimentally

obtained studentized residuals in Figure 5-11(a). The straight line formed in Figure 5-11(a) implies that the studentized residuals follow a normal distribution (Salahi et al., 2013). The studentized residuals versus predicted removal efficiency of TPH is plotted in Figure 5-11(b). As expected, this plot was a random scatter implying that the variation in the original observations and the value of the response are not related to each other.

In Figure 5-12(c), the outlier t plot that indicates the magnitude of the residuals for each run for all runs of removal efficiency of TPH is depicted. Typically, a limit of three standard deviations is defined as a boundary of an outlier. In Figure 5-12(c), all data were located inside this interval that demonstrated the consistency of the model for all the data. The actual and predicted removal efficiency of TPH by Eq. (5-18) are plotted in Figure 5-12(d). All of these graphs were produced by software Design-Expert 7.1.

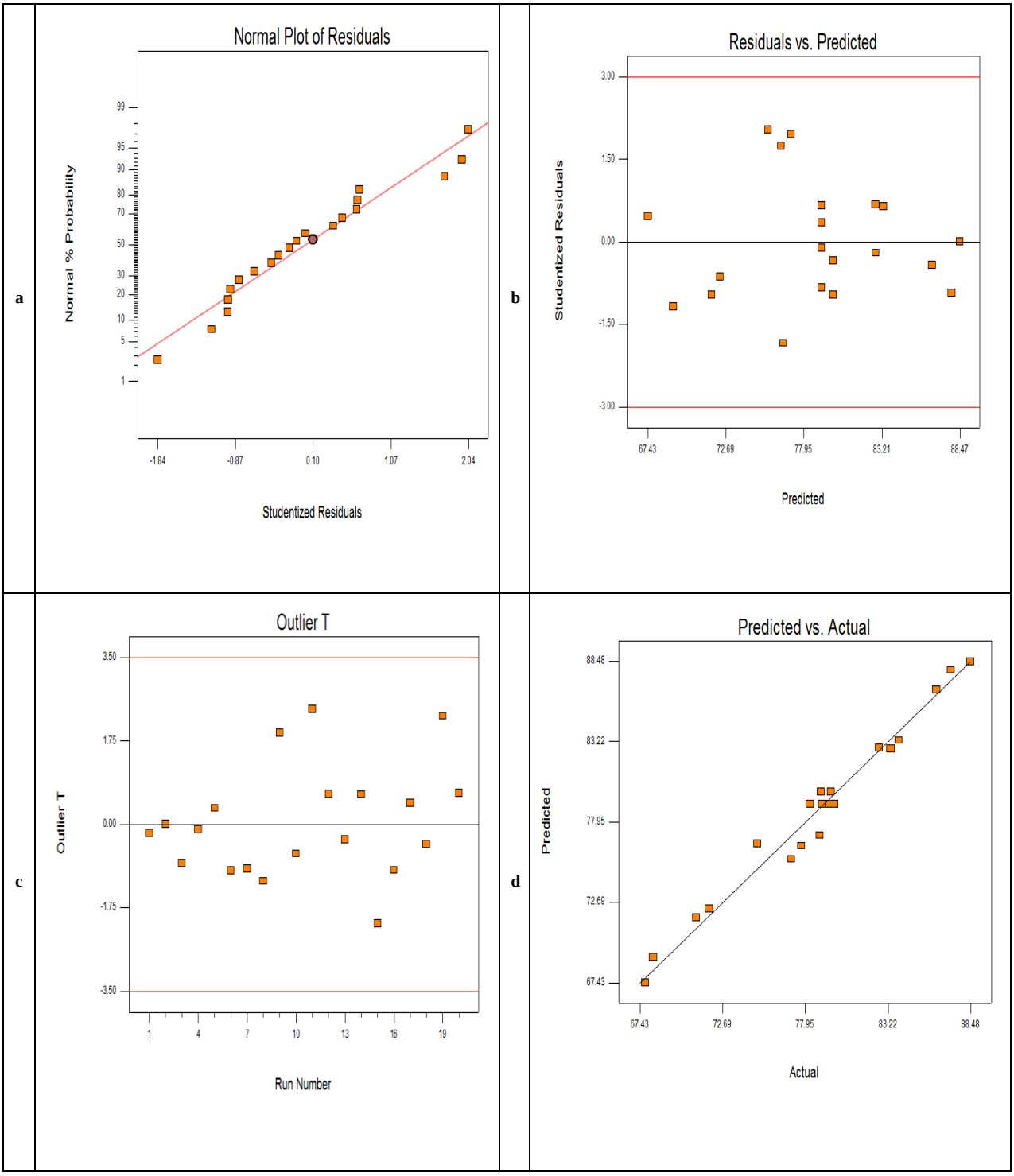

Figure 5-11: (a) Normal% probability and studentized residual plot. (b) The studentized residuals and predicted response plot. (c) The outlier t plot (d) The actual and predicted plot

5.2.4.3 The effect of pH and EL on TPH removal efficiency

The removal efficiency of TPH at different HA and pH is shown in Figure 5-12(a) at EL=35%. Based on the information on Figure 5-12(a), a decrease in EL

and an increase in pH led to the increase in removal efficiency of TPH. By decreasing EL and increasing pH, the removal efficiency of TPH increased. The maximum value of removal efficiency with increase in HA had occurred in a wider range of EL and after about HA=97mg/l, higher values of pH resulted.

5.2.4.4 The effect of HA and EL on TPH removal efficiency

The removal efficiency of TPH at different HA and pH is shown in Figure 5-13 (b) at HA=100mg/l. By increasing EL%, the maximum removal efficiency of TPH occurred in a wider HA limit and at higher pH values. The maximum value of the removal efficiency, 80.60%, had disappeared at approximately EL=38%. After approximately EL=42%, the maximum removal efficiency occurred at low HA and pH values.

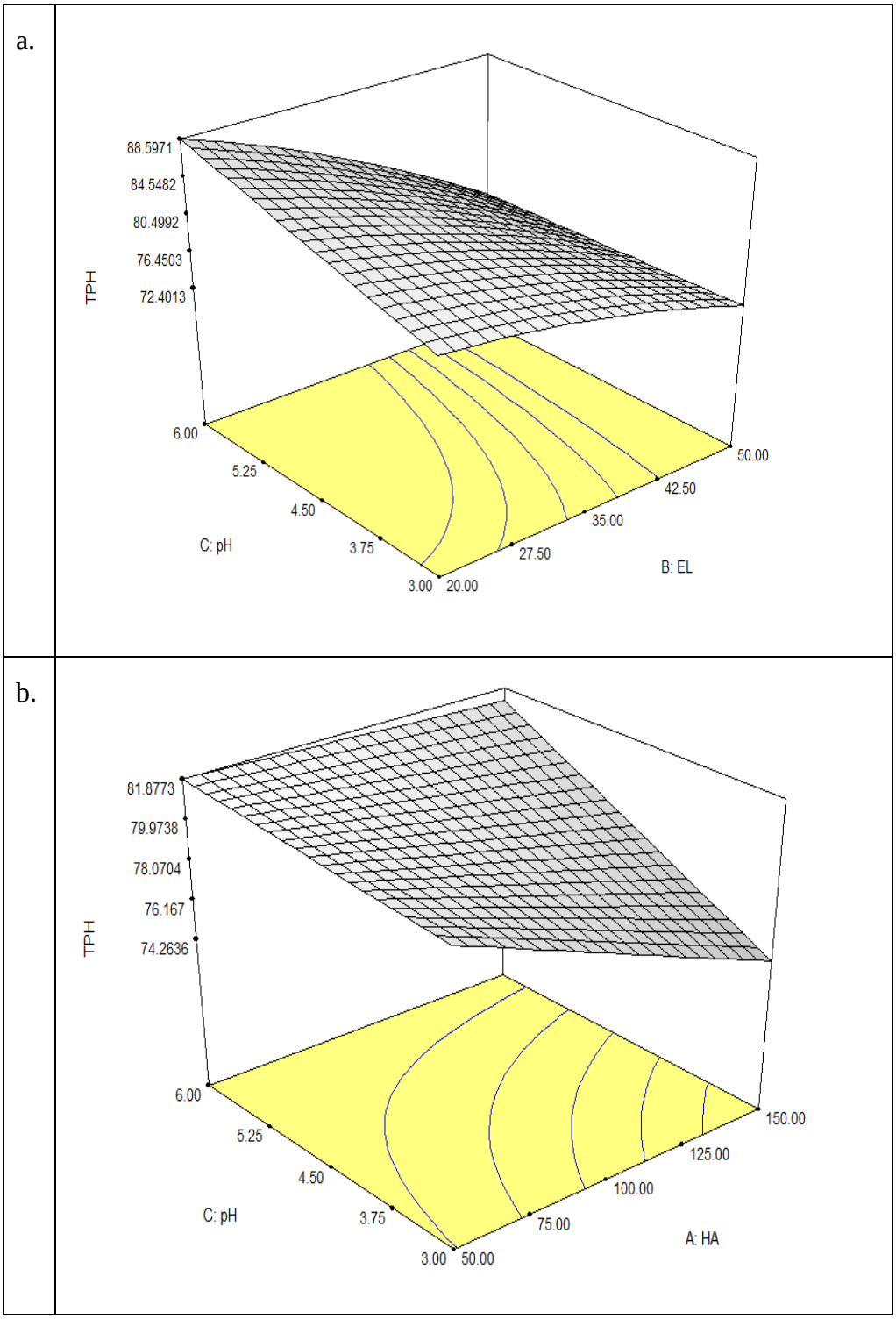

Figure 5-12: a. the effect of pH and EL on removal efficiency of TPH at constant HA=100mg/l, b. the effect of pH and HA on removal efficiency of TPH at constant EL=35%

5.2.4.5 Process optimization and verification

The optimum conditions for maximum removal efficiency of TPH based on HA, EL, and pH were determined from the predictive equation of RSM. The maximum removal efficiency of TPH was predicted at HA=51.76mg/l, EL=20.93%, and pH=5.99. The experiment was conducted at these values. The predicted value by the RSM equation and the value obtained from the experiment were compared to verify the validity of the model. The predicted value was 88.48% while the measured value was 84.93%, a difference of 3.55%, which verified the validity of the model.

5.3 Concluding Remarks

This work studied the effects of EL%, H_2O_2 concentration and L/S on Fenton oxidation of TPH in contaminated soil. Increasing H_2O_2 concentration from 0.1 M to 2 M at L/S=2 and EL=25% increased the removal efficiency of TPH after 4 h from 68.41% to 90.21%. By increasing EL% from 10% to 68%, the removal efficiency for TPH decreased from 96.74% to 89.6%, respectively. The lowest L/S, i.e. L/S=1, had the highest TPH removal efficiency of 85.77%. An optimum EL% of 10% was determined from parametric batch studies to increase the Fenton reaction efficiency. The EL-based Fenton reaction changed the distribution of the three fractions in TPH, by decreasing the percentage of fraction 1 and increasing the percentage of fractions 2 and 3. The data from kinetic experiments fitted well to the power law kinetic and pseudo-first order equations. Addition of HA and its effect on removal efficiency of TPH by Fenton reaction showed increase for fraction 1 from HA=10 mg/l and increase for fraction 2 for HA=150mg/l and no increase till addition of HA=150mg/l for

fraction 3. RSM was carried out to consider the effects and interactions of three variables s, HA, EL% and H_2O_2 and to optimize the process. The results showed that a decrease in EL and an increase in pH at constant EL=35% led to increased removal efficiencies. The optimum conditions for maximum removal efficiency of TPH were at HA=51.76mg/l, EL=20.93%, and pH=5.99. The predicted TPH removal efficiency with the close value with the experimental value verified the validity of the model.

CHAPTER 6: ETHYL LACTATE-FENTON COLUMN STUDIES FOR REMEDIATION OF TPH-CONTAMINATED SOIL

6.1. Introduction

Column study is used for simulating the situation in real cases of in-situ field application. By comparison with batch experiment in terms of weight of studied soil, 30 times more soil was examined. The prediction of the economic aspect of Fenton reaction depends on having information regarding to this treatment in large scale. One of the major costs in this area is providing the reagents thus determining the optimum values of the related variables to the reagent is crucial. Besides the economic issues, some practical matters, such as the existence of H_2O_2 in the presence of EL, also need consideration. Since column experiments are a better representative of in-situ soil remediation treatments than batch experiments, this chapter aims to explore EL-Fenton for remediation of TPH-contaminated soil via column setup. The effects of different variables, i.e. overall L/S, EL% and H_2O_2 concentration on TPH removal have been investigated. Additionally, the effects of EL on H_2O_2 stability was also studied.

6.2. Results and Discussion

6.2.1. Effect of H_2O_2 concentration on remaining diesel in soil

Figure 6-1 shows the effect of increasing H_2O_2 molarity on the remaining diesel in soil. By increasing the H_2O_2 molarity from 0.1 M to 0.5 M, the remaining diesel in soil decreased from 154.66 mg/kg soil to 107.52 mg/kg soil in section 5 for TPH. However, further increase in H_2O_2 molarity up to 2 M led to an increase till 122.09 mg/kg of remaining diesel for TPH in soil. It has been reported that H_2O_2 can act as a quencher of OH° radicals and there is an optimum value for H_2O_2 concentration (Huling et al., 2001; Georgi et al., 2007). There are reported results related to a decrease in the removal efficiency due to the increase in H_2O_2 concentration while in some other cases, no changes were reported (Ferrarese et al., 2008; Yeh et al., 2008). The observed results in Figure 6-1 suggested that the optimum value for H_2O_2 molarity was less than 2 M. For fraction 1, after this optimum value at approximately 0.5 M, the remaining diesel in soil had not changed with increase in H_2O_2 concentration while for fractions 2, 3 and TPH, the remaining diesel in soil increased after this optimum value.

By moving from section 1 at the top of the column to section 5 at the bottom of the column, the remaining diesel in soil had increased as could be expected. The higher concentration of the Fenton reagents at the entrance at the top of the column resulted in more destruction of TPH.

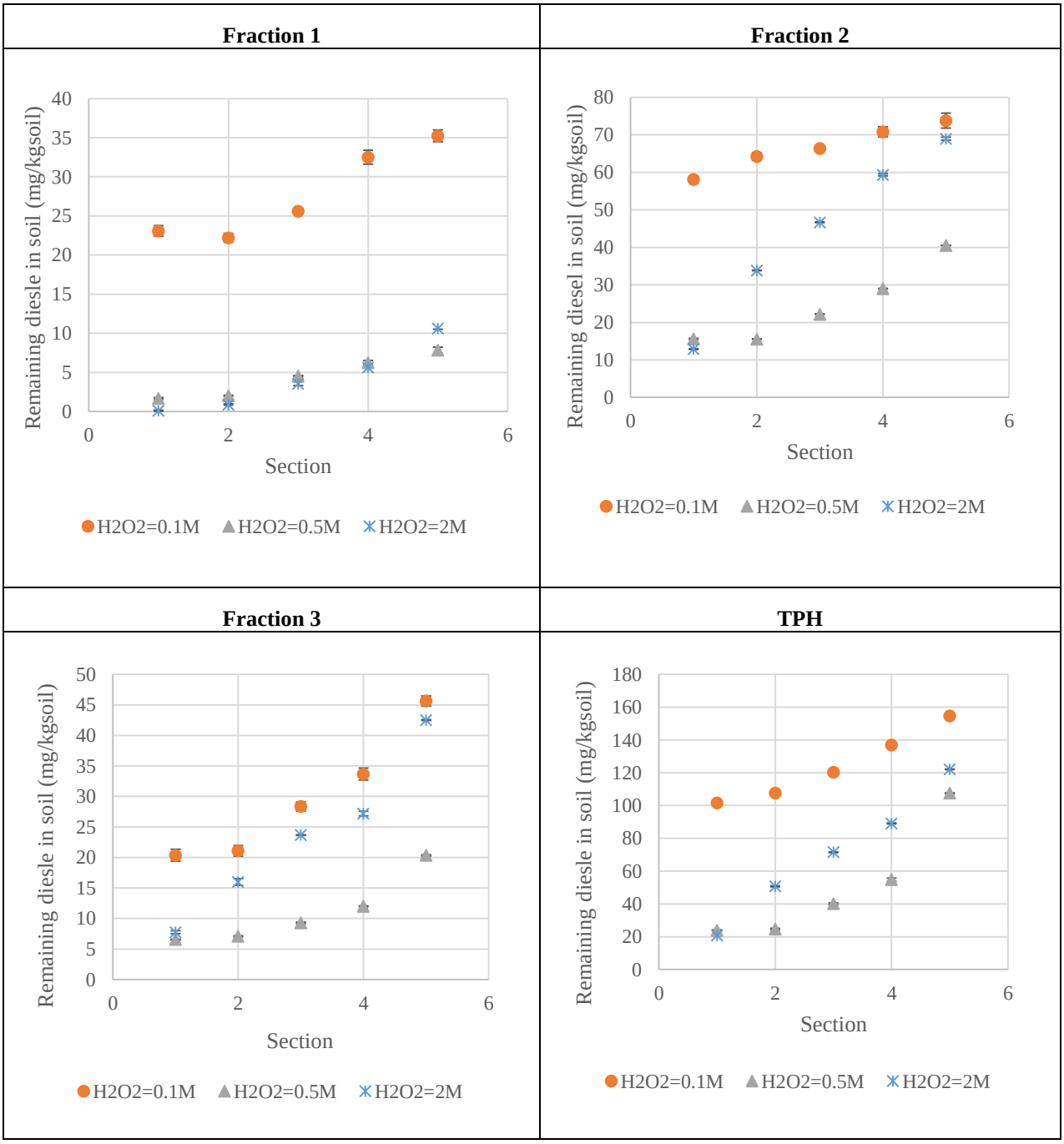

Figure 6-1: Remaining diesel in soil at H_2O_2= 0.1M, 0.5M, and 2M at constant Fe^{2+}=0.05 M, EL=10%, and LS=1/2, fraction 1, fraction 2, fraction 3 and TPH

6.2.2. Effect of overall soil slurry volume, L/S, on remaining diesel in soil

In Figure 6-2, the effect of overall L/S is depicted. It should be noted here that each section is representing different L/S ratio. The L/S of the final section is considered as the overall L/S. As can be observed, the remaining of diesel had

not changed considerably. This showed that increase in L/S did not have a significant effect on the remaining diesel in soil. This is potentially helpful in determining the amount of Fenton reagents for field applications. The remaining diesel in soil had increased from section 1 to section 5, as expected and previously explained due to the higher concentration of Fenton at the top of the column.

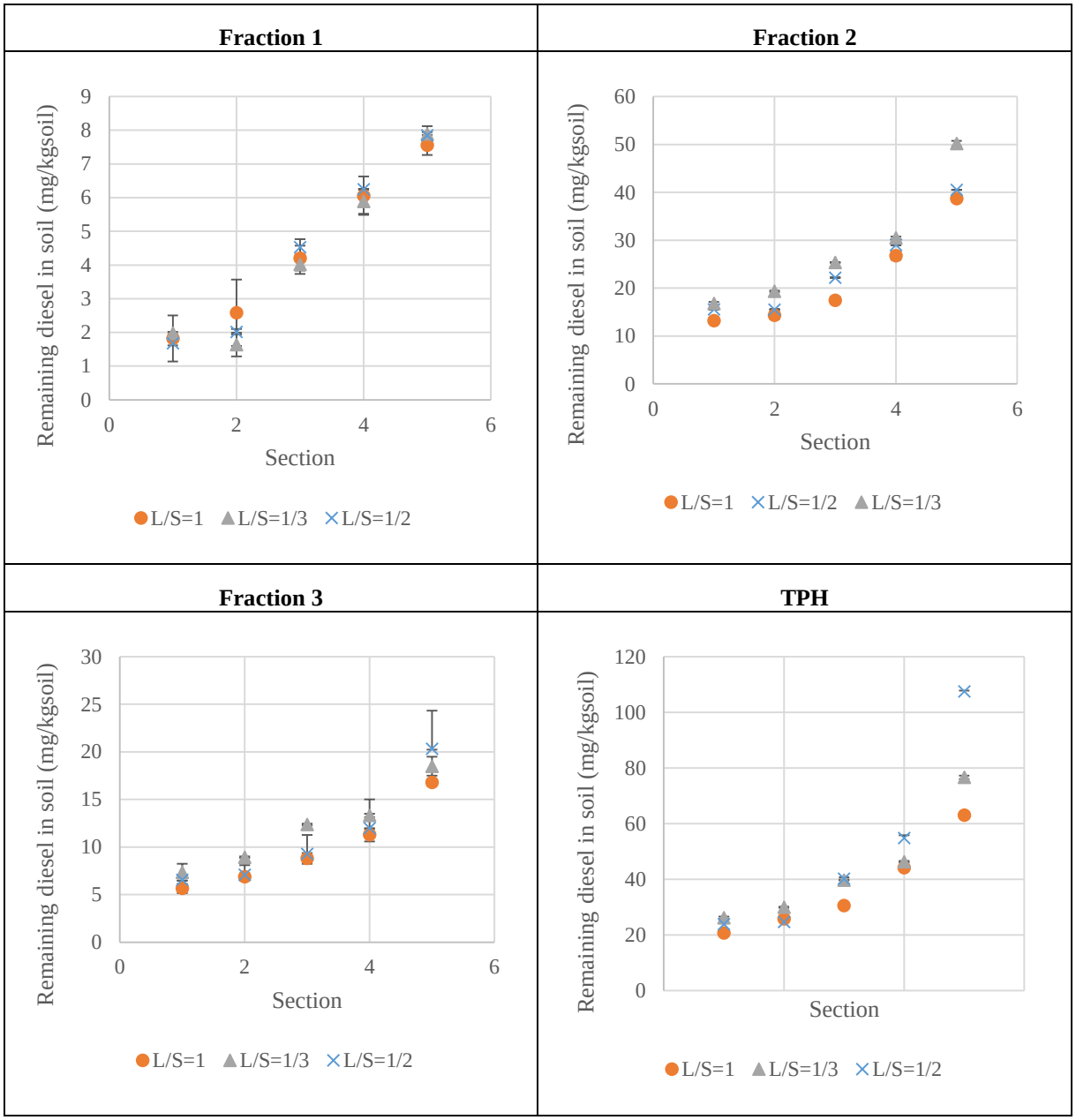

Figure 6-2: Remaining diesel in soil at L/S=1/3, 1/2, 1 at constant H_2O_2=0.5 M, Fe^{2+}=0.05M, and EL=10%, fraction 1, fraction 2, fraction 3 and TPH

6.2.3. Effect of EL% on remaining diesel in soil, H_2O_2, and velocity

The results of the effect of EL% on remaining diesel in soil are illustrated in Figure 6-3. The experiment without EL had the lowest remaining TPH in soil. By increasing the EL%, the remaining TPH increased from 93.41 mg/kg soil for EL=10% to 565.64 mg/kg soil for EL=50% at section 5 for TPH which was the highest remaining TPH value in soil. This could possibly be caused by the more

reactive Fenton reagents in solutions with higher water content. For fraction 1, both EL=10% and 25% did not have considerable differences as compared to EL=0%. For fractions 2 and 3, the difference between EL=10% and EL=0% was not significant, but the remaining diesel in soil for EL=25% had increased.

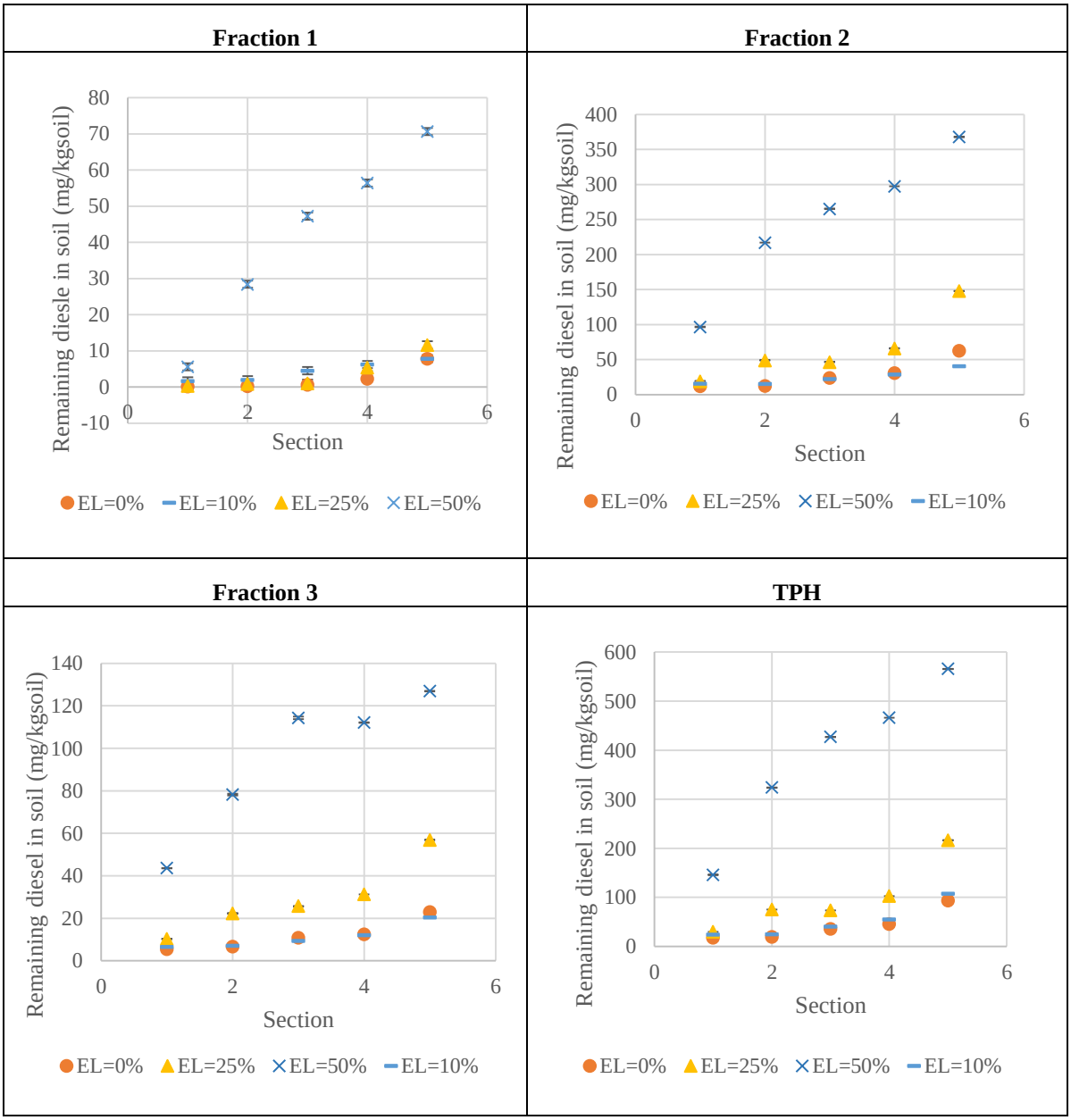

Figure 6-3: Remaining diesel in soil at EL%= 0%, 25%, and 50% at constant H_2O_2=0.5 M, Fe^{2+}=0.05M, and LS=1/2, fraction 1, fraction 2, fraction 3 and TPH

The remaining diesel in soil had increased from section 1 to section 5 because of the higher concentration of Fenton reagent in the higher column sections. However, the change in section 1 to section 5 was lower than the case with change in H_2O_2 concentration. The high value of the remaining diesel in soil for EL=50%, 565.64 mg/kg soil for section 5 of TPH, could also be caused by dissolution of diesel in EL, but not decomposed by Fenton reaction. In this case,

the dissolved diesel was transported with the liquid phase to the lower sections. This finding indicated that choosing an appropriate percentage of solvent is important as it can change the fate of the pollutants and in this case increase the solubility and ultimately, availability of TPH. For this reason, the ratio of Fenton reagents and EL should be chosen accordingly.

The H_2O_2 in the effluent were analysed to see how an increase in EL% could change the H_2O_2 decomposition. Figure 6-4 shows the H_2O_2 in the effluent at EL=0%, 10%, 25%, and 50%. As shown, by adding EL, the remaining H_2O_2 in the effluent increased dramatically from the case without EL, EL=0%, to the higher EL% values from C/C_0=0.03 for EL=0% to C/C_0=0.32 for EL=50% after 15 min for TPH. This suggested that EL increased the stability of H_2O_2. By increasing EL% from 10% to 50%, the H_2O_2 in the effluent had increased slightly. One of the main issues in in-situ application of Fenton reaction is the instability of H_2O_2 and its decomposition at 1-2 m of injection point (Vicente et al., 2011). This research indicated that EL can be an effective stabilizer for H_2O_2. This property can be even more helpful for the aged contaminated soil as desorption of the pollutants requires longer contact time. By choosing an appropriately small value of EL, the stability of H_2O_2 can be increased.

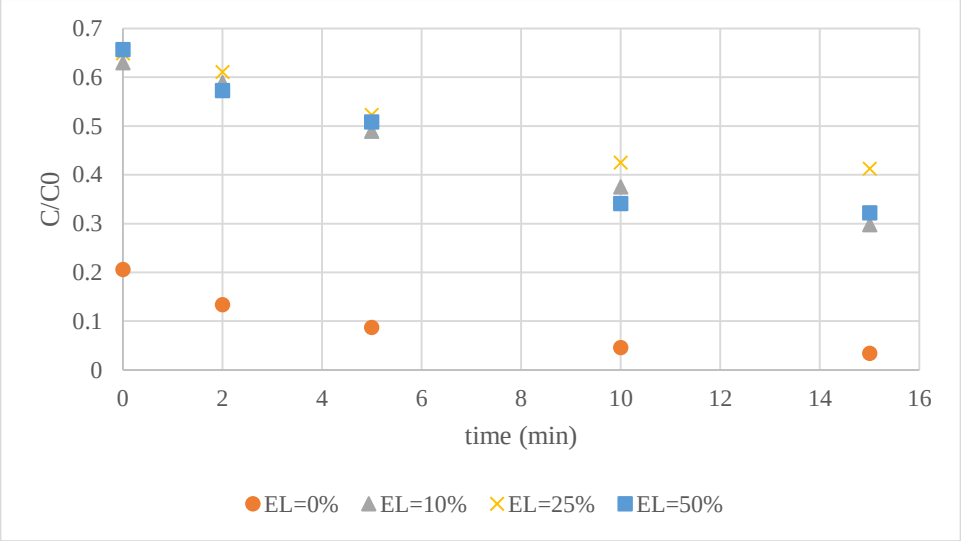

Figure 6-4: Effect of EL% on H_2O_2 decomposition

The effect of EL% on velocity is depicted in Figure 6-5. As can be observed, the flow with EL=10% had the highest velocity. This could be linked to the increase in EL% which increased the density of the flow slightly leading to the decrease in velocity. Conversely, in the case of EL=0%, the reaction was very fast and was accompanied by bubbling on top of the column that resulted in lower velocity.

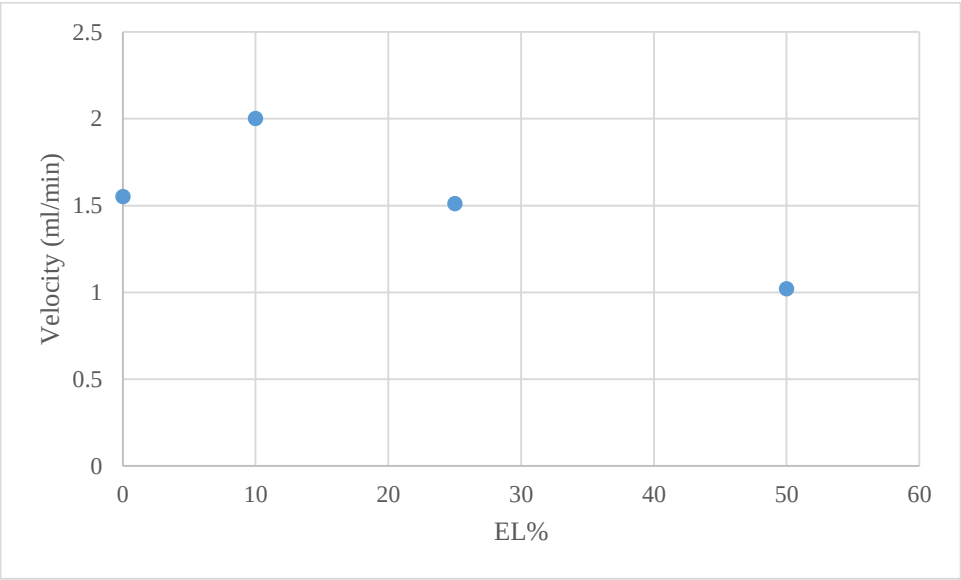

Figure 6-5: Effect of EL% on velocity

6.3 Concluding Remarks

To study the fate of petroleum hydrocarbons under field conditions, EL-Fenton reactions were studied using column set-up. The effects of different variables on remaining diesel in column set-up were examined. An increase in H_2O_2 molarity from 0.1 M to 0.5 M decreased the remaining diesel in soil while further increase to 2 M led to an increase in the remaining diesel in soil. The results showed that the destruction reaction had not changed by increasing the overall L/S to more than L/S=1/3. An increase in EL increased the stability of H_2O_2. C/C_0 values for EL=0% and EL=50% after 15 min for TPH increased from C/C_0=0.03 to C/C_0=0.32, respectively.

CHAPTER 7: CONCLUSIONS AND RECOMMENDATIONS FOR FUTURE WORK

7.1 Conclusions

This study reports a novel EL based Fenton treatment for the remediation of diesel-contaminated soil. The applied solvent in this study, EL, is classified as a green solvent. A sequential remediation process was studied starting with a desorption pretreatment followed by Fenton oxidation. The main conclusions derived from this study are summarised below.

Due to its unique properties, EL serves as an excellent solubilizing and extracting agent. The removal efficiency via desorption of TPH in different fractions was enhanced with addition of EL, and this solvent could even desorb diffused contaminants which showed its potential in treating aged contaminated soil. In desorption kinetic study, the existence of a very fast initial step followed by a very slow and equilibrium step was detected. With the fluctuation in desorption experiments, it was hypothesized that there were different compartments with different adsorption/desorption affinities. Desorption kinetics were well described by the pseudo-second order model. The effects of different variables, EL%, L/S, and initial contamination levels, on the initial desorption rate are examined. Increase in EL% leads to the increase in initial desorption rate, increase in initial contamination level results in decrease in initial desorption rate and L/S=2 had the lowest initial desorption rate.

At higher concentration, EL could hinder the Fenton reaction due to the insolubility of $FeSO_4.7H_2O$ in EL. On the other hand, it was proved that EL could increase the stability of H_2O_2 in Fenton reaction, a property that is highly desirable in field applications especially for remediation of sites with long contamination history. The effects of EL%, H_2O_2 concentration and L/S on Fenton oxidation of TPH in contaminated soil was investigated through parametric batch studies. After 4 h, removal efficiency of TPH increased from 68.41% to 90.21% by increasing H_2O_2 concentration from 0.1 M to 2 M at L/S=2 and EL=25%. By increasing EL% from 10% to 68%, the removal efficiency for TPH decreased. The TPH removal efficiency had the highest value of 85.77% for the lowest L/S=1. Fenton reaction had the highest TPH removal efficiency for EL=10% . Based on the curve-fitting results of the Fenton reaction, power law equation and pseudo-first order equation are reported as the best equations that are able to model the results.

This study further extended previous findings regarding the effect of HA on Fenton reaction. The results showed how the fractions with different molecular weights responded to the increase in HA. Furthermore, HA addition for TPH till 100 mg/l was less than the HA=0 case with a value of 87.95%, and an increase to HA=150 resulted in the increase in removal efficiency to 93.23%. The results suggested the presence of an optimum value for HA which was mostly dependent on the molecular weight of the pollutants for petroleum hydrocarbons. Adding EL contributed towards making accessible the diffused part of TPH.

The effects and interactions of three variables, HA (A), EL % (B), and pH (C), on removal efficiency of Fenton reaction and finally optimization of the process were studied by RSM. Based on the obtained results, increase in removal efficiency was observed at constant EL=35% as a result of decrease in EL and increase in pH. HA=51.76mg/l, EL=20.93%, and pH=5.99 are calculated as the optimum values.

To study the fate of petroleum hydrocarbons under field conditions, the effects of different Fenton variables on remaining diesel in column set-up were examined. An increase in H_2O_2 molarity from 0.1 M to 0.5 M decreased the remaining diesel in soil while further increase to 2 M led to an increase in remaining diesel in soil. The results showed that the reaction was almost complete for fraction 1 by passing the overall L/S=1/3 and higher than this value did not affect the remaining diesel in soil. Meanwhile, for fractions 2 and 3 and TPH, an increase from 1/3 to 1/2 and 1, respectively led to inconsiderable decreases in remaining diesel. An increase in EL increased the stability of H_2O_2.

7.2 Recommendations for future work

The potential of EL in soil remediation requires further study in order to fully develop its application in the area of soil remediation. Based on the findings of this study, two main recommendations for future work are suggested as follows:

1. Study of EL-Fenton reaction with different iron catalysts, such as native iron, Fe^{3+}, or inorganic iron sources might shed light on the reaction of these catalysts with H_2O_2.
2. Due to the high potential of EL for desorption of petroleum hydrocarbon and the stability of H_2O_2 in EL, exploring the application of EL-based

Fenton treatment in actual contaminated sites would be helpful in expanding the application of this green solvent.

References

Aksu Z. (2005) Application of biosorption for the removal of organic pollutants: a review. Process Biochem 40:997–1026

Al-Abed S. R., Jegadeesan G., Purandare J., Allen D. (2008) Leaching behavior of mineral processing waste: Comparison of batch and column investigations. J. Hazard. Mater. 153(3):1088-1092

Albergaria J.T., Conceição M., Alvim-Ferraz M., and Delerue-Matos C. (2012) Remediation of sandy soils contaminated with hydrocarbons and halogenated hydrocarbons by soil vapour extraction. Journal of Environmental Management 104:195-201

Allen S.J., Mckay G., Porter J.F. (2004) Adsorption isotherm models for basic dye adsorption by peat in single and binary component systems. J. Colloid Interface Sci. 280:322–333

Altenor S., Carene B., Emmanuel E., Lambert J., Ehrhardt J.-J., Gaspard S. (2009) Adsorption studies of methylene blue and phenol onto vetiver roots activated carbon prepared by chemical activation. J. Hazard. Mater. 165:1029–1039

Aparicio S., Alcalde R. (2009/a) The green solvent ethyl lactate: an experimental and theoretical characterization. Green Chem.11:65-78

Aparicio S., Alcalde R. (2009/b) Insights into the ethyl lactate + water mixed solvent. J. Phys. Chem. B, 113:14257–14269

Aparicio S., Halajian S., Alcalde R., Leal B. G. J. M. (2008) Liquid structure of ethyl lactate, pure and water mixed, as seen by dielectric spectroscopy, solvatochromic and thermophysical studies. J. Phys. Chem. Lett 454:49–55

Arias-Estévez M. (2012) Comparison of batch, stirred flow chamber, and column experiments to study adsorption, desorption and transport of carbofuran within two acidic soils. Chemosphere 88:106–112

Azizian S. (2004) Kinetic models of sorption: a theoretical analysis. J. Colloid Interface Sci. 276:47–52

Bandala E.R., Pel´aez A.M., Salgado M.J., and Torres L. (2008) Degradation of sodium dodecyl sulphate in water using solar driven Fenton-like advanced oxidation processes J. Hazard. Mater.151:578–584

Barnier C., Ouvrard S., Robin C., and Morel J.L. (2014) Desorption kinetics of PAHs from aged industrial soils for availability assessment. Sci Total Environ 470–471:639–645

Başar C. A. (2006) Applicability of the various adsorption models of three dyes adsorption onto activated carbon prepared waste apricot. J. Hazard. Mater. B135:232–241

Batzias F.A., Sidiras D.K. (2007) Simulation of dye adsorption by beech sawdust as affected by pH. J. Hazard. Mater. 141:668–679

Bayley R.W., and Biggs C.A. (200/a) Characterisation of an attrition scrubber for the removal of high molecular weight contaminants in sand. Chem. Eng. J. 111:71–79

Bayley R.W., and Biggs C.A. (200/b) Evaluation of the jet pump scrubber as a novel approach for soil remediation. Process Safety and Environmental Protection 83 (B4):381–386

Bermúdez-Couso A., Fernández-Calviño D., Rodríguez-Salgado I., Nóvoa Muñoz J. C., Arias-Estévez M. (2012) Comparison of batch, stirred flow chamber, and column experiments to study adsorption, desorption and transport of carbofuran within two acidic soils. 88 (1):106-112

Besha A.T., Bekele D. N., Naidu R., Chadalavada S. (2017) Recent advances in surfactant-enhanced in-situ chemical oxidation for the remediation of non-aqueous phase liquid contaminated soils and aquifers. Environmental Technology & Innovation. http://dx.doi.org/10.1016/j.eti.2017.08.004

Birdwell J., Cook R.L., Thibodeaux L.J. (2007) Desorption kinetics of hydrophobic organic chemicals from sediment to water: A review of data and models. Environ. Toxicol. Chem. 26 (3):424–434

Bogan B. W., and Trbovic V. (2003/a) Effect of sequestration on PAH degradability with Fenton's reagent: roles of total organic carbon, humin, and soil porosity. J. Hazard. Mater. B100:285–300

Bogan B.W., Trbovic V., and Paterek J.R. (2003/b) Inclusion of vegetable oils in Fenton's chemistry for remediation of PAH-contaminated soils. Chemosphere 50:15–21

Brusseau M.L., and Rao P.S.C. (1990) Modelling solute transport in structured soils: A review. Geoderma 46:169-192

Reference method for the Canada-wide standard for petroleum hydrocarbons in Soil - Tier 1 method, Canadian Council of Ministers of the Environment (CCME)

Castaldi P., Alberti G. , Merella R., and Pietro Melis (2005) Study of the organic matter evolution during municipal solid waste composting aimed at identifying suitable variables for the evaluation of compost maturity. Waste Manage. 25:209–213

Chen C. T., Tafuri A. N., Rahman M., Foerst M. B. (1998) Chemical oxidation treatment of petroleum contaminated soil using Fenton's reagent. J. Environ. Sci. Health. A33(6):987-1008

Chen G., Hoag G. E., Chedda P., Nadim F., Woody B. A., and Dobbs G. M. (2001) The mechanism and applicability of in situ oxidation of trichloroethylene with Fenton's reagent. J. Hazard. Mater. 87:171–186

Cheng M., Zeng G., Huang D., Lai C., Xu P., Zhang C., Liu Y. (2015) Hydroxyl radicals based advanced oxidation processes (AOPs) for remediation of soils contaminated with organic compounds: a review. Chem. Eng. J. 284:582-598

Chern J.-M., Wu C.-Y. (2001) Desorption of dye from activated carbon beds: effect sof temperature, pH, and alcohol. Wat. Res. 35(17)4159–4165

Connaughton D.F., Stedlnger J.R., Llon L.W., and Shuler M.L. (1993) Description of Time-Varying Desorption Kinetics: Release of Naphthalene from Contaminated Soils. Environ. Sci. Technol. 27:2397-2403

Contaminated Land Management and Control Guidelines No. 1: Malaysia Recommended Site Screening Levels for Contaminated Soil Land

Cornelissen G., Van Noort P.C.M., Govers H.A.J. (1998) Mechanism of slow desorption of organic compounds from sediments: A study using model sorbents. Environ. Sci. Technol. 32:3124-3131

Cundy A. B., Hopkinson L., and Whitby R. L.D. (2008) Use of iron-based technologies in contaminated land and groundwater remediation: A review. Sci. Total Environ. 400: 42-51

Dąbrowski A. (2001) Adsorption_ from theory to practice. Adv. Colloid Interface Sci. 93:135-224

Delay M., Lager T., Schulz H. D., and Frimmel F. H. (2007) Comparison of leaching tests to determine and quantify the release of inorganic contaminants in demolition waste. Waste Manage. 27:248–255

Doick K., Burauel P. , Jones K. C., Semple K. (2005) Distribution of aged 14C-PCB and14C-PAH residues in particle-size and humic fractions of an agricultural soil. Environ. Sci. Technol. 39:6575-6583

EPA 402-R-99-004B, United States Office of Air and Radiation, Environmental Protection Agency, 1999

Fan C., Horng C-Y., Li S.-J. (2013) Structural characterization of natural organic matter and its impact on methomyl removal efficiency in Fenton process. Chemosphere 93:178–183

Ferguson S.H., Woinarski A.Z., Snape I., Morris C.E., and Revill A.T. (2004) A field trial of in situ chemical oxidation to remediate long-term diesel contaminated Antarctic soil. Cold Regions Science and Technology 40:47– 60

Ferrarese E., Andreottola G., Oprea I.A. (2008) Remediation of PAH-contaminated sediments by chemical oxidation. J Hazard Mater 152:128–139

Foo K.Y., Hameed B.H. (2010) Insights into the modelling of adsorption isotherm systems. Chem. Eng. J. 156:2–10

Georgi A., Schierz A., Trommler U., Horwitz C.P., Collins T.J., Kopinke F.-D. (2007) Humic acid modified Fenton reagent for enhancement of the working pH range. Appl. Catal., B: Environmental 72:26–36

Goi A., Kulik N., and Trapido M. (2006) Combined chemical and biological treatment of oil contaminated soil. Chemosphere 63:1754–1763

Gong Z., Alef K., Wilke B-M., and Li P. (200/b) Dissolution and removal of PAHs from a contaminated soil using sunflower oil. Chemosphere 58:291–298

Gong Z., Alef K., Wilke B-M., and Li P. (2007) Activated carbon adsorption of PAHs from vegetable oil used in soil remediation. J. Hazard. Mater. 143:372–378

Gong Z., Wang X., Tu Y., Wud J., Sun Y., and Li P. (2010) Polycyclic aromatic hydrocarbon removal from contaminated soils using fatty acid methyl esters. Chemosphere 79:138–143

Gong Z., Wilke B.-M., Alef K., and Li P. (2005/a) Influence of soil moisture on sunflower oil extraction of Polycyclic Aromatic Hydrocarbons from a manufactured gas plant soil. Sci. Total Environ. 343:51– 59

Gong Z., Wilke B.-M., Alef K., Li P., Zhou Q. (2006) Removal of polycyclic aromatic hydrocarbons from manufactured gas plant-contaminated soils using sunflower oil: Laboratory column experiments. Chemosphere 62:780–787

Grathwohl P., and Susset B. (2009) Comparison of percolation to batch and sequential leaching tests: Theory and data. Waste Manage. 29:2681–2688

Gunasekara A. S., and Xing B. (2003) Sorption and desorption of Naphthalene by soil organic matter: Importance of aromatic and aliphatic components. J. Environ. Qual. 32:240–246

G¨unay A., Arslankaya E., Tosun ˙I. (2007) Lead removal from aqueous solution by natural and pretreated clinoptilolite: Adsorption equilibrium and kinetics. J. Hazard. Mater. 146:362–371

Guo H., Wang W., Sun Y., Li H., Ai F., Xie L., and Wang X. (2010) Ethyl lactate enhances ethylenediaminedisuccinic acid solution removal of copper from contaminated soils. . J. Hazard. Mater. 174:59–63

Gustafson J.B., Tell J. G., and Orem D. (1997) Selection of Representative TPH Fractions Based on Fate and Transport Considerations. Total Petroleum Hydrocarbon Criteria Working Group Series, 3

He L., Song J., Peng P. (2008) Characterization of extractable and non-extractable polycyclic aromatic hydrocarbons in soils and sediments from the Pearl River Delta, China. Environ. Pollut. 156:769–774

He Y., Xu J., Wang H., Zhang Q., Muhammad A. (2006) Potential contributions of clay minerals and organic matter to pentachlorophenol retention in soils. Chemosphere 65:497–505

Heath J. S., Koblis K., Sager S.L. (1993) Review of chemical, physical, and toxicologic properties of components of total petroleum hydrocarbons. Journal of Soil Contamination 2 (1)

Ho Y.-S., (2006/a) Second-order kinetic model for the sorption of cadmium onto tree fern: A comparison of linear and non-linear methods. Water Res. 40:119 – 125

Ho Y.-S. (2006/b) Review of second-order models for adsorption systems. J. Hazard. Mater. B136:681–689

Hossain M.A., Ngo H.H., Guo W.S., Setiadi T. (2012) Adsorption and desorption of copper (II) ions onto garden grass. Bioresour. Technol. 121:386–395

Ghosh U., Talley J. W., Luthy R. G. (2001) Particle-scale investigation of PAH desorption kinetics and thermodynamics from sediment. Environ. Sci. Technol. 35:3468-3475

Guo H., Wang W., Sun Y., Li H., Ai F., Xie L., Wang X. (2010) Ethyl lactate enhances ethylenediamine disuccinic acid solution removal of copper from contaminated soils. J. Hazard. Mater. 174:59–63

Huang S.W., Chiang P.N., Liu J.C., Hung J.T., Kuan W.H., Tzou Y.M., Wang S.L., Huang J.H., Chen C.C., Wang M.K., Loeppert R.H. (2012) Chromate reduction on humic acid derived from a peat soil – Exploration of the activated sites on HAs for chromate removal. Chemosphere l.87:587–594

Huang Y.-Y., Wang S.-L., Liu J.-C., Tzou Y.-M., Chang R.-R., Chen J.-H., (2008) Influences of preparative methods of humic acids on the sorption of 2,4,6-trichlorophenol. Chemosphere 70:1218–1227

Huling S. G., Arnold R. G., Siekra R. A., Miller M. R. (2001) Influence of peat on Fenton oxidation Wat. Res. 35(7):1687–1694

Isosaari P., T. Tuhkanen, and T. Vartianen (2001) Use of olive oil for soil extraction and ultraviolet degradation of polychlorinated dibenzo-p-dioxins and dibenzofurans. Environ. Sci. Technol. 35(6):1259-1265

Jalilian A. S. P., Suyin Gan, Hoon Kiat Ng, Suhaimi Abdul Talib (2017) Evaluation of ethyl lactate as solvent in Fenton oxidation for the remediation of total petroleum hydrocarbon (TPH)-contaminated soil. Environ Sci Pollut Res, 24(21):17779-17789

Jamialahmadi N., Gitipour S., Jamialahmadi O., Baghdadi M. (2015) Remediation of a Diesel-Contaminated Soil Using a Fenton-Like Advanced Oxidation Process: Optimization by Response Surface Methodology. Soil Sediment Contam: An International Journal, 24:609–623

Johnson M. D., Weber W. J. Jr. (2001) Rapid prediction of long-term rates of contaminant desorption from soils and sediments. Environ. Sci. Technol. 35:427-433

Jones J., Pham T., Smart K., Splinter D., Steele M. (2003) Ethyl Lactate Production. Capstone Design Project- University of Oklahoma

Jonsson S., Persson Y., Frankki S., van Bavel B., Lundstedt S., Haglund P. , M. TysklindKanel S.R. (2007) Degradation of polycyclic aromatic hydrocarbons (PAHs) in contaminated soils by Fenton's reagent: A multivariate evaluation of the importance of soil characteristics and PAH properties. J. Hazard. Mater. 149:86–96

Kalbe U., Berger W., Eckardt J., Simon F.-G. (2007) Evaluation of leaching and extraction procedures for soil and waste. Waste Manag. 28(6):1027-1038

Kanel S.R., Neppolian B., Choi H., and Yang J.W. (2003) Heterogeneous catalytic oxidation of phenanthrene by hydrogen peroxide in soil slurry: kinetics, mechanism, and implication. Soil Sediment Contam 12(1):101-117

Kang N., Hua I. (2005) Enhanced chemical oxidation of aromatic hydrocarbons in soil systems. Chemosphere 61:909‑922

Kang N., Hua I., Rao P. S. C. (2006) Enhanced Fenton's destruction of non-aqueous phase perchloroethylene in soil systems. Chemosphere 63 (2006) 1685–1698

Kannan N., Sundaram M. M. (2001) Kinetics and mechanism of removal of methylene blue by adsorption on various carbons—a comparative study. Dyes Pigm 51 (2001) 25–40

Kawahara F. K., Davila B., Al-Abed S. R., Vesper S. J., Ireland J. C., Rock S. (1995) Polynuclear aromatic hydrocarbon (PAH) release from soil during treatment with Fenton's reagent. Chemosphere. 31(9): 4131-4142.

Khan A. R., Al-Bahri T. A., Al-Haddad A. (1997/a) Adsorption of phenol based organic pollutants on activated carbon from multi-component dilute aqueous solutions. Wat. Res. Vol. 31(8):2102 2112

Khan A. R., Ataullah R., Al-Haddad A. (1997/b) Equilibrium adsorption studies of some aromatic pollutants from dilute aqueous solutions on activated carbon at different temperatures. J. Colloid Interface Sci. 194:154–165

Khan A. R., Riazi M. R., Al-Roomi Y. A. (2000) A thermodynamic model for liquid adsorption isotherms. Sep. Purif. Technol. 18:237–250

Khodadoust A.P., Bagchi R., Suidan M.T., Brenner R.C., and Sellers N.G. (2000) Removal of PAHs from highly contaminated soils found at prior manufactured gas operations. J. Hazard. Mater. B80:159–174

Koshlaf E., Shahsavar E., Aburto-Medina A., Taha M., Haleyur N., Makadia T. H., Morrison P. D., Ball A. S. (2016) Bioremediation potential of diesel-contaminated Libyan soil. Ecotoxicol Environ Saf. 133:297–305

Kleineidam S., Schuth C., Grathwohl P. (2002) Solubility-Normalized Combined Adsorption-Partitioning Sorption Isotherms for Organic Pollutants. Environ. Sci. Technol. 36:4689-4697

Khodadoust A.P., Suidan M.T. Acheson C.M., and Brenner R.C. (1999) Solvent extraction of Pentachlorohenol from contaminated soils using water-ethanol mixtures. Chemosphere 38 (11):2681-2693

Kim I., Lee M. (2012) Pilot scale feasibility study for in-situ chemical oxidation using H2O2 solution conjugated with biodegradation to remediate a diesel contaminated site. J. Hazard. Mater. 241– 242:173– 181

Kong S.-H, Watts R. J., Choi J-H. (1998) Treatment of Petroleum-Contaminated Soils Using Iron Mineral Catalyzed Hydrogen Peroxide. Chemosphere, 37 (8):1473-1482

Koranteng – Addo E.J, Owusu – Ansah E, Boamponsem L. K, Bentum J. K, Arthur S. (2011) Levels of zinc, copper, iron and manganese in soils of abandoned mine pits around the Tarkwa gold mining area of Ghana. Adv Appl Sci Res. 2 (1): 280-288

Kosaka J., Honda C., Izeki A. (1961) Fractionation of humic acid by organic solvents. J. Soil Sci. Plant Nutr. 7(2):48-53

Kulik N., Goi A., Trapido M., Tuhkanen T. (2006) Degradation of polycyclic aromatic hydrocarbons by combined chemical pre-oxidation and bioremediation in creosote contaminated soil. J. Environ. Manage. 78:382–391

Kumar K. V., Porkodi K. (2006) Relation between some two- and three-parameter isotherm models for the sorption of methylene blue onto lemon peel. J. Hazard. Mater. 138:633–635

Kumar P. S., Ramalingam S., Senthamarai C., Niranjanaa M., Vijayalakshmi P., Sivanesan S. (2010) Adsorption of dye from aqueous solution by cashew nut shell: Studies on equilibrium isotherm, kinetics and thermodynamics of interactions. Desalination 261:52–60

Kuppusamy S., Thavamani P., Venkateswarlu K., Lee Y. B., Naidu R., Megharaj M. (2016) Remediation approaches for polycyclic aromatic hydrocarbons (PAHs) contaminated soils: Technological constraints, emerging trends and future directions. Chemosphere. 1-25

Lee B-D, Hosomi M. (2001) Fenton oxidation of ethanol-washed distillation-concentrated bBenzoa(a)pyrene: reaction product identification and biodegradability. Wat Res 35(9): 2314–2319

Lee B-T., and Kim K-W. (2002) Ozonation of diesel fuel in unsaturated porous media. Appl Geochem 17:1165–1170

Lee L.S., Zhai X., and Lee J. (2006) Lab testing and field implementation of soil flushing. Joint Transportation Research Program Purdue Libraries

Leifeld J., and Kogel-Knabner I. (2001) Organic carbon and nitrogen in fine soil fractions after treatment with hydrogen peroxide. Soil Biol Biochem 33:2155-2158

Lewis J., and Sjöstrom J. (2010) Optimizing the experimental design of soil columns in saturated and unsaturated transport experiments. J. Contam. Hydrol. 115:1–13

Li X., Dua Y., Wua G., Li Z., Li H., and Sui H. (2012) Solvent extraction for heavy crude oil removal from contaminated soils. Chemosphere 88:245–249

Liao C., Chung T., Chen W., and Kuo S. (2007) Treatment of pentachlorophenol-contaminated soil using nano-scale zero-valent iron with hydrogen peroxide. J. Mol. Catal. A: Chemical 265:189–194

Lim M. W., Lau E. V., Poh P. E. (2016) A comprehensive guide of remediation technologies for oil contaminated soil—Present works and future directions. Marine Pollution Bulletin.

Lindsey M., Tarr M.A. (2000) Inhibition of hydroxyl radical reaction with aromatics by dissolved natural organic matter. Environ. Sci. Technol. 34:444-449

Liu Y., Li Q., Li Y., Bao J., Hu Z., Hao D., Song D., Wang Y., Yang M. (2015) Detection of nanoscale soil organic matter by middle infrared spectrum for forensic science. Hindawi Publishing Corporation Journal of Chemistry Volume 2015

Loehr R.C., Lamar M.R., and Poppendieck D.G. (2003) A protocol to estimate of anthropogenic hydrocarbons from contaminated soils. Environ. Toxicol. Chem. 22(9):2202–2208

Lu M., Zhang Z., Qiao W., Guan Y., Xiao M., and Chong Peng (2010/a) Removal of residual contaminants in petroleum-contaminated soil by Fenton-like oxidation. J. Hazard. Mater.179:604–611

Lu M., Zhang Z., Qiao W. ,Wei X., Guan Y., Maa Q., and Guan Y. (2010/b) Remediation of petroleum-contaminated soil after composting by sequential treatment with Fenton-like oxidation and biodegradation. Bioresour. Technol. 101:2106–2113

Lundstedt S., Persson Y., and Lars Oberg (2006) Transformation of PAHs during ethanol-Fenton treatment of an aged gasworks' soil. Chemosphere 65:1288–1294

Ma X.-H., Zhao L., Dong Y.-H., Chen H., Zhong M. (2018) Enhanced Fenton degradation of polychlorinated biphenyls in capacitor-oil contaminated soil by chelating agents. Chem. Eng. J. 333:370–379

Maurya N. S., Mittal A. K., Cornel P., Rother E. (2006/a) Biosorption of dyes using dead macro fungi: Effect of dye structure, ionic strength and pH. Bioresour. Technol. 97:512–521

Maurya N. S., Mittal A. K. (2006/b) Applicability of Equilibrium Isotherm Models for the Biosorptive Uptakes in Comparison to Activated Carbon-Based Adsorption. J. Environ. Eng. 1589-1599

McKay G. (1983) The Adsorption of dyestuffs from aqueous solutions using activated carbon. III. Intraparticle diffusion processes. J. Chem. Tech. Biotechnol. 33A:196-204

Mackay D., Shui W.Y., and Ma K.C. (1999) Illustrated Handbook of physical-chemical properties and environmental fate for organic chemicals. vol.1-4. Lewis Publishers, Chelsea, MI.

Mann M.J. (1999) Full-scale and pilot-scale soil washing. J. Hazard. Mater.66:119–136

Mater L., Sperb R.M., Madureira L.A.S., Rosin A.P., Correa A.X.R., and Radetski C.M. (2006) Proposal of a sequential treatment methodology for the safe reuse of oil sludge-contaminated soil. J. Hazard. Mater.B136:967–971

Miller C. T., Weber Jr. W. J. (1986) Sorption of hydrophobic organic pollutants in saturated soil systems. J. Contam. Hydrol. 1:243-261

Millioli V. S., Freire D. D.C., Cammarota M. C. (2003) Petroleum oxidation using Fenton's reagent over beach sand following a spill. J. Hazard. Mater.B103:79–91

Mohan D., Singh K. P., Sinha S., Gosh D. (2004) Removal of pyridine from aqueous solution using low cost activated carbons derived from agricultural waste materials. Carbon 42:2409–2421

Navalon S., Alvaro M., and Garcia H. (2010) Heterogeneous Fenton catalysts based on clays, silicas and zeolites. Appl. Catal. B 99:1–26

Ncibi M.C., Mahjoub B., Gourdon R. (2007) Effects of aging on the extractability of naphthalene and phenanthrene from Mediterranean soils. J. Hazard. Mater. 146:378–384

Neyens E., and Baeyens J. (2003) A review of classic Fenton's peroxidation as an advanced oxidation technique. J. Hazard. Mater. B98:33–50

Northcott G., Jones K. C. (2001) Partitioning, extractability, and formation of nonextractable PAH residues in Soil. 1. Compound differences in aging and sequestration. Environ. Sci. Technol. 35:1103-1110

Ojinnaka C., Osuji L., and Achugasim O. (2012) Remediation of hydrocarbons in crude oil-contaminated soils using Fenton's reagent. Environ. Monit. Assess. 184:6527–6540

Oh S.-Y., Shin D.-S. (2014) Treatment of diesel-contaminated soil by Fenton and persulfate oxidation with zero-valent iron. Soil Sediment Contam. 23:180–193

Pannu J.K., Singh A., and Ward O.P. (2004) Vegetable oil as a contaminated soil remediation amendment: application of peanut oil for extraction of polycyclic aromatic hydrocarbons from soil. Process Biochem. 39:1211–1216

Parker JR G. R. (1995) Optimum Isotherm Equation and Thermodynamic Interpretation for Aqueous 1,1,2-Trichloroethene Adsorption Isotherms on Three Adsorbents. Adsorption 1:113-132

Pérez-Gregorio M.R., M.S. García-Falcón., J. Simal-Gándara (2010) Removal of polycyclic aromatic hydrocarbons from organic solvents by ashes wastes. J. Hazard. Mater. 178(1–3) 2010:273-281

Pighin E., Díez V.K., Cosimo J. I. D. (2016) Synthesis of ethyl lactate from triose sugars on Sn/Al2O3 catalysts. Appl. Catal. A General. 517:151-160

Pikaar I., Koelmans A. A., van Noort P. C.M. (2006) Sorption of organic compounds to activated carbons. Evaluation of isotherm models. Chemosphere 65:2343–2351

Qiu H., LV L., PAN B.-c., Zhang Q.-j, Zhang W.-m., Zhang Q.-x. (2009) Critical review in adsorption kinetic models. J Zhejiang Univ Sci A. 10(5):716-724

Quinn J., Geiger C., Clausen C., Brooks K ., Coon C., O'hara S., Krug T., Major D., Yoon W., A. Gavaskar, and T. Sholdsworth (2005) Field Demonstration of DNAPL Dehalogenation Using Emulsified Zero-Valent Iron. Environ. Sci. Technol. 39:1309-1318

Quin˜ones I., Guiochon G. (1996/a) Derivation and Application of a Jovanovic–Freundlich Isotherm Modelfor Single-Component Adsorption on Heterogeneous Surfaces. J. Colloid Interface Sci. 183:57–67

Quin˜ ones I., Guiochon G. (1996/b) Isotherm models for localized monolayers with lateral interactions. Application to single-component and competitive adsorption data obtained in RP-HPLC. Langmuir 12:5433-5443

Quin˜ones I., Guiochon G. (1998) Extension of a Jovanovic–Freundlich isotherm model to multicomponent adsorption on heterogeneous surfaces. J. Chromatogr. A, 796:15–40

Reemtsma T., Mehrtens J. (1997) Determination of Polycyclic Aromatic Hydrocarbon (PAH) leaching from contaminated soil by a column test with on-line phase extraction. Chemosphere 35(11):2491-2501

Reference Method for the Canada-Wide Standard for Petroleum Hydrocarbons in Soil - Tier 1 Method

Rivas J., Gimeno O., de la Calle R.G., Portela J.R., de la Ossa E.M. (2009) Remediation of PAH spiked soils: Concentrated H2O2 treatment/continuous hot water extraction–oxidation. J. Hazard. Mater. 168:1359–1365

Romero A., Santos A., Cordero T., R-Mirasol J., Maria Rosasa J., Vicente F. (2011) Soil remediation by Fenton-like process: Phenol removal and soil organic matter modification. Chem. Eng. J. 170:36–43

Romero A., Santos A., Vicente F., Rodriguez S., Lafuente A. L. (2009) In situ oxidation remediation technologies: Kinetic of hydrogen peroxide decomposition on soil organic matter. J. Hazard. Mater. 170:627–632

Ruthven D.M. (1984) principles of adsorption and adsorption processes

Salahi A., Noshadi I., Badrnezhad R., Kanjilal B., Mohammadi T. (2013) Nano-porous membrane process for oily wastewater treatment: Optimization using response surface methodology. J Environ Chem Eng 1:218–225

Sedlak D. L., Andren A. W. (1994) The effect of sorption on the oxidation of polychlorinated biphenyls (PCBs) by hydroxyl radicals. Water Resource. 28 (5):1207-1215

Silva A., Delerue-Matos C., Fiuza A. (2005) Use of solvent extraction to remediate soils contaminated with hydrocarbons. J. Hazard. Mater. B124:224–229

Silva P. T. d S., Silva V. L. da, Neto B. de B., Simonnot M-O. (2009) Phenanthrene and pyrene oxidation in contaminated soils using Fenton's reagent. J. Hazard. Mater. 161:967–973

Sirguey C., Silva P. T. S., Schwartz C., and Simonnot M.-O. (2008) Impact of chemical oxidation on soil quality. Chemosphere 72:282–289

Shahbeig H., Bagheri N., Ghorbanian S. A., Hallajisani A., Poorkarimi S. (2013) A new adsorption isotherm model of aqueous solutions on granular activated carbon. World Journal of Modelling and Simulation 9(4):243-254

Sherwood M. K., and Daniel P. Cassidy (2014) Modified Fenton oxidation of diesel fuel in arctic soils rich in organic matter and iron. Chemosphere 113:56–61

Shor L.M., Rockne K.J., Taghon G.L., Young L.Y., and Kosson D.S. (2003) Desorption kinetics for field-aged Polycyclic Aromatic Hydrocarbons from sediments. Environ. Sci. Technol. 37:1535-1544

Smith B. A., Teel A. L., Watts R. J. (2006) Mechanism for the destruction of carbon tetrachloride and chloroform DNAPLs by modified Fenton's reagent. J. Contam. Hydrol. 85:229‑246

Song J., Peng P., Huang W. (2002) Black carbon and kerogen in soils and sediments. 1. Quantification and characterization. Environ. Sci. Technol. 36:3960-3967

Sparks D. L. (2003) Environmental soil chemistry. Amsterdam; Boston: Academic Press, 2nd ed

Subramanian B., Namboodiri V., Khodadoust A.P., and Dionysiou D.D. (2010) Extraction of pentachlorophenol from soils using environmentally benign lactic acid solutions. J. Hazard. Mater. 174:263–269

Sui H., Hua Z., Li X., Li H., Wu G. (2014) Influence of soil and hydrocarbon properties on the solvent extraction of high-concentration weathered petroleum from contaminated soils. Environ. Sci. Pollut. Res. 21:5774-5784

Sun H.-W., Yan Q.-S. (2007) Influence of Fenton oxidation on soil organic matter and its sorption and desorption of pyrene. J. Hazard. Mater. 144:164–170

Teel A. L., Warberg C. R., Atkinson D. A., Watts R. J. (2000) Comparison of mineral and soluble iron Fenton's catalysts for the treatment of trichloroethylene. Wat. Res. 35(4):977-984

Texas natural resource conservation commission, 1006, Revision 03, 2001

TNRCC METHOD 1006, Characterization of NC6 to NC35 Petroleum Hydrocarbons in Environmental Samples

Trellu C., Mousset E., Pechaud Y., Huguenot D., van Hullebusch E. D., Esposito G., Oturan M. A. (2015) Removal of hydrophobic organic pollutants from soil washing/flushing solutions: A critical review. J. Hazard. Mater. 306(5):149-174

Tsai T.T., and Kao C.M. (2009) Treatment of petroleum-hydrocarbon contaminated soils using hydrogen peroxide oxidation catalyzed by waste basic oxygen furnace slag. J. Hazard. Mater. 170:466–472

Umpleby R. J., Baxter S. C., Chen Y., Shah R. N., Shimizu K. D. (2001) Characterization of molecularly imprinted polymers with the Langmuir-Freundlich isotherm. Anal. Chem. 73:4584-4591

Usman M., Faure P., Hanna K., Abdelmoula M., Ruby C. (2012) Application of magnetite catalyzed chemical oxidation (Fenton-like and persulfate) for the remediation of oil hydrocarbon contamination. Fuel 96:270–276

US EPA, United States Environmental Protection Agency. Method 3050B (Revision 2): Acid digestion of Sediments, Sludges and Soils. 1996

Van Vliet B. M., Weber Jr W. J., Hozumi H. (1980) Modeling and prediction of specific compound adsorption by activated carbon and synthetic adsorbents Water Res. Vol. 14, pp. 1719 to 1728

Varanasi P., Fullana A., Sidhu S. (2007) Remediation of PCB contaminated soils using iron nano-particles. Chemosphere 66:1031–1038

Vicente F., Rosas J.M., Santos A., Romero A. (2011) Improvement soil remediation by using stabilizers and chelating agents in a Fenton-like process. Chem. Eng. J. 172:689– 697

Vijayaraghavan K., Padmesh T.V.N., Palanivelu K., Velan M. (2006) Biosorption of nickel(II) ions onto Sargassum wightii: Application of two-parameter and three-parameter isotherm models. J. Hazard. Mater. B133 (2006) 304–308

Voelker B., Sulzberger B. (1996) Effects of fulvic acid on Fe(II) oxidation by hydrogen peroxide. Environ. Sci. Technol. 30:1106-1114

Wang F. F., Wu Y., Gao Y., Li H., Chen Z. (2016) Effect of humic acid, oxalate and phosphate on Fenton-like oxidation of microcystin-LR by nanoscale zero-valent iron. Sep. Purif. Technol. 170:337-343

Watts R. J., ASCE M., Teel A. L. (2005) Chemistry of modified Fenton's reagent Catalyzed H2O2 Propagations–CHP, for In situ soil and groundwater remediation. Journal of Environmental Engineering 131:612-622

Watts R.J., Dilly S.E. (1996) Evaluation of iron catalysts for the Fenton –like remediation of diesel contaminated soils. Hazardous Material 51:209-224

Watts R. J., Stanton P. C. (1999) Mineralization of sorbed and NAPL-phase hexadecane by catalysed hydrogen peroxide. Water Resource 33 (6):1405-1414

Watts R. J., Stanton P. C., Howsawkeng J., Teel A. L.(2002) Mineralization of a sorbed polycyclic aromatic hydrocarbon in two soils using catalyzed hydrogen peroxide. Water Research 36:4283–4292

Weber W. J., Huang W. (1996) A distributed reactivity model for sorption by soils and sediments. 4. Intraparticle heterogeneity and phase-distribution relationships under nonequilibrium conditions. Environ. Sci. Technol. 30:881-888

Weisz P.B. (1967/a) Sorption-Diffusion in Heterogeneous Systems Part 1.-General Sorption Behaviour and Criteria. Journal of Transaction of Faraday society 63:1801-1806

Weisz P. B., Hicks J. S. (1967/b) Sorption-Diffusion in Heterogeneous Systems Part 2.-Quantitative Solutions for Uptake Rates. Journal of Transaction of Faraday society 63:1807-1814

Wu G-Z., Coulon F., Y-W. Y., Hong L., Hong S. (2013) Combining solvent extraction and Bioremediation for Removing Weathered Petroleum from Contaminated Soil. Pedosphere 23 (4):455–463

Wu F.-C., Tseng R.-L., R.-S. Juang (2001) Kinetic modelling of liquid-phase adsorption of reactive and metal ions on chitosan. Wat. Res. 35(3):613-618

Xiao B., Yu Z., Huang W., Song J., Peng P. (2004) Black carbon and kerogen in soils and sediments. 2. Their roles in equilibrium sorption of less-polar organic pollutants. Environ. Sci. Technol. 38:5842-5852

Xu P., Achari G., Mahmoud M., Joshi R. C. (2006) Application of Fenton's reagent to remediate diesel contaminated soils. Practice Periodical of Hazardous, Toxic, and Radioactive Waste Management 10:19-27

Yang L., Jin M., Tong C., Xie S. (2013) Study of dynamic sorption and desorption of polycyclic aromatic hydrocarbons in silty-clay soil. J. Hazard. Mater. 244– 245:77– 85

Yang Y., Zhang N., Xue M., Tao S. (2010) Impact of soil organic matter on the distribution of polycyclic aromatic hydrocarbons (PAHs) in soils. Environ. Pollut. 158:2170-2174

Yap C.L., Gan S., Ng H.K. (2012/a) Evaluation of solubility of polycyclic aromatic hydrocarbons in ethyl lactate/water versus ethanol/water mixtures for contaminated soil remediation applications. J Environ Sci. (China) 24 (6):1064–1075

Yap C.L. (2012/b) Ethyl lactate based Fenton treatment for the remediation of polycyclic aromatic hydrocarbon-contaminated soils. PhD thesis of faculty of chemical and environmental engineering, University of Nottingham, Malaysia

Yeh C. K., Hsu C.Y., Chiu C.H., Huang K.L. (2008) Reaction efficiencies and rate constants for the goethite-catalyzed Fenton-like reaction of NAPL-form aromatic hydrocarbons and chloroethylenes. J. Hazard. Mater. 151:562–569

Yeh C. K.-J., Wu H.-M., Chen T.-C. (2003) Chemical oxidation of chlorinated non-aqueous phase liquid by hydrogen peroxide in natural sand systems. J. Hazard. Mater. B96:29–51

Yoo J.-C., Lee C., Lee J.-S., Baek K. (2016) Simultaneous application of chemical oxidation and extraction processes is effective at remediating soil Co-contaminated with petroleum and heavy metals. J. Environ. Manage. 1-6

Yu D-Y., Kang N., Bae W., Banks M. K. (2007) Characteristics in oxidative degradation by ozone for saturated hydrocarbons in soil contaminated with diesel fuel. Chemosphere 66:799–807

Yousefi A. S., Bostani A. (2012) Effect of hydrogen peroxide concentration in remediation of oil-contaminated soils with use of Fenton reaction. Journal of Chemical Health Risks 2(4):9-12

Zhang H., Ma D., Qiu R., Tang Y., Du C. (2016) Non-thermal plasma technology for organic contaminated soil remediation: a review. Chem. Eng. J. 313(1):157-170

http://www.caslab.com/Petroleum-Hydrocarbon-Ranges/

https://en.wikipedia.org/wiki/Ethyl_lactate

Appendix 1:

The overall equation is explained in Eq.(A1-1):

$$\eta = \beta_0 + \sum_{j=1}^{k} \beta_j x_j + \sum_{j=1}^{k} \beta_{jj} x_j^2 + \sum_i \sum_{<j=2}^{k} \beta_{ij} x_i x_j + e_i \qquad \text{Eq.(A1-1)}$$

where η is response, $x_i$and x_j are the independent factors, β_0 the constant coefficient, β_j, β_{jj} and β_{ij} denote the coefficient for linear, quadratic and interaction effect and e_i is the error (Salahi et al., 2013).

Suitability of the proposed polynomial was examined by the R^2 and R^2_{adj} as defined by Eqs.(A1-2) and (A1-3) (Salahi, 2013), respectively:

$$R^2 = 1 - \frac{SS_{residual}}{SS_{model} + SS_{residual}} \qquad \text{Eq.(A1-2)}$$

$$R^2_{adj} = 1 - \frac{SS_{residual}/DF_{residual}}{(SS_{model} + SS_{residual})/(DF_{model} + DF_{residual})} \qquad \text{Eq.(A1-3)}$$

In these equations, DF is the degree of freedom, P is the number of model variable, SS is the sum of squares, and n indicates the number of experiment.

Appendix 2:

Table A2-1: Experimental design results for fraction 1, fraction 2, fraction 3, and TPH removal efficiency

Run	Block	HA	EL	pH	Removal efficiency of TPH, actual value	Removal efficiency of TPH, predicted value
1	1	-1	-1	-1	82.65	82.80
2	1	-1	-1	1	88.48	88.47
3	1	0	0	0	78.25	79.13
4	1	0	0	0	79.01	79.13
5	1	0	0	0	79.50	79.13
6	1	1	1	1	71.00	71.72
7	1	1	-1	1	87.22	87.91
8	1	1	1	-1	68.26	69.13
9	1	1	-1	-1	77.69	76.40
10	1	-1	1	1	71.81	72.28
11	1	-1	1	-1	77.04	75.53
12	1	0	0	0	79.82	79.13
13	-1	0	0	0	79.59	79.93
14	-1	0	0	1.633	83.89	83.31
15	-1	0	0	-1.633	74.90	76.56
16	-1	0	0	0	78.94	79.93
17	-1	0	1.633	0	67.75	67.43
18	-1	0	-1.633	0	86.30	86.59
19	-1	1.633	0	0	78.86	77.09
20	-1	-1.633	0	0	83.39	82.78

Appendix 3:

The correlation coefficient results for the second order kinetic rate.

Table (A3-1): Second order kinetic rate correlation coefficient for Fenton reaction without HA

Experimental Conditions				Fraction 1	Fraction 2	Fraction 3	TPH
H_2O_2,M	EL%	L/S	Fe^{2+},M	R^2			
0.1	25	2	0.05	**0.6577**	**0.7645**	**0.5567**	**0.6689**
0.5	25	2	0.05	**0.6399**	**0.6849**	**0.6487**	**0.6847**
2	25	2	0.05	**0.5899**	**0.6933**	**0.8036**	**0.6322**
4	0	2	0.2	**0.5836**	**0.7321**	**0.7466**	**0.7029**
4	25	2	0.2	**0.6123**	**0.7569**	**0.7123**	**0.6987**
4	50	2	0.2	**0.6099**	**0.6842**	**0.6984**	**0.6128**
0.5	25	1	0.05	**0.6822**	**0.5769**	**0.5987**	**0.5974**
0.5	25	5	0.05	**0.4989**	**0.7364**	**0.6328**	**0.7163**

Table (A3-2): Second order kinetic rate correlation coefficient for Fenton reaction with HA

Experimental Conditions	Fraction 1	Fraction 2	Fraction 3	TPH
HA	R^2			
0	**0.6789**	**0.5578**	**0.6488**	**0.6213**
10	**0.5978**	**0.6987**	**0.5876**	**0.6098**
50	**0.4966**	**0.4876**	**0.5498**	**0.7436**
100	**0.7032**	**0.7843**	**0.4489**	**0.5789**
150	**0.6947**	**0.6698**	**0.6912**	**0.6622**